UNIVERSITY OF MISKOLC

MIKOVINY SAMUEL DOCTORAL SCHOOL OF EARTH SCIENCES

Head of the doctoral school: Prof. Dr. Péter Szűcs

MATRIX ACIDIZING IN CARBONATE RESERVOIRS: OPTIMIZATION OF CARBONIC ACID INJECTION AND INNOVATIVE ACID DIVERSION TECHNIQUES

Thesis of the doctoral dissertation (Ph.D.)

Authur:

Abdulameer Mohsin Kadhim Almalichy

Scientific supervisor:

Associate Professor Dr. Zoltan Turzo

UNIVERSITY OF MISKOLC

FACULTY OF EARTH AND ENVIRONMENTAL SCIENCES AND ENGINEERING

INSTITUTE OF MINING AND ENERGY

Miskolc, 2025

HUNGARY

Table of Contents

List of Figures

List of tables

List of Abbreviations

API	American Petroleum Institute
BPR	back pressure regulator
CCS	carbon capture and storage
CI	corrosion inhibitor
CO_2	Carbon dioxide
CT	Computed Tomography
DI	Deionized water
DP	Differential pressure
EOR	enhance oil recovery
HP/HT	high pressure/high temperature
HCl	hydrochloric acid
ICP	inductively coupled plasma
ICP-OES	inductively coupled plasma optical emission spectroscopy
IL	Indiana limestone
IR	injection rate
MSA	Methanesulfonic acid
NMR	Nuclear Magnetic Resonance
NTA	nitrilotriacetic acid
PLA	Polylactic acid
PV	pore volume
PVBT	Pore volume to breakthrough
SC-CO_2	supercritical carbon dioxide
TBT	Time to Breakthrough
VES	viscoelastic surfactant
SDA	self-diverting acid
Vi	interstitial velocity
Vwh	wormhole volume
WB	wormhole growth B-factor
Weff	wormhole efficiency factor
XRD	x-ray diffraction

Recommendation of the Supervisor

The scientific research conducted by Mr. Abdulameer Almalichy represents a significant and original contribution to understanding and further development of matrix acidizing of carbonate reservoirs. He evaluated an alternative, environmental friendly fluid, carbonic acid instead of the commonly used HCl. Carbonic acid has many advantage against HCl. Based on many labor experiments he determined the necessary information required for successful design of acidizing with carbonic acid. He also evaluated the usage of acid diverter (VES) in combination of carbonic acid. Acid diverters used in heterogenous reservoirs for more even distribution of acids. During his research he developed a new method with the associated laboratory measuring equipment for evaluation of acidizing in horizontal wells. The new equipment has five evenly distributed acid inlets and two outlets. This new method with the corresponding equipment is a great contribution in understanding the acidizing process in horizontal wells. In case of the developed method and equipment the patent application has been filed.

Mr. Abdulameer Almalichy demonstrated strong analytical skills, scientific independence, and an exceptional ability to synthesize the results into coherent interpretations. His conclusions are well supported, providing new insights into matrix acidizing of heterogeneous carbonate reservoirs. The thesis is clearly written, well structured, and supported by high-quality figures and tables. Throughout his PhD studies, the candidate showed remarkable dedication, creativity, and independence in both laboratory and interpretive work. Mr. Abdulameer Almalichy published his new scientific achievements in four conferences and seven scientific article in well ranked scientific journals (Heliyon, Scientific Report, Energy&Fuels, etc.) confirming the originality and scientific value of his results.

Both reviewers recognized the scientific integrity, depth, and significance of the study, confirming that it meets international PhD standards. Based on its scientific quality, originality, and contribution, I recommend the thesis for public defense and support the award of the Doctor of Philosophy (PhD) degree to Mr. Abdulameer Almalichy.

Miskolc, 20/11/2025

Dr. Zoltán Turzó
supervisor

Summary

Matrix acidizing is a stimulation technique used to remove the damaged zone around the wellbore caused by drilling and completion. In this process, the intended acid is pumped into the wellbore at a pressure below the formation breakdown pressure, thereby avoiding formation fractures. When injected, acid penetrates carbonate formations, dissolves carbonate minerals, and generates conductive flow channels called wormholes that enhance well productivity. Hydrochloric acid (HCl) is preferred due to its cost-effectiveness and strong ability to dissolve carbonate rocks, making it an ideal choice for matrix acidizing. Its reaction products are typically soluble, preventing clogging, and its low cost makes it an economical choice for enhancing oil production. However, HCl also has notable drawbacks, including its rapid reaction with carbonates at high temperatures, which causes face dissolution and high acid volume consumption, thus limiting deep penetration into the formation. Additionally, it causes severe tubing corrosion, resulting in high inhibition costs.

To overcome these drawbacks, carbonic acid, which consists of water and carbon dioxide (CO_2), can be considered an environmentally friendly alternative to hydrochloric acid. The gradual increase in CO_2 emissions is causing severe environmental and economic concerns regarding global climate change, and utilizing large volumes of CO_2 in industrial projects can reduce greenhouse gas emissions. Over the past decade, significant attention has been directed toward CO_2 injection for enhanced oil recovery (EOR) and carbon capture and storage (CCS) as promising approaches to achieving zero-net carbon. Using carbonic acid as a stimulation acid in carbonate reservoirs can reduce emissions and mitigate the corrosion issues common with HCl acidizing, while also improving permeability, removing drilling-induced formation damage, and increasing production.

Creating a long, dominant wormhole is a primary objective during matrix acidizing, and finding the optimal injection rate is crucial for achieving the longest penetration radius with the minimum acid volume. Experimentally, the optimum injection rate is determined by the minimum injected acid pore volume required to generate a wormhole in a core sample, a parameter known as the minimum pore volume to breakthrough (PVBT). This parameter is influenced by factors such as rock mineralogy, acid type, formation temperature, permeability, and core dimensions.

In the first part of the research, since each acid has an optimum injection rate, similar core-flooding experiments were conducted with carbonic acid to determine its optimum injection conditions.

A major limitation of traditional acidizing techniques is their tendency to flow into high-permeability zones, leaving low-permeability regions untreated. This selective flow reduces the overall

effectiveness of the acidizing treatment, resulting in poor reservoir stimulation. Diversion techniques have been developed to overcome this limitation and are generally categorized into mechanical and chemical methods. Mechanical diversion relies on physical barriers to block high-permeability areas, while chemical diversion uses specialized fluids to alter the acid's flow paths. Foam-based acids can effectively block high-permeability zones and slow the acid–rock reaction, but they often suffer from poor stability, especially in high-temperature reservoirs. Emulsified acids can penetrate deeper and offer corrosion protection, but they require complex preparation, have high pumping friction, and are unsuitable for low-temperature wells or fine-particle production. Polymer-based in-situ gelled acids provide strong diversion but can leave damaging residues, suffer from crosslinker precipitation at high temperatures, and lose efficiency in high-permeability contrast cases. In contrast, viscoelastic surfactants (VES)-based self-diverting acids offer high thermal stability, residue-free cleanup, effective diversion in high-salinity environments, and easy viscosity breakdown after treatment, thereby minimizing formation damage while ensuring selective stimulation.

The second part of this research introduces a novel approach that integrates carbonic acid with a viscoelastic surfactant (VES) to divert acid in a heterogeneous carbonate reservoir. This combination aims to enhance acid distribution and deliver both environmental and operational benefits, including reduced hydrochloric acid consumption, minimized corrosion, and alignment with CCS objectives.

In the final part of this study, unlike previous laboratory experiments that relied on conventional single- or dual-core flooding systems, a new method is proposed for simulating matrix acidizing in horizontal wells, incorporating five separate injection points and two outlet lines. This design provides a more representative simulation of flow behavior in horizontal wells and allows for direct observation of wormhole initiation, competition, and propagation in heterogeneous reservoirs.

Abdulameer Mohsin Kadhim Almalichy

November 2025, Miskolc, Hungary

Acknowledgments

I would like to express my sincere appreciation to my supervisor, Associate Professor **Dr. Zoltan Turzo**, for his continuous support, guidance, and invaluable expertise throughout the development of this work. I am also deeply grateful to **Dr. Ahmed Al-Yaseri** and **Dr. Murtada Saleh Aljawad** for their thoughtful evaluation and constructive feedback; their dedication and encouragement helped me overcome many challenges along the way.

I also sincerely **thank King Fahd University of Petroleum and Minerals**, particularly the **College of Petroleum Engineering and Geoscience (CPG)**, for providing the facilities and support necessary to conduct this research. I'm deeply appreciative of the lab engineers who guided and assisted me during the experimental work: **Hani Salman Al Mukainah**, **Ammar M. Al-Ramadhan, Ridha Al-Abdrabalnabi, and Eassa Abdulah**. Their expertise and invaluable contributions were instrumental in completing the laboratory work for this study. I also extend my appreciation to **Missan Oil Company** for their moral and financial support and for granting me the opportunity to pursue my studies in Hungary.

My heartfelt gratitude goes to my family, especially my **father and mother**, whose patience, prayers, and understanding sustained me while I was far from home, even during times when they needed me most. I'm equally thankful to **my brothers**, particularly **Akram** and **Samer**, for their constant sacrifices, which allowed me to remain focused on my academic journey.

My deepest thanks go to **my wife**, whose strength, patience, and willingness to travel long distances to stand by my side brought me comfort and stability. To my children, my little angels, thank you for the joy, motivation, and daily energy that pushed me forward even on the most challenging days.

Finally, I extended my appreciation to everyone who supported me during this journey, as well as to my colleagues and professors in the Department of Petroleum Engineering at the University of Miskolc. I would also like to thank **Dr. Usama Alamedy** and **Dr. Hasan Alsaedi** for their support and continuous encouragement.

1 Introduction

1.1 Research Objectives and Scope

The objectives of this dissertation are:

1. Introducing carbonic acid as a matrix acid for carbonate formations and studying its effects on wormhole generation, permeability enhancement, and porosity improvement while determining its optimum injection rate.
2. Developing a novel approach by effectively mixing carbonic acid with viscoelastic surfactants (VES) to acidize heterogeneous carbonate formations.
3. Introduce a novel design to study acid diversion, offering an alternative to the conventional designs commonly used in literature.

1.2 Dissertation Structure

The dissertation is divided into the following chapters:

1. Introduction: The background of HCL alternatives, optimum injection rate, acid diversion, and the objectives of this study will be discussed.
2. Optimization of Injection Rates Using Carbonic Acid: Experimental methods, results, and analysis for determining the optimum injection rate.
3. Dual-Core Flooding for Acid Diversion: Comparing acid systems in dual-core setups to evaluate their diversion efficiency.
4. Single-Core Flooding with Novel Design for Acid Diversion: Evaluating the newly developed single-core holder for advanced acid placement.

1.3 Background on matrix acidizing

Matrix acidizing is a stimulation technique used to remove the damaged zone around the wellbore caused by drilling and completion processes; the intended acid is pumped into the wellbore at a pressure below the formation breakdown pressure, avoiding formation fractures. When injected, acid penetrates carbonate formations, dissolving carbonate minerals and generating flow channels called wormholes that enhance well productivity (Almalichy et al., 2022; Bazin et al., 1995; Daccord et al., 1989; Wang et al., 1993).

However, HCl has several drawbacks, including high corrosivity, rapid reaction rates at high-temperature/high-pressure (HT/HP) conditions, inefficient acid penetration into deeper formations, increased costs, and the need for corrosion inhibitors (Chacon and Pournik, 2022). As a result, researchers are actively seeking alternative acid systems that offer the benefits of HCl with lower reaction rates and reduced corrosivity (Rodrigues et al., 2021).

In rocks with varying properties, a significant difference in permeability may significantly decrease the effectiveness of stimulation treatments since the acid will predominantly flow into the zones with higher permeability. Inadequate design will result in unequal treatment of target areas and unsuccessful acid treatment (Zakaria and Nasr-El-Din, 2016a). This phenomenon will be worse in a thick or horizontal reservoir. Consequently, the industry has extensively adopted mechanical and chemical diverters, selecting the most effective approach to mitigating this effect for each lithology (Ba Alawi et al., 2020).

The gradual increase in carbon dioxide (CO_2) emissions is raising serious environmental and economic concerns about global climate change. Utilizing large volumes of CO_2 in industrial projects can reduce greenhouse gas emissions (Bashir et al., 2024; Caldeira and Wickett, 2003; Ma et al., 2021). In the last decade, much focus has been placed on CO2 injection-enhanced oil recovery (EOR) and carbon geostorage (CGS) as promising methods to achieve zero-net carbon (Al-Yaseri et al., 2023; Elsayed et al., 2023; Thomas et al., 2022). Using carbonic acid, which consists of DI water and CO_2, as a stimulation acid for carbonate reservoirs should reduce emissions and tubular corrosion, which are common with HCl acid stimulation.

1.4 Background on HCl Alternatives

Matrix acidizing, a widely used well-stimulation technique, involves injecting acid solutions below the formation's fracture pressure to enhance productivity by eliminating formation damage and creating new flow channels called "wormholes" (Usama Alameedy et al., 2023; Almalichy et al., 2022). Since the 1890s, hydrochloric acid has been the dominant choice in treating oil and gas reservoirs due to its effectiveness in dissolving carbonate formations. However, HCl has several drawbacks, including high corrosivity, rapid reaction rates at high-temperature/high-pressure (HT/HP) conditions, inefficient acid penetration into deeper formations, increased costs, and the need for corrosion inhibitors (Chacon and Pournik, 2022). As a result, researchers are actively seeking alternative acid systems that offer the benefits of HCl with lower reaction rates and reduced corrosivity (Rodrigues et al., 2021)

Organic acids such as methanesulfonic acid (MSA) and acetic acid are among the most promising alternatives. MSA's lower reactivity, resulting from its lower H+ activity coefficient and higher pKa value than HCl, allows for deeper penetration into carbonate formations and more effective wormhole creation (Ortega, 2015; Shank and McCartney, 2013). Similarly, acetic acid and other weak acids, such as formic acid, have shown slower reaction kinetics, facilitating deeper stimulation (Al-Douri et al., 2013; Chang et al., 2008).

Retarded acid systems, including gelled acids, in-situ gelled acids, and emulsified acids, have emerged as effective alternatives to control acid reactivity. Gelled acids are a prominent approach to managing acid reaction rate by increasing the acid's viscosity, which

helps prevent fluid loss and improve acid placement. This approach is particularly practical in formations with heterogeneous permeability, where conventional acids might preferentially enter high-permeability zones, leaving low-permeability areas untreated (Ratnakar et al., 2012). In-situ gelled acids, which form a gel within the reservoir through pH or temperature-triggered reactions, further enhance acid placement by treating less permeable zones (AlOtaibi et al., 2020). Emulsified acids, consisting of HCl droplets dispersed in an oil phase, slow down the acid-rock interaction, enabling deeper penetration. Surfactant-stabilized emulsions reduce acid consumption near the wellbore and improve wormhole propagation (Lynn and Nasr-El-Din, 2001; Zakaria and Nasr-El-Din, 2016a). Biopolymeric resin-based retarded HCl also shows promise, as polymers slow down the mobility of hydrogen ions, improving acid penetration in high-temperature environments (Al-Othman et al., 2017).

Chelating agents like ethylenediaminetetraacetic acid (EDTA) and nitrilotriacetic acid (NTA) have also been explored for deep penetration and uniform acid distribution. These agents form stable complexes with calcium ions, thereby controlling reaction rates and minimizing near-wellbore spending, making them effective in high-temperature carbonate reservoirs (Al-Othman et al., 2017; Frenier et al., 2000; Shafiq et al., 2018).

Foamed acids, which incorporate nitrogen gas into HCl, present another practical approach for controlling acid reactivity. By reducing contact between acid and rock, foamed acids slow reaction rates, promote wormhole growth, and reduce overall acid consumption. This system has proven particularly effective in heterogeneous formations, ensuring more uniform stimulation and deeper penetration even at low injection rates (Al Ayesh et al., 2017; Yan et al., 2019a).

1.5 Background on Optimum Injection Rate

Creating a long, dominant flow channel, called a wormhole, is desirable during matrix acidizing. Finding the optimal injection rate is key to achieving the longest penetration radius with the minimum acid volume. Experimentally, the optimum injection rate is determined by the minimum injected acid pore volume required to generate a wormhole in a core sample, a parameter called the minimum pore volume to breakthrough (PVBT). Many factors, including rock minerals, acid type, formation temperature, permeability, and core dimensions, influence the optimum injection rate. Core flooding experiments on the selected rock and acid type are typically conducted to determine the optimum injection rate and the corresponding PVBT. The selection of acid concentration, acid volume, and injection rate is based on this fundamental characteristic. Thus, a similar study should be conducted on carbonic acid to determine its optimal injection conditions, which is an environmentally

friendly alternative to hydrochloric acid (Buijse, 1997; Chacon and Pournik, 2022; Fredd and Fogler, 1998; T. Huang et al., 2000).

Numerous researchers have examined the optimal injection rate both theoretically and experimentally. Wang et al. were the first to experimentally determine the optimal injection rate through acid core flooding experiments (Wang et al., 1993). They found that the optimal value varies with injection rate, rock mineralogy, reaction temperature, and acid concentration. The results indicate that rock mineralogy has the greatest impact on the optimal injection rate. Higher injection rates are needed for formations with higher temperatures. Furthermore, the study revealed that increasing the acid viscosity or decreasing the acid diffusivity could be advantageous. According to the theory, a reduction in wormhole radius results in a lower volume of acid required to achieve a given depth of penetration (Bazin, 2001; Wang et al., 1993).

Bazin studied the effect of core length, acid concentration, and injection rate on wormhole propagation. He found that the wormhole propagation rate is proportional to $u^{2/3,}$ where u is the acid injection rate. Furthermore, researchers found that a balance between convection and acid consumption determines the maximum wormhole depth in long cores. They also identified the optimal injection rate, which varies with core length, marking the transition between convection-limited and mass transfer-limited regimes (Bazin et al., 1995; Ghommem et al., 2015).

Buijse studied the mechanism of wormhole formation in carbonate reservoirs and demonstrated that the core geometry significantly influences leak-off properties and wormhole competition, thereby impacting the upscaling of lab results to the field scale. Wormhole growth rate, breakthrough volumes, etc., vary with core size. Larger-diameter cores exhibit more developed side branches and lower breakthrough volumes. The results indicate that wormhole models that depend on the outcomes of laboratory flooding experiments should be used cautiously (Buijse, 2000, 1997).

Buijse and Glasbergen developed a semiempirical model to determine the relationship between acid injection rate and the propagation velocity of wormholes. This model aims to fit experimental data from acidizing core flooding experiments. Two essential parameters that can be obtained from the core flooding experiment and used to fit the model are the optimum interstitial velocity and the associated PVBT. The study revealed that upscaling the optimal injection rate from a linear core-flow experiment to field conditions is not straightforward. Pumping the acid at its maximum rate while avoiding the fracturing pressure could be the best option in a radial flow scenario (Buijse and Glasbergen, 2005). Later, another model was developed by Furui, which builds on Buijse and Glasbergen's semiempirical model. This study upscaled the lab-scale core flooding experiments to field conditions (Furui et al., 2011; Panga et al., 2004).

Fredd and Fogler studied how the reaction rate of the acid and transport phenomena interact to generate wormholes using Damköhler number concepts. They found that the optimal Damköhler number was 0.29 across all acid systems and rock types. The study revealed that a low injection rate leads to unwanted face dissolution and that the injected acid is consumed at the sample inlet. At a slightly higher injection rate, the acid enters the sample and forms a wormhole, with acid loss from the wormhole wall, leading to an increase in the acid PVBT; this type of wormhole is called a conical wormhole. At an intermediate injection rate, a single, less branched, dominant wormhole is generated, requiring the minimum pore volume to break through; this desirable type of wormhole is called a dominant wormhole. At higher injection rates, the acid reaches the tiny pores, increasing contact with surface area and leading to greater acid consumption and branched flow channels; this type of wormhole is called a ramified wormhole (Fredd and Fogler, 1998).

Dong et al. also studied the optimal injection rate in carbonate acidizing, accounting for rock lithology, acid concentration, temperature, and rock-pore-size distribution in their model. He approved that the model accurately predicts optimal rates for acidizing-core flood experiments, consistent with experimental results. Furthermore, the study reveals that wormhole-propagation velocity is directly proportional to the acid-diffusion coefficient for diffusion-limited reactions under optimal conditions, as confirmed experimentally and theoretically. Since the model was not limited by flow geometry, it can be applied to field scales, as demonstrated in the study (Dong et al., 2016; Tianping Huang et al., 2000).

Talbot and Gdanski analyzed various experimental results using hydrochloric acid, accounting for factors such as temperature, acid concentration, core aspect ratio, porosity, and permeability. The authors developed a universal function to describe all the data, enabling the data to be collapsed into a master curve. Regardless of the aspect ratio, this master curve enables the prediction of the optimal flow rate for acid wormhole experiments on various rocks (Talbot and Gdanski, 2008; Ziauddin and Bize, 2007).

Later, Dong developed a novel wormhole propagation model for acidizing processes, explicitly examining wormhole characteristics as they reach specific lengths in core plugs. He discovered, through numerical simulations and lab experiments, that when a wormhole reaches a critical length, its propagation velocity becomes stable due to the establishment of a consistent fluid-loss profile. The authors show that factors including the distribution of pore sizes in the rock, the overall reaction rate, and the diffusion coefficient influence the propagation speed. He incorporated an optimal tip flux model into a mechanistic growth model (Dong, 2018).

Aljawad et al. used a two-scale continuum model to investigate the impact of temperature on acid stimulation in carbonate reservoirs, specifically limestone, dolomite, and mixed-mineralogy formations. The key findings emphasized that the heat generated during the

reaction had a negligible effect on wormhole propagation, whereas the injected acid's temperature significantly affected its efficiency. Increasing the temperature of the acid enhanced the effectiveness of dolomite stimulation but decreased the efficiency of limestone. At low temperatures, acid targets limestone more than dolomite in separate layers, whereas at elevated temperatures, it penetrates both layers equally. Wormhole propagation was enhanced in cases with mixed mineralogy, resembling the behavior observed in pure calcite under high-temperature conditions (Aljawad et al., 2021).

1.6 Background on Acid Diversion

Carbonate reservoirs comprise over 70% of the world's proven oil and gas reserves and play a crucial role in global energy production. Despite their significance, these reservoirs pose considerable challenges to effective hydrocarbon recovery due to their natural heterogeneity, complex fracture networks, and varying permeability (Mohammed and Velledits, 2024a, 2024b; Zheng et al., 2024). Conventional acidizing treatments have been widely used to enhance oil production by dissolving carbonate minerals, thereby increasing permeability and improving fluid flow within the formation. These acid treatments create channels, or wormholes, that facilitate the movement of hydrocarbons (Almalichy et al., 2022). However, a major limitation of traditional acidizing techniques is their tendency to flow into high-permeability zones, leaving low-permeability regions untreated. This selective flow reduces the overall effectiveness of the acidizing treatment and results in poor reservoir stimulation (Ba Alawi et al., 2020; Garrouch and Jennings, 2017).

Two primary categories of diversion techniques have been developed to overcome this issue: mechanical diversion and chemical diversion. These methods ensure uniform acid distribution throughout the reservoir, thereby enhancing stimulation in both high- and low-permeability zones. Mechanical diversion relies on physical barriers to block high-permeability areas, while chemical diversion uses specialized fluids to alter the acid's flow paths (Al-Shargabi et al., 2023).

Mechanical diversion techniques use physical tools to isolate zones within the wellbore, thereby directing acid to specific areas. Mechanical diversion methods include ball sealers, packers, and coiled tubing (Al-Shargabi et al., 2023). Ball sealers are injected with acid into the wellbore, carried to perforations in the high-permeability zones, and then held in place by the ball's larger diameter relative to the perforated hole diameter. Once in place, they temporarily block these zones, diverting the acid into the lower-permeability areas that require stimulation (Evgenievich Folomeev et al., 2021). The effectiveness of ball sealer operations is influenced by factors such as ball density, fluid viscosity, pump rate, perforation density, and well conditions like inclination and formation permeability contrasts, making process optimization complex (Chang et al., 2007; Kalfayan and Martin, 2009).

Similarly, packers are mechanical devices that come in different types but share standard functions. They are placed at the end of the tubing to create a physical barrier between different well sections, isolating specific zones for acid treatment. Packers can also make a secondary flow path through the annulus to the formations above, isolating two zones in a single installation (Bale, 1984; Chang et al., 2007; Kalfayan and Martin, 2009). Coiled tubing provides another method of zonal isolation, allowing for selective acid injection into targeted intervals of the formation. Moreover, a mechanical diverter can be installed at the end of the coiled tubing to transport and divert the acid to the targeted zone. It also has a compact design, resulting in less rig-up/down time and, therefore, reduced costs. This method also benefits horizontal wells or extended-reach drilling, where zonal isolation is critical for effective acid placement (Khan and Raza, 2015; Thomas et al.,1998).

Although mechanical diversion methods are effective, they tend to be more complex and costly than chemical diversion techniques (Coulter and Jennings, 1999). Chemical diversion can be divided into viscous fluid and particulate diverters (Domelen and S, 2017). The particulate diverter is widely used in fracturing (Akrad and Miskimins, 2023; Al-Hulail et al., 2019; Peiwu et al., 2023; Zhang et al., 2019) and matrix acidizing (Al-Othman et al., 2017; Gonzalez et al., 2017; Huang et al., 2018; Safari et al., 2017; Shahri et al., 2017) because particulate diverters offer temporary, biodegradable blockage, are cost-effective, environmentally friendly, adaptable to reservoir conditions, minimize long-term formation damage, and are simple to apply (Chen and Lu, 2023; Reddy and Cortez, 2013). Common particulate diverters include polylactic acid (PLA), benzoic acid, Rock salt, Naphthalene, Wax beads, and oil-soluble resins, with PLA being the most widely used. Its popularity is due to its biodegradable properties and the ability to adjust its chemical composition for use in different reservoir temperature and pressure conditions. In contrast, other diverters face temperature limitations or lack self-degradability (Shah et al., 2020).

All particulate diverters operate similarly. When pumped into the formation, they target the zones with the highest permeability, forming a barrier of low-permeability particle pack on the formation face or within the perforations. This blockage increases flow resistance in those areas, directing the acid flow to other untreated interval sections (Domelen and S, 2017). Chen and Lu provided the most comprehensive review of degradable polylactic acid diverters used in fracture and matrix acidizing (Chen and Lu, 2023). Al-Othman et al. introduced a new approach in two Jurassic wells using biodegradable particulates and fiber blends emulsified with acid for matrix stimulation. They found that the volume of diversion required was smaller than that of other chemical diverters, and all materials were fully degradable, causing no formation damage (Al-Othman et al., 2017). Shahri et al. optimized particulate diverter systems to create temporary seals (jamming and plugging) in flow paths, enhancing fluid redistribution during acidizing or fracturing. Using a scientifically verified

analytical model that incorporates Computational Fluid Dynamics (CFD) and the Discrete Element Method (DEM), they improved the design of particulate systems, reducing excessive diverter use and lowering operational costs (Shahri et al., 2017).

The second category of chemical diversion involves viscous fluids, which are classified into various types based on the diverting agent used. These include in situ gelled (polymer- and VES-based), foam-based, and emulsified acids.

Foam was first introduced by Smith et al. in 1969 as a diverter (Zerhboub et al., 1994). In single-core acidizing, Foam-based acids consist of a two-phase fluid system of liquid and gas (such as nitrogen or carbon dioxide). The gas acting as the discontinuous phase occupies the medium's large void space. In contrast, the liquid phase, typically the wetting phase, forms a thin layer, or lamellae, covering the rock face and spanning the pore throats. The addition of surfactant provides foam stabilization, allowing the lamellae to break and reform as the acid moves (Bernadiner et al., 1992).

In multistage acid diversion, foam injection traps 80-99% of the gas in porous media, even at high-pressure gradients. This significantly reduces gas mobility, lowering water saturation and decreasing water relative permeability. The foam in a high-permeability or undamaged layer reduces liquid saturation and relative liquid permeability, limiting the acid flow into foam-saturated areas during acid injection and redirecting it into low-permeability or damaged formations. Effective acid diversion relies on gas injected into high-permeability zones during foam injection, which is then trapped during subsequent acid injection (Letichevskiy et al., 2017; Li et al., 2008). Foam diversion frequently encounters stability issues and inconsistent performance, particularly with surface-generated foam, which motivates the researchers to develop an in-situ foam generation technology based on the chemical reaction of HCl with carbonate rock to produce supercritical CO2. With foam agents and stabilizers added, the produced CO_2 forms in situ foam, which acts as a diverter during matrix acidizing (Yan et al., 2019b).

Foam acidizing offers various advantages, including plugging high-permeability zones to target low-permeability zones, selectively stimulating the bearing layer, and enhancing the removal of residual acid through gas expansion, thereby reducing formation damage. Moreover, its retardant nature slows acid rock reaction, enabling deeper acid treatment (Zhang et al., 2021). The primary challenge in applying foamed acids is their stability, which becomes difficult to sustain, especially in high-temperature reservoirs (Liu et al., 2015; Zheng et al., 2024).

Emulsified acids also provide an effective method for acid diversion. Emulsified is a mix of two immiscible fluids, aqueous and oil phases, with an emulsifier. The emulsion can be classified based on the dispersion medium (water-in-oil or oil-in-water), the droplet size of the dispersed phase (nanoemulsion, microemulsion, macroemulsion), and the emulsifier

(Pickering and surfactant agents) (Yousufi et al., 2024). The oil phase slows the reaction rate of hydrochloric acid with carbonate formation to half that of hydrochloric acid alone, allowing the acid to penetrate the formation more deeply, making it an effective solution for high-temperature reservoir acidizing (Abdollahi et al., 2021). It also provides a corrosion inhibitor for well equipment. Despite the benefits, emulsified acid has various drawbacks, including the preparation of acid in the field, not applicable in low temperature and shallow wells with small diameter due to the high friction of pumping; additionally, the acid is not recommended for wells that produce fine particles, as these particles can stabilize the emulsion leading to reduced acid performance (Lynn and Nasr-El-Din, 2001). A new, innovative polymer-assisted emulsified acid was introduced to better treat high-temperature formations by combining the benefits of gelled and emulsified acids (Zakaria and Nasr-El-Din, 2016b, 2015).

Polymer-based in-situ gelled acids, also referred to as self-viscosifying acids, are formulated using hydrochloric acid (HCl), a polymer such as partially hydrolyzed polyacrylamide (PHPA), a crosslinker, and a breaker (Usama Alameedy et al., 2023). The mechanism of these acids is based on the pH-dependent crosslinking of the polymer. Initially, when the acid is injected, its pH is near zero, resulting in low viscosity. As the acid reacts with carbonate formations, the pH gradually rises above 2; at this point, the polymer begins to crosslink with the iron or zirconium ions (Gomaa et al., 2010). This crosslinking increases the viscosity of the acid, forming a gel that helps plug the high-permeability zones and divert the remaining acid to untreated or low-permeability zones. As the acid reacts, the pH rises to around 4, activating the breaker, dissociating crosslinked polymer chains, and reducing viscosity to a low value for easy flowback (AlOtaibi et al., 2020). Gomaa et al. studied the effect of permeability contrast on in-situ gelled acid diversion. At a 1:2 permeability contrast, acid was effectively diverted; at 1:20–25, diversion occurred only below 10 cm^3/min due to reduced gel viscosity at higher rates (Gomaa et al., 2011). Retnakar et al. presented an experiment-based model for gelling acids, showing that viscosity depends on temperature, shear rate, and pH. It also demonstrated that gels improve wormhole branching and flow diversion compared to Newtonian acids (Ratnakar et al., 2012). Many researchers (Chang et al., 2001; Taylor and Nasr-El-Din, 2003, 2002)have reported that polymer residue left after flowback can reduce permeability. Lynn and Nasr-El-Din observed that iron crosslinkers tend to precipitate at high temperatures, further contributing to formation damage and permeability reduction (Lynn and Nasr-El-Din, 2001). To address the problems caused by iron participation, researchers have explored other crosslinkers, including zirconium (Zr^{4+}) (Moffitt et al., 1996), chromium (Cr^{3+}) (Jain et al., 2005), aluminum (Al^{3+}) (Fatah et al., 2008), and metallic-based (AlOtaibi et al., 2020) crosslinkers.

On the other hand, one of the most effective chemical diversion methods is self-diverting acids, typically formulated with viscoelastic surfactants (VES). Upon injection, these acids exhibit low viscosity, allowing them to be easily pumped into the formation. As the acid reacts with the carbonate rock, the pH and Ca^{+2} increase, prompting the VES molecules to organize into rod-like micelles, thereby increasing viscosity. This increase in viscosity temporarily blocks high-permeability zones, diverting the acid into low-permeability regions. The high viscosity of acid can be fully broken down by a solvent flush or contact with carbonate during flowback, without leaving any residual plugging materials behind (Almalichy et al., 2025; Jafarpour et al., 2018). The VES was first introduced by Chang et al. as an alternative to polymers. Unlike polymer, he confirmed the core face was clean after the flooding, with no residual material remaining inside the core (Chang et al., 2001). The limitation of the VES developed by Chang was its stability up to 200°F (93°C). Later, Taylor et al. developed a new, non-damaging self-diverting acid, and rheology tests demonstrated its stability up to 300°F (150°C) (Taylor et al., 2003). The viscoelastic surfactant was first used at the field scale in Kuwait in 17 wells, increasing the production from 8000 BPD to 32000 PBD, exceeding the 21000 BPD expected if treated with conventional acid (Al-Mutawa et al., 2003); similar outcomes were observed when used to simulate gas wells in Bahrain and simulating low-temperature dolomitic oil reservoir in Egypt (Nasr-El-Din and Samuel, 2007). The physical and chemical properties of VES were extensively studied by Lungwitz et al., who also reported that self-diverting acid (SDVA) cleanup was easier than conventional gelled acid cleanup (Lungwitz et al., 2007). Nasr-El-Din et al. introduced amphoteric VES as a new class and studied the effects of various additives. He found that factors such as temperature, pH, and additives, including corrosion inhibitors, iron control agents, and mutual solvents, significantly affect the apparent viscosity of the acid system (Nasr-El-Din et al., 2008). Liu et al. investigated different HCl concentration and their effects on the reaction rate, developing a relationship between reaction rate and HCl concentration (Liu et al., 2013). A comprehensive study conducted by Al-Sadat et al. revealed that the VES exhibited dominant elastic properties, shear-thinning, and thermal stability up to 150 °C; the viscosity was also affected by methanol, salt, pH, and temperature (Al-Sadat et al., 2014). Al-Ghamdi et al. showed that the use of VES as a diverting agent is limited by the initial permeability ratio, with diversion being ineffective for a ratio above 10 (Al-Ghamdi et al., 2014); this limitation can be addressed by combining the VES with Foam, enabling acid diversion for permeability contrast of up to 20 (Zhang et al., 2021). Many researchers have developed models to study various aspects of acidizing, including the effects of pH value and calcium concentration on rheological behavior (Liu et al., 2015), the diversion ability and the factors influencing diversion within the rock (Mou et al., 2015), the impact of heterogeneity on wormhole propagation (Liu and Liu, 2016), and the influence of spent acid

on wormhole propagation (Zhu et al., 2022), additionally, an equation was formulated to relate the reaction rate constant, temperature, molecular diffusion coefficient (Li et al., 2018).

2 Equipment and tools

2.1 Core Handling and Flooding Equipment

2.1.1 Core Holders

The core holders used for single and dual-core flooding, shown in Figure 1, are designed to house core samples up to 12 inches in length and 1 or 1.5 inches in diameter. Constructed from Hastelloy, they provide excellent resistance to highly acidic environments. With an operational pressure of up to 10,000 psi, they are ideal for high-pressure experiments.

The novel single-core holder, depicted in Figure 2, is also made of Hastelloy and developed explicitly for acid diversion studies. It accommodates core samples up to 12 inches long and 1.5 inches in diameter. This advanced design features five injection points distributed along its length for precise acid placement and two production outlets for efficient monitoring and flow control. Capable of withstanding up to 10,000 psi and 120°C, it is highly robust and well-suited to challenging experimental conditions.

Figure 1 Core holder used for single and dual-core flooding experiments

Figure 2 The novel core holder

2.1.2 Syringe Pump

The Teledyne ISCO Model 100DX Syringe Pump, Figure 3, is a highly accurate and adaptable tool for high-pressure applications that require a precisely controlled liquid flow rate. With an operating pressure of up to 10,000 psi and a syringe volume of 103 mL, it is ideal for lab experiments such as core flooding and enhanced oil recovery. This pump provides exceptional accuracy, maintaining a flow precision of ±0.3% and ensuring consistent performance across a range of flow rates from 0.01 µL/min to 50 mL/min. It effectively manages aggressive substances, such as acids and brines, constructed from corrosion-resistant materials, including Nitronic 50, PTFE, and Hastelloy C-276. This pump was essential in my laboratory work, used to apply confining pressure, sustain back pressure, and inject required fluids for core flooding experiments.

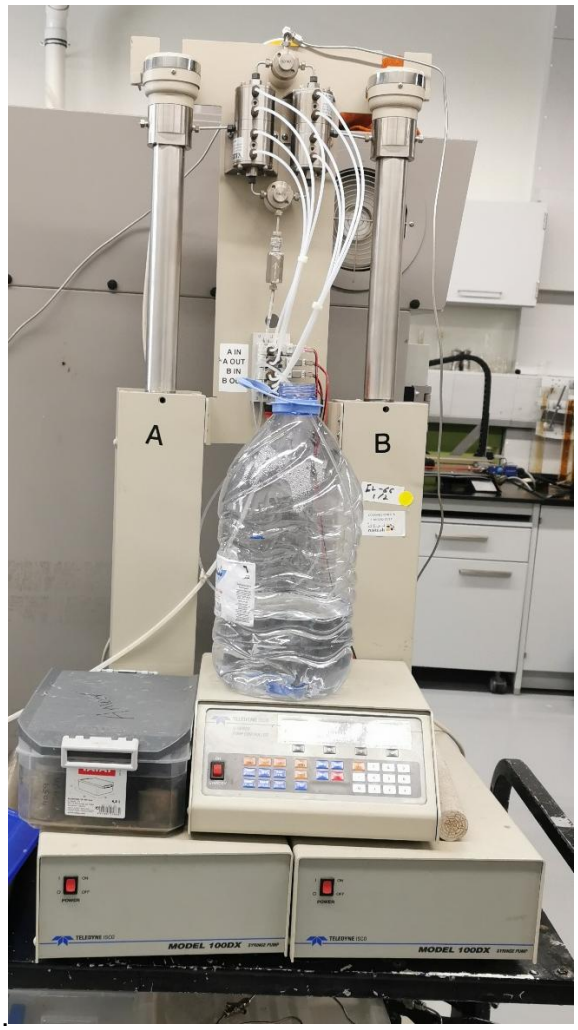

Figure 3 Syringe Pump

2.1.3 Pressure Sensors

The 33X series pressure transmitters, Figure 4, employ digital compensation via a mathematical model to achieve remarkable accuracy of 0.05% FS (±7 psi); within the temperature range of 10 to 40 °C, this corresponds to the total error band. Further measurements and selections may be employed to attain a precision of 0.01% FS. This sensor has been used in my lab work to record the pressure before and after the core holder, allowing me to measure the pressure difference between the inlet and the outlet.

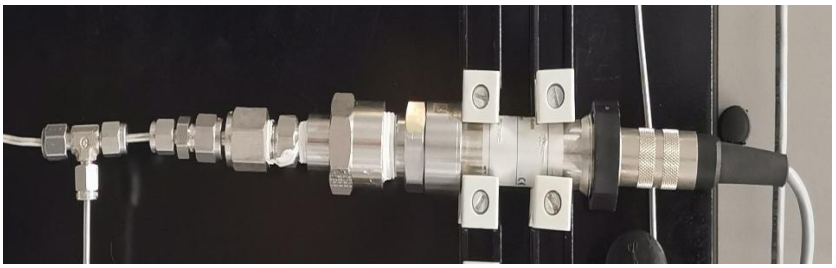

Figure 4 Pressure Sensors

2.1.4 Back Pressure Regulator

The back pressure regulator BPR, shown in Figure 5, is used in core flooding experiments to maintain the back pressure at a specific value on the outlet side of the core holder to simulate the reservoir pressure. It can maintain back pressure even at low flow rates. It is located downstream of the core holder to keep the back pressure. The operation pressure is up to 10000 psi, and the temperature is up to 250 °C. It is commonly made of stainless steel to resist corrosion.

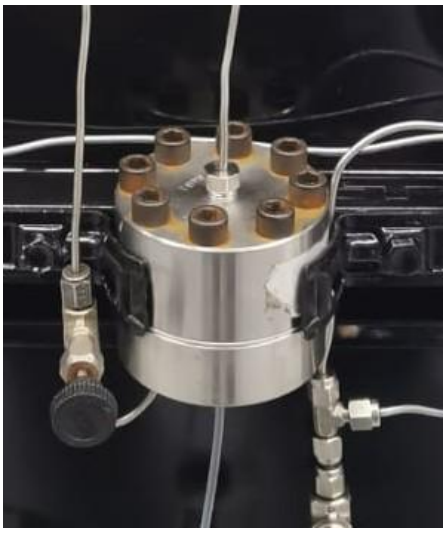

Figure 5 Back pressure regulator

2.1.5 Rheometer

The AMETEK Chandler Engineering Model 5550 HPHT Viscometer, shown in Figure 6, is engineered to determine the viscosity of fluids under high-pressure, high-temperature conditions, simulating downhole environments. It operates at temperatures up to 600°F (316°C) and pressures up to 20,000 psi. This viscometer is designed to deliver real-time viscosity measurements, ensuring accurate shear stress and shear rate analysis in extreme conditions. Its durable design resists corrosive chemicals, facilitating reliable operation in challenging situations.

Figure 6 Viscometer

2.1.6 Overhead Stirrer (Normal and Titanium)

The Silverson L5M Overhead Stirrer (Figure 7) and the IKA T25 Digital Ultra-Turrax Overhead Stirrer (Figure 8) are designed for mixing in laboratory environments. The Silverson LM5 offers accurate speed control up to 25,000 rpm and is ideal for preparing and mixing viscous fluids. It's compact, intuitive design and easy-to-read digital display for an enhanced user experience. The IKA T25 Titanium Overhead Stirrer, with its titanium

components, offers exceptional durability and corrosion resistance, making it ideal for mixing reactive or corrosive solutions. I have used the IKA T25 stirrer in my lab work for mixing HCl with VES and calcium chloride ($CaCl_2$), demonstrating its effectiveness in handling chemically aggressive mixtures. In contrast, the Silverson L5M stirrer is used for regular mixing. Both stirrers feature high-torque motors to ensure reliable performance across a wide range of fluid viscosities. They are commonly used in chemical and materials science research.

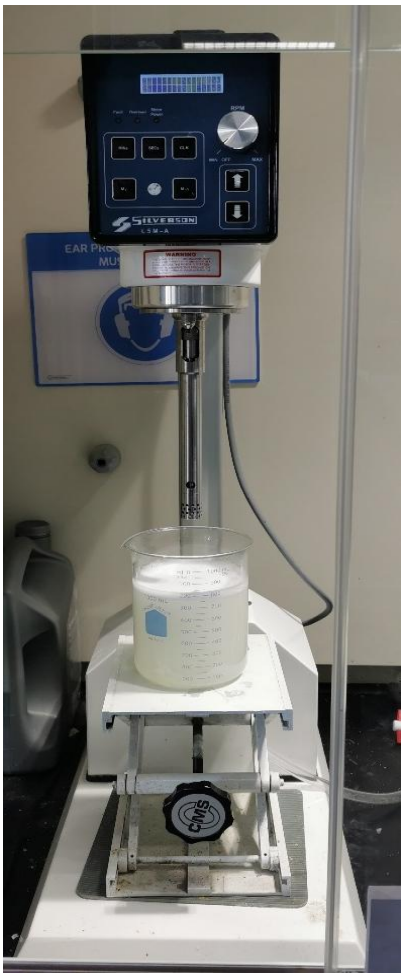

Figure 7 Overhead stirrer

Figure 8 Titanium overhead stirrer

2.1.7 Auto Core Saturator

An Automatic Core Saturator Figure 9 was used in the lab to saturate core samples with fluids under controlled conditions. This apparatus is designed to simultaneously handle up to 3 samples, each 2.5 inches long. The stainless steel core holder can accommodate various core sample sizes and ensures uniform fluid saturation. The system is equipped with a vacuum pump to efficiently remove air from the samples, ensuring complete saturation of the core samples with the required fluid.

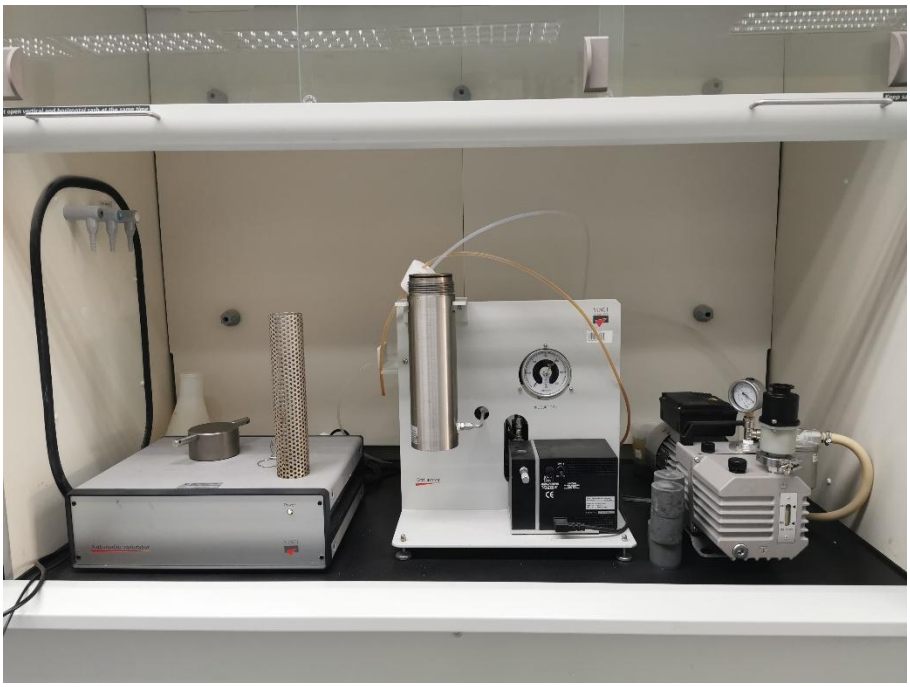

Figure 9 Automatic saturator

2.1.8 Oven

A Memmert drying oven (Figure 10), constructed from stainless steel and equipped with a digital temperature control panel, is required for laboratory and industrial applications. The oven is designed to dry samples efficiently and offers precise temperature control with uniform heat distribution, making it ideal for applications requiring consistent thermal conditions. It can reach temperatures of up to 300°C. Our work has used the oven to dry samples before porosity measurements and for other laboratory applications.

Figure 10 Oven

2.1.9 Sample Collector

Core effluent samples were systematically collected using a sample collector during flooding. These samples were subsequently analyzed to determine calcium ion concentration.

2.1.10 Hand Mixer

Hand Mixer (Figure 11) is used for hand-mixing carbonic acid by combining water and CO_2. The process typically takes 10 minutes, ensuring that the CO_2 is fully dissolved in the water to form a uniform carbonic acid solution.

Figure 11 Hand mixer

2.1.11 Core Cutter

The Mecatome ST310 (Figure 12) is a high-precision core-cutting machine designed to prepare core samples to the desired length. It is equipped with a cooling system to minimize heat generation during cutting and reduce dust, ensuring sample integrity and a safer working environment.

Figure 12 Core cutter

2.1.12 Toluene Cleaning Apparatus

The apparatus depicted in Figure 13 is a Toluene Cleaning Apparatus, designed to cleanse and remove impurities from core samples using toluene as the solvent. The device ensures effective and thorough cleaning by integrating a heating system and solvent recirculation.

Figure 13 Toluene Cleaning Apparatus

2.2 Advanced Analytical Equipment

2.2.1 Porosity Measurement Tools

The porosity of the core sample was measured using a Helium Porosimeter (AP-608), Figure 14, which operates by injecting helium gas into the core sample to determine the pore volume. Porosity measurements were conducted before and after core flooding to evaluate changes in porosity resulting from the acid reaction with calcite. The porosimeter can measure the porosity of core samples with 1 inch or 1.5 inch diameters and lengths of up to 12 inches.

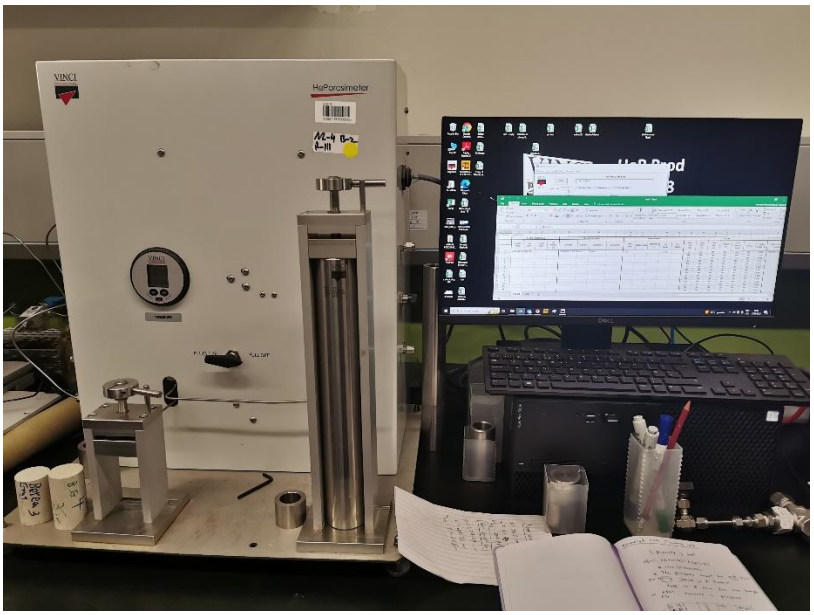

Figure 14 Porosimeter

2.2.2 Permeability Measurement Tools

The samples' permeability was initially measured using an auto-scan device (Figure 15) to obtain a rough estimate of core permeability. This method was chosen because the auto-scan can measure the permeability of more than 30 samples simultaneously. Afterward, the samples were clustered based on the auto-scan results, and their permeability was measured more accurately using the Liquid Permeameter LP-100A (Figure 16).

Figure 15 auto scan

Figure 16 Liquid permeameter

2.2.3 Nuclear Magnetic Resonance (NMR)

NMR (Figure 17) is a powerful, non-destructive tool widely used at laboratory and field scales as a wireline logging tool. NMR measurements detect the presence of hydrogen protons. During NMR analysis, it is possible to detect the amounts and characteristics of the fluids present, as well as the diameters of the pores that contain them. NMR measurements were conducted before and after acidizing to determine the core sample's T2 relaxation time and diffusion tortuosity, and to assess the effect of carbonated water on the pore-size distribution. Before the NMR measurement, the cores were dried in the oven

for 24 hours at 60°C, vacuumed for three hours, and then saturated with DI water at 2000 psi for 24 hrs.

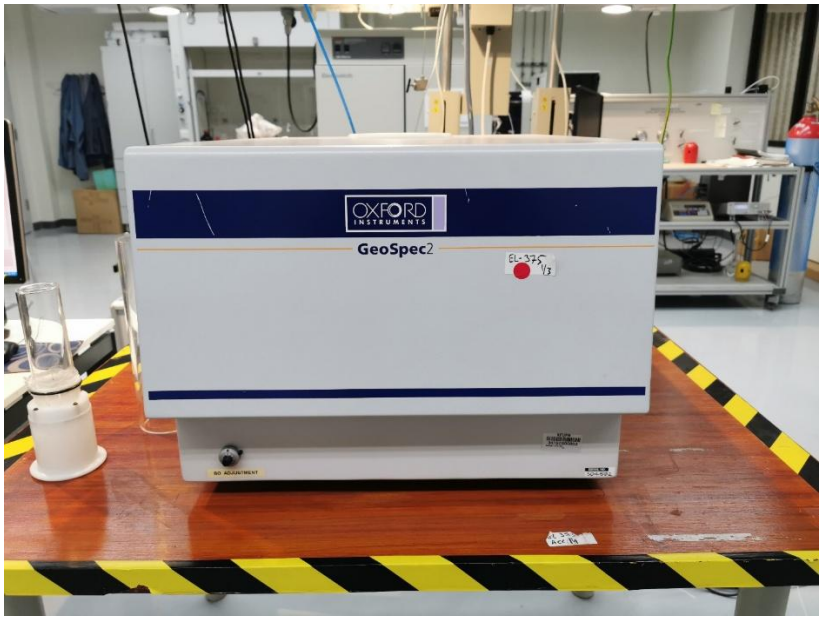

Figure 17 Nuclear Magnetic Resonance

2.2.4 CT Scan Computed Tomography (CT) Scan

Computed tomography is a non-invasive method that utilizes X-rays to produce a sequence of 2D cross-sectional images of the rock sample. The program can generate a 3D model of the sample from the pictures. Software may analyze images to identify the rock sample's porosity, permeability, mineral composition, wormhole presence, and pore-size distribution. The CT scan comprises four components: an X-ray source system, a mechanical motion system, a data-gathering system, and an image production system. The wormhole length can be objectively determined by using a standard curve. The X-ray source emits X-rays that penetrate and weaken as they pass through the rock, a process influenced by mineral density. A detector captures the weakened X-rays to generate a projected image. The rock sample is rotated by 180 or 360 degrees to create a sequence of projection images, as described. In our study, the CT scan was conducted after the flooding experiments to visualize the wormhole and estimate its volume using PerGeos software.

Due to the limitation of micro-CT, a medical CT scan was used for long samples measuring 12" in length to analyze the wormhole structure. The Toshiba Aquilion CT scanner was employed for non-destructive measurements, enabling visualization of the pore structure and network within the core samples. This scanner provides a spatial resolution of 0.3-0.6 mm and operates at 80–140 kVp. It is equipped with software for image reconstruction. The

Toshiba scanner features a 150 cm table, making it suitable for measuring cylindrical core samples up to 70 cm long.

Figure 18 Medical CT scan

Figure 19 Micro CT scan

2.2.5 Inductively Coupled Plasma (ICP) Spectrometer

Inductively coupled plasma, ICP, represents a powerful method of investigation for trace component detection in all types of samples using the combined principles of atomic emission spectroscopy and mass spectrometry. Calcium, a common element in carbonate rocks, plays a crucial role in influencing the efficiency of acid treatments. Accurate

monitoring of calcium content is imperative for optimizing acid formulation and predicting reservoir response.

The Shimadzu ICPE-9800 Series Inductively Coupled Plasma Emission Spectrometer (ICP-OES) is a preferred analytical instrument for elemental analysis due to its high sensitivity, precision, and ability to simultaneously analyze multiple elements. ICP-OES is especially effective for detecting calcium, a significant component of carbonate minerals such as calcite and dolomite, which constitute the majority of carbonate reservoirs.

During matrix acidizing, the dissolution of calcium-rich minerals significantly alters rock permeability and porosity, ultimately influencing reservoir productivity. Accurate measurement of calcium levels before and after acid treatment is critical for evaluating the effectiveness of the stimulation process.

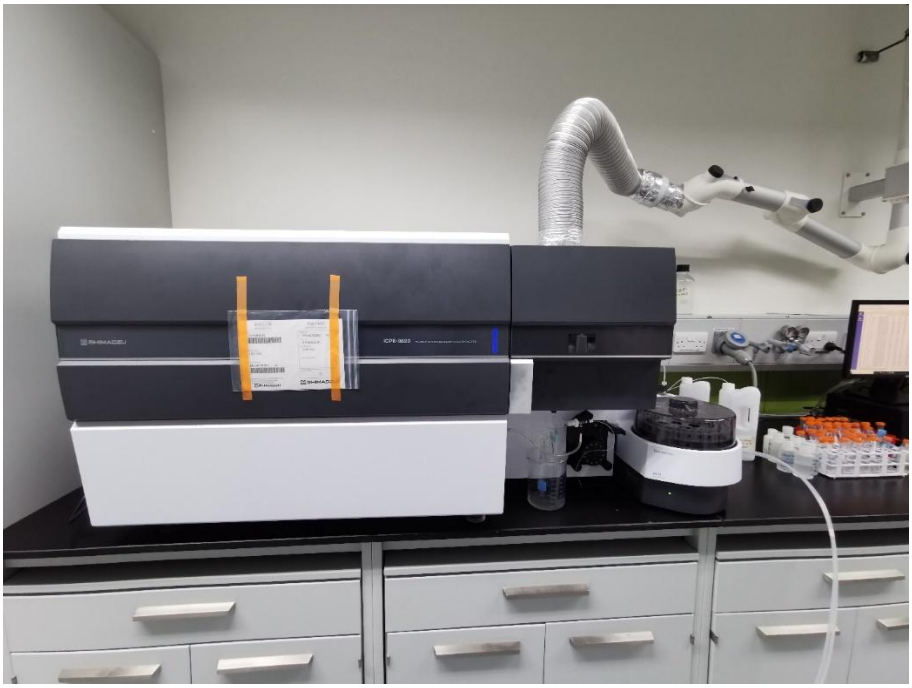

Figure 20 Inductively Coupled Plasma Spectrometer

3 Optimization of Injection Rates Using Carbonic Acid

3.1 Introduction

This chapter explores the optimization of carbonic acid injection rates during matrix acidizing in carbonate formations, emphasizing their effects on wormhole formation, dissolution efficiency, and changes in rock petrophysical properties. Indiana limestone core samples, with 14% to 16% porosity and permeability from 7 to 12 mD, were selected for flooding experiments at varying injection rates (0.5, 1, 2, and 5 cm^3/min correspond to 3, 6, 12, 30 x10-5 m^3/h, respectively) to identify the optimal injection rate Carbonic acid was prepared by mixing 70% DI water with 30% sc-CO_2 under conditions of 1500 psi and room temperature.

Advanced tools were utilized to analyze the outcomes. Micro-CT scanning provided visualizations of wormhole patterns, enabling measurements of wormhole dimensions and calculation of the optimum Damköhler number. Inductively coupled plasma (ICP) analysis quantified calcium concentrations in effluent samples collected at different time points, providing insights into acid dissolution behavior. Two analytical models were employed to determine the optimal injection rate. The first model proposed by Wang et al., based on pore volumes to breakthrough (PVBT) as a function of injection rate, identified 2 cm^3/min as optimal, with a corresponding PVBT of 22 (Wang et al., 1993). The second model, proposed by Buijse and Glasbergen, correlating PVBT with interstitial velocity (Vi), yielded an optimal injection rate of 1.7 cm^3/min, equivalent to an interstitial velocity of 1 cm/min (Buijse and Glasbergen, 2005). Notably, the calculated Damköhler number deviated significantly from the established value of 0.29 proposed by Fredd and Fogler, indicating unique dynamics in carbonic acid reactivity (Fredd and Fogler, 1999, 1998).

This introduction establishes the foundation for understanding the behavior of carbonic acid in matrix acidizing applications. It highlights its potential as a sustainable alternative to conventional acids, thereby enhancing well productivity in carbonate reservoirs.

3.2 Experimental Setup and Materials

3.2.1 Samples

Four core samples from Indiana limestone (outcrop formation), 2.5" in length and 1.5" in diameter, were used in this study. The experiments were conducted at 60 °C and 2000 psi backpressure, which represents the formation reservoir pressure. The initial porosity of the

sample was measured using a helium porosimeter (AP-608), shown in Table 1. The liquid permeability was measured, yielding an initial permeability of around 8-12 mD. XRD measurements indicate that the Indiana limestone is 100% calcite. A shrink tube was used to cover the core and to avoid cross-flow from the core sides.

Table 1 Core sample characteristics and properties

Core No.	D (cm)	L (cm)	Porosity (%)	Permeability (mD)
IL1	3.78	6.468	15.41	12
IL2	3.77	6.336	14.95	8
IL3	3.767	6.595	12.99	9.7
IL4	3.771	6.518	15.20	11.9

3.2.2 Carbonic Acid Preparation

In this study, carbonic acid was prepared for testing by mixing 30% CO_2 and 70% DI water using a high-pressure/high-temperature accumulator, as shown in Figure 21. The procedure involved filling accumulator No. 2 with CO2 until the pressure reached 650 psi, followed by precise filling of accumulator No. 1 with 700 cm^3 of DI water. Both accumulators were then connected to the isco pump according to the schematic in Figure 21, ensuring proper alignment. The connection between the accumulators was closed, valve No.2, and the pump was set to constant pressure mode to reach 650 psi, with close monitoring to prevent over pressurization. Subsequently, the pump was switched to constant flow rate mode, and the connection between the accumulators and valve No. 2 was opened to initiate DI water transfer to the CO_2 accumulator at a controlled rate of 50 cm^3/min until the targeted volume of 750 cm3 was reached. After that, disconnect the accumulator containing the resulting carbonic acid (accumulator No. 2) and manually mix for 10 minutes to ensure thorough incorporation of CO_2 into the DI water. Finally, the prepared accumulator was placed in an oven set to 60°C to allow sufficient time for equilibration and to reach the specified temperature for optimal performance.

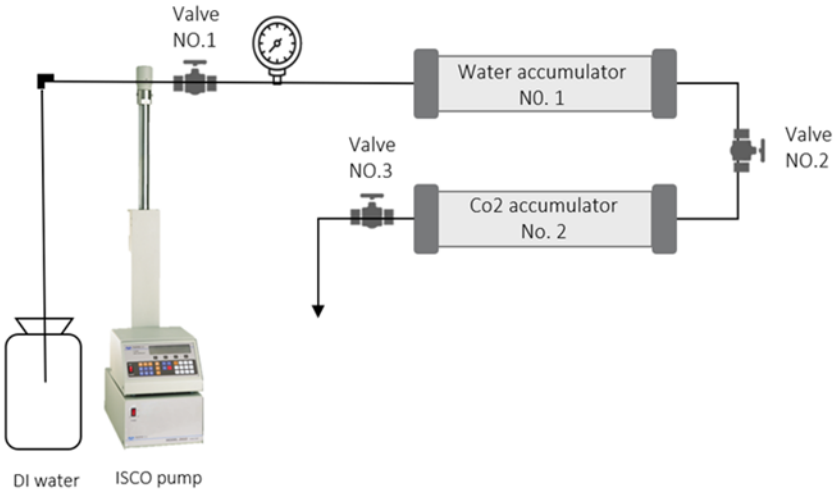

Figure 21 Schematic diagram of the carbonic acid preparation system

3.2.3 Experimental Procedure

As shown in Figure 22, the experimental procedure begins by measuring two critical petrophysical properties: porosity, which determines the void space within the rock, and permeability, which measures the ability of fluids to flow through the rock. The core sample's dimensions were measured with a caliper, weighed in a dry state, and porosity was measured with a helium porosimeter; permeability was roughly estimated using the Auto scan. The core sample was dried at 100°C overnight in an oven. Vacuum the core sample for 3 hours, then saturate it with DI water at 2000 psi for 24 hours. Core flooding followed, as detailed in the core flooding procedure section, during which the differential pressure (DP) and pore volume to breakthrough (PVBT) were recorded, along with the collection of effluent samples for ICP analysis. The core samples were dried in the oven at 100° C for 24 hours. Computerized Tomography (CT) scans were then used to visualize the wormhole and measure its size. As the last step in the laboratory work, porosity was measured after acidizing, and effluent samples collected during core flooding were analyzed by Inductively Coupled Plasma (ICP).

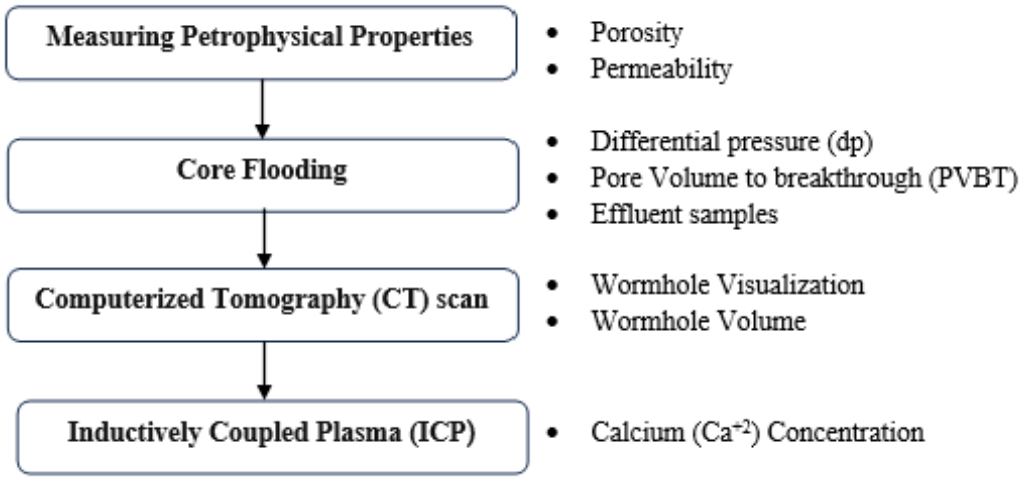

Figure 22 The experimental workflow outlined above integrates various techniques to study flooding in carbonate formations using carbonic acid

3.2.4 Core Flooding Setup

Figure 23 shows the schematic diagram of the flooding system used for Indiana limestone core flooding experiments using carbonic acid. The operating pressure and temperature of the system are 10,000 psi and 150 °C, respectively. The core holder and lines are made of high-resistance material (Hastelloy) for acid at high temperatures, which is a consolidated description of the core flooding system components and their functions. The HP/HT Core holder, made of Hastelloy, resists acidity and houses the core sample. Before the experiment, the core is loaded inside and exposed to 3500 psi confining pressure. The core holder inlet is connected to two DI water and carbonic acid accumulators. The outlet is linked to the production line for effluent sample collection. A syringe pump applies 2000 psi back pressure. The isco pump injected carbonic acid at varying flow rates (0.5, 1, 2, and 5 cm^3/min). The pressure transducer measures the pressure difference between the inlet and outlet. Lastly, the sample collector collects effluent samples.

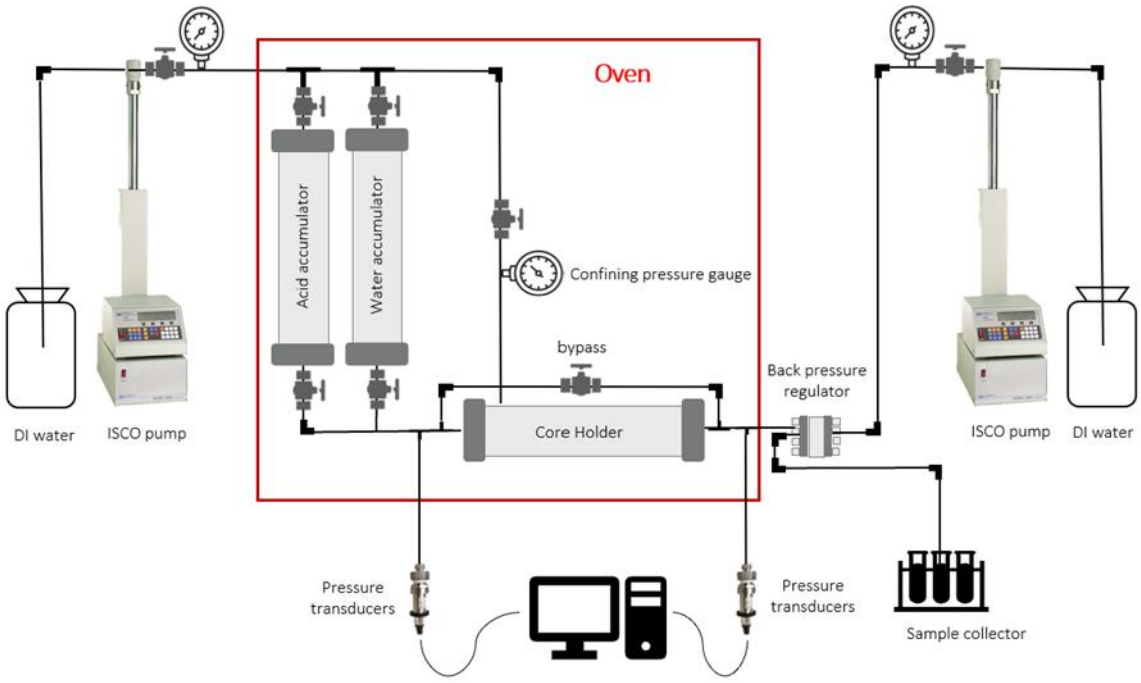

Figure 23 Schematic diagram of a single-core flooding system

3.2.5 Core Flooding Procedure

At the outset, the core flooding experiments started by covering the core sample with a shrink tube, loading it into the core holder, and placing it in the oven. A confining pressure of 3500 psi and a back pressure of 2000 psi were applied. Before each experiment, DI water was pumped at 1, 2, 4, and 8 cm3/min, respectively, and the differential pressure was recorded to calculate the core sample's water permeability before flooding. Injection experiments were performed using an HP/HT isco pump at four different injection rates (0.5, 1, 2, and 5 cm^3/min). The injection was stopped after a breakthrough occurred. Effluent samples were collected at each of the two-pore volumes for the ICP test to measure the Ca^{+2} concentration.

3.3 Results and Analysis

3.3.1 Pressure profiles

Four core flooding experiments were conducted to determine the optimal injection rate (IR) of carbonic acid in carbonate formation. The injection rate is the flow rate at which acid is injected into the core sample. The specifics of each experiment are outlined in Table 2. In the initial experiment, conducted at a 0.5 cm^3/min rate, the time to breakthrough (TBT) represents the point at which pressure drop across the core sample reaches zero, indicating

the acid has successfully penetrated the core sample, was observed after 14.8 hours (890 minutes), coinciding with a breakthrough pore volume (PVBT) of 40.2, as depicted in Figure 24. Subsequently, the second experiment was performed at a rate of 1 cm^3/min. Figure 25 illustrates that the pressure drop across the core sample reached zero after 6.3 hours (379 minutes), with a PVBT of 39.7. The third experiment involved a flow rate of 2 cm^3/min. As depicted in Figure 26, the pressure decreased across the core sample, reaching zero after 1.9 hours (116 minutes), corresponding to a PVBT of 21.9. Finally, the fourth experiment was conducted at a flow rate of 5 cm3/min. As shown in Figure 27, the pressure drop across the core sample ceased after 1.5 hours (89 minutes), with a breakthrough pore volume (PVBT) of 41. These results provide valuable insights into the relationship between injection rate and breakthrough behavior, which is crucial for optimizing carbonic acid injection in carbonate formations.

Table 2 The carbonic acid volume consumed at different injection rates

Core No	IR (cm^3/min)	TBT (min)	PV (cm^3)	Volume (cm^3)	PVBT
IL4	0.5	890	11.065	445	40.2
IL3	1	379	9.551	379	39.7
IL2	2	116	10.59	232	21.9
IL1	5	89	11.218	445	41.0

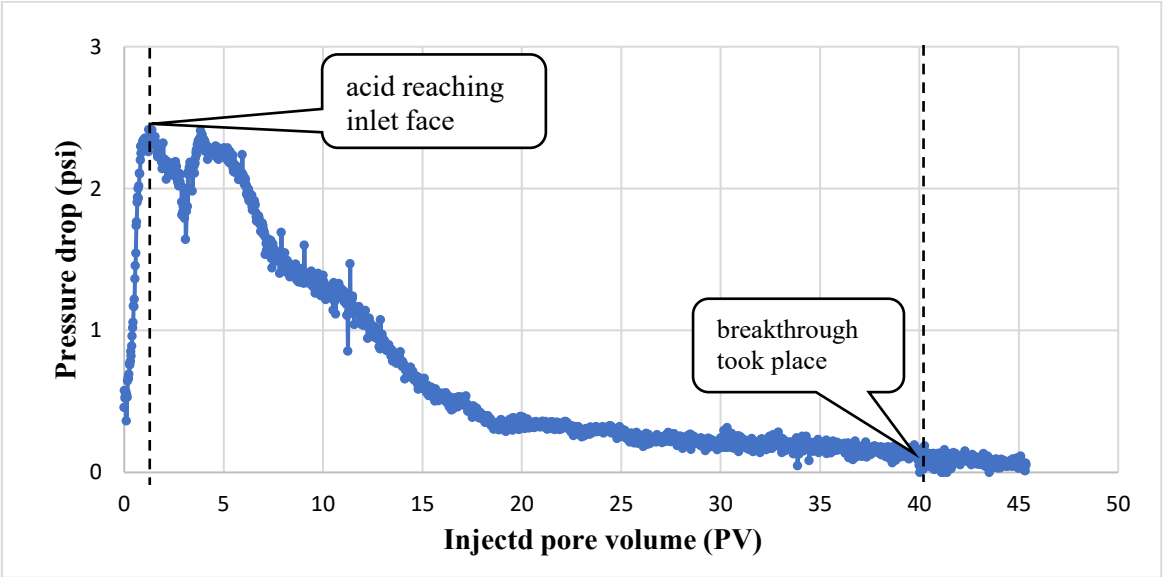

Figure 24 Pressure drop a cross IL4 sample with 0.5 (cm^3/min) injection rate

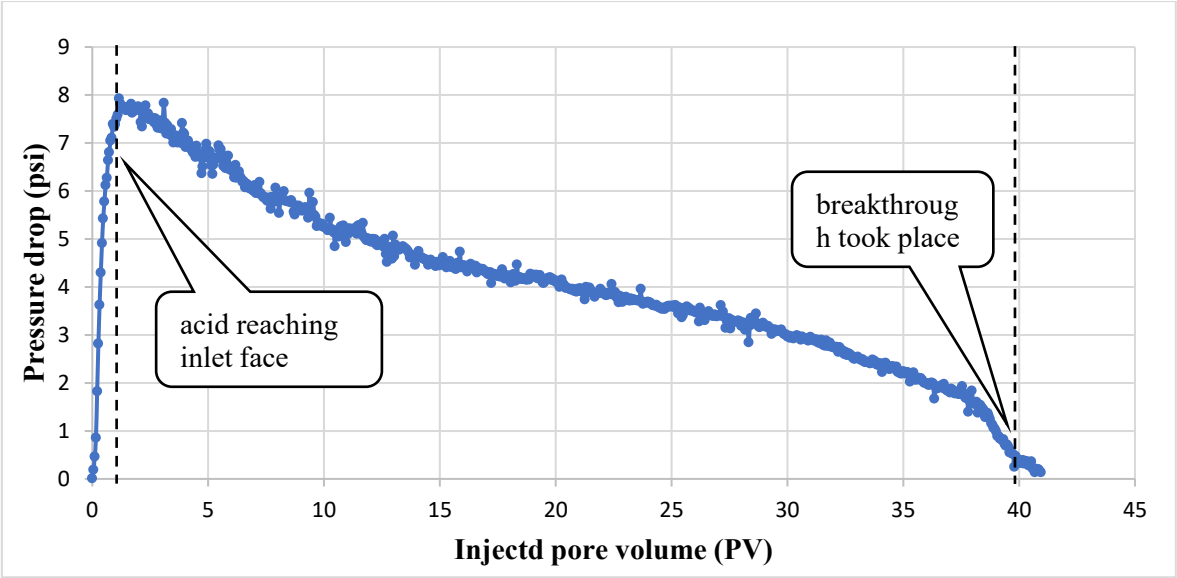

Figure 25 Pressure drop a cross IL3 sample with 1 (cm^3/min) injection rate

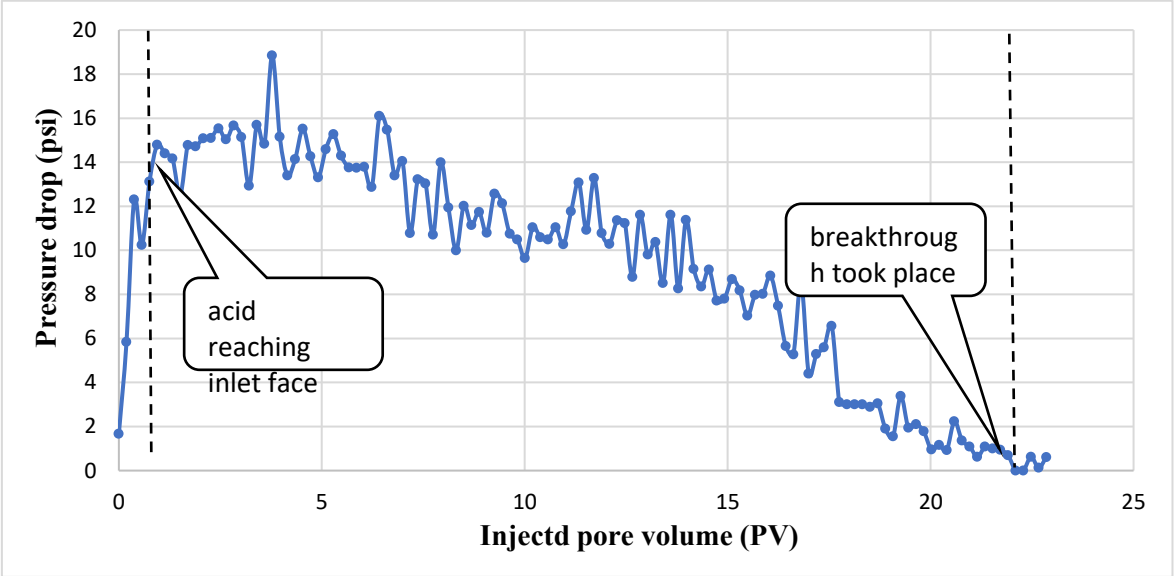

Figure 26 Pressure drop a cross IL2 sample with 2 (cm^3/min) injection rate

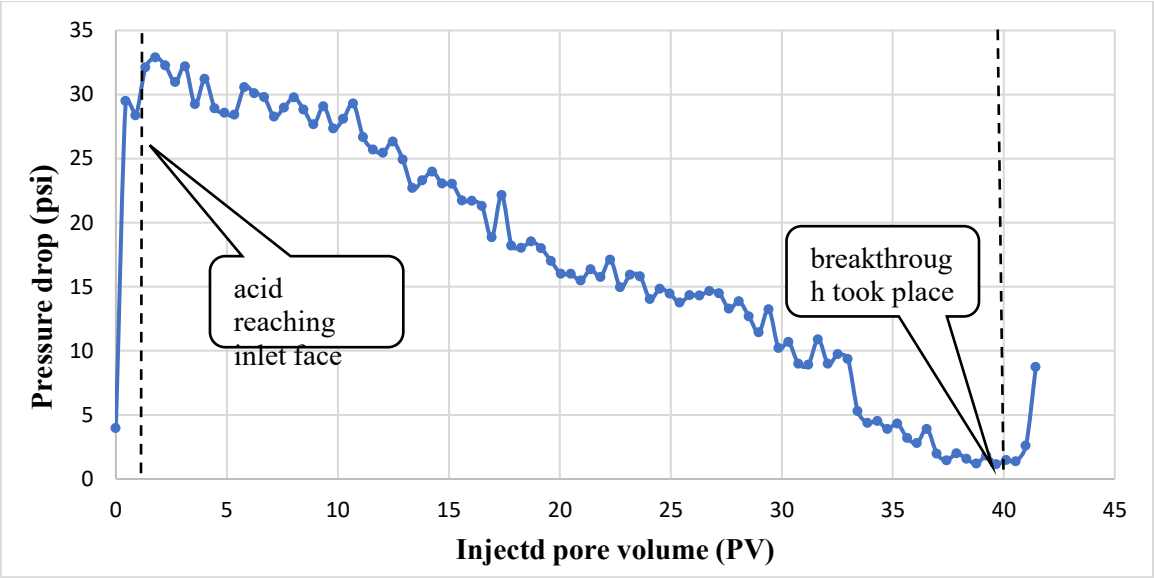

Figure 27 Pressure drop a cross IL1 sample with 5 (cm^3/min) injection rate

3.3.2 Optimum injection rate

Wang, for the first time, studied the investigation into the influence of injection rate, particularly the determination of the optimal rate. He established that the optimal injection rate is characterized by generating the most efficient wormhole with the least PVBT (Wang et al., 1993). Our study constructed the curve using four injection rates (0.5, 1, 2, and 5 cm^3/min). The pore volume to breakthrough ($PVBT_{experiments}$), as shown in Table 3, can be estimated using the following expression. (Alghamdi, 2011; Cao et al., 2021):

$$PVBT_{experiments} = \frac{IR \,.\, TBT}{PV} \qquad (1)$$

Where $PVBT_{experiments}$ are the acid volume consumed until the breakthrough (dimensionless), IR is the injection rate of acid (cm^3/min), TBT is the time to break through (min), and PV is the pore volume of the sample (cm^3).

Based on our experimental results, the optimum injection rate is 2 cm^3/min, as shown in Figure 28, where breakthrough occurred with the minimum acid volume. This indicates that, at this rate, the acid is used more efficiently to form a dominant wormhole pathway. Therefore, 2 cm^3/min is considered the optimal injection rate as it provides the best balance between effective wormhole formation and minimal acid consumption, in agreement with wangs finding.

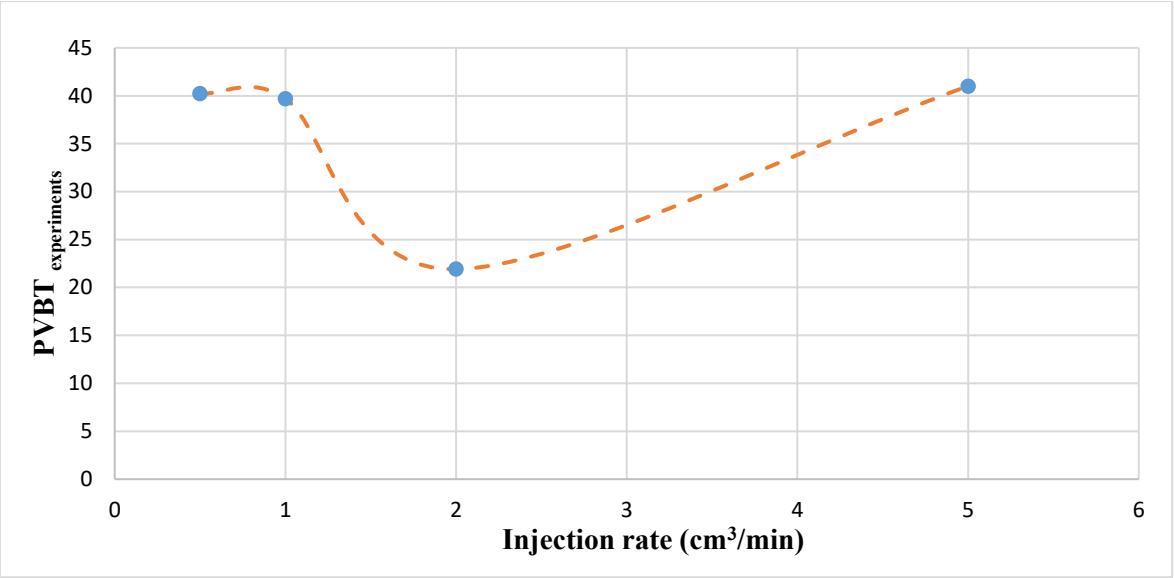

Figure 28 Experimental optimum injection rate graph

Another model developed by Buijse and Glasbergen States that the wormhole's progression rate is represented by the injection rate of acid or precisely dependent on the acid velocity within the pores (interstitial velocity), as shown in the following formula (Buijse and Glasbergen, 2005):

$$V_i = \frac{IR}{\frac{1}{4}\pi d_{sample}^2 \cdot \varphi} \quad (2)$$

Where Vi is the interstitial velocity (cm/min), representing the average velocity of acid within the sample pores, IR is the injection rate of acid (cm^3/min), d is the sample diameter, and φ is the sample porosity.

The relationship between the pore volume to breakthrough ($PVBT_{model\ fit}$) and wormhole growth rate (V_{wh}) (cm/min) is as follows:

$$PVBT_{model\ fit} = \frac{V_i}{V_{wh}} \quad (3)$$

Where the expression of wormhole growth is :

$$V_{wh} = W_{eff} \cdot V_i^{\frac{2}{3}} \cdot B(V_i) \quad (4)$$

W_{eff} is the efficiency factor of the wormhole $(cm/min)^{1/3}$, $B(V_i)$ is illustrating the compact dissolution regime.W_{eff} and $B(V_i)$ This can be estimated by the following formulas, respectively:

$$W_{eff} = \frac{V_{i-opt}^{1/3}}{PVBT_{-opt}} \quad (5)$$

$$B(V_i) = \left(1 - \exp\left(-W_B \cdot V_i^2\right)\right)^2 \quad (6)$$

W_B is constant in the wormhole model $(cm/min)^{-2}$, can be obtained by the following formula:

$$W_B = \frac{4}{V_{i-opt}^2} \quad (7)$$

After determining all the parameters, the curve can be constructed by plotting the PVBT model fit vs. interstitial velocity Vi. Table 3 presents the calculations for this study, and the results are plotted in Figure 29. As we can see from the table, the optimum interstitial velocity and the optimum injection rate according to this model are 1 (cm/min) and 1.7 (cm^3/min), respectively.

Table 3 PVPT fitting parameters (Buijse and Glasbergen model)

Core No.	d (cm)	φ (%)	q (cm^3/min)	PVBT (experiments)	Vi (cm/min)	Weff $(cm/min)^{1/3}$	W_B $(cm/min)^{-2}$	B (vi)	PVBT (model fit)
IL1	3.79	0.154	5	41.0	2.885	0.018	2.79	1	52
IL2	3.77	0.149	2	21.9	1.197			0.96	22
IL3	3.83	0.151	1	39.7	0.573			0.36	29
IL4	3.83	0.151	0.5	40.2	0.286			0.04	124

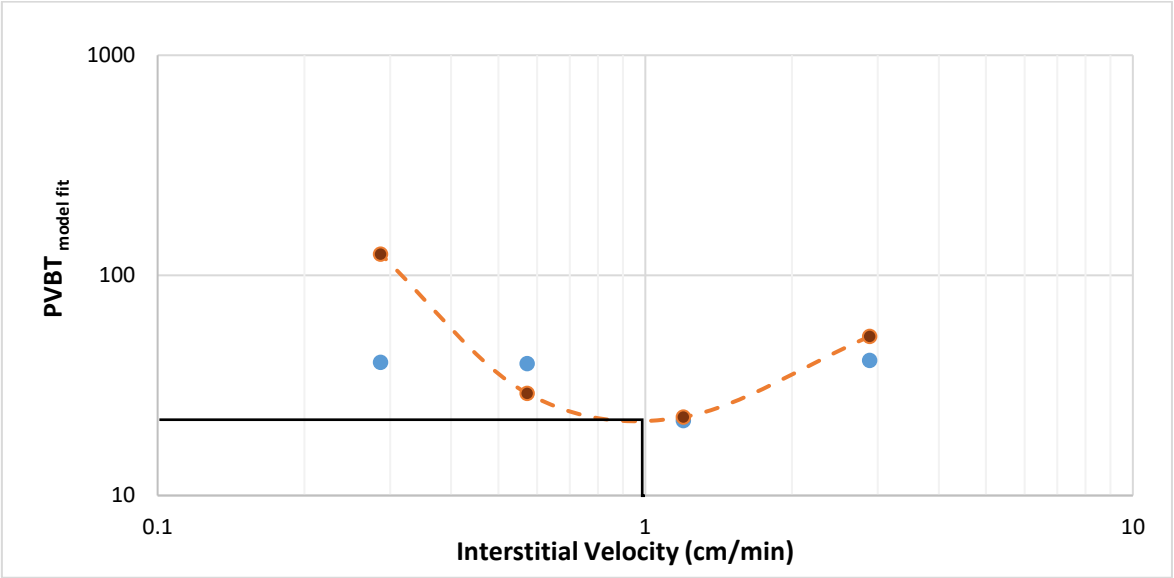

Figure 29 Optimum interstitial velocity based on the Buijse and Glasbergen model

When considering the outcomes of the two methods proposed by Wang and the one proposed by Buijse and Glasbergen (2005), it is evident that both approaches aim to identify the injection rate to achieve a breakthrough with the minimum acid volume. Wang's method utilizes experimental observation and curve fitting to determine the optimal injection rate. In this study, the rate of 2 cm^3/min was established based on experimental data.

However, Buijse and Glasbergen's model presents a more detailed and systematic comprehension of how the injection rate, interstitial velocity, and wormhole growth are interconnected. Their method produces a different and more accurate injection rate. Based on our experiments, the optimum injection rate was 1.7 cm^3/min, with an optimal interstitial velocity of 1 cm/min. These values are obtained through thorough calculations that consider

various factors, including sample diameter, porosity, injection rate, and pore volume to breakthrough.

As compared with several researchers have investigated the optimal injection rates for various acid treatments in limestone formations, revealing a spectrum of outcomes (Daccord et al., 1989; Fredd and Fogler, 1999; Glasbergen et al., 2009; Punnapala et al., 2014). For example, one study determined that employing 3.4 wt% HCl at 75°C required an injection rate of 3.5 cm^3/min to achieve optimal results. However, at 50°C, this rate dropped significantly to 1 cm^3/min (Wang et al., 1993). In contrast, employing foam acid, comprising 15 wt% HCl and 2 vol% foaming agent, at 60°C significantly reduced the optimal injection rate to 1.5 cm^3/min (Cao et al., 2021). Another investigation exploring the efficacy of 10% acetic acid at 121°C indicated a further decrease in the optimal injection rate to 1.2 cm^3/min (T. Huang et al., 2000). Conversely, the use of 10 wt% methanol sulfamic acid (MSA) at 80°C resulted in an increased injection rate of 6 cm^3/min, which notably dropped to 2 cm^3/min at room temperature (Ortega, 2015). Interestingly, gelled acid, in-situ gelled acid, and regular acid (all at 5 wt% HCl) exhibit the same optimal injection rate at 120°C: 7 cm^3/min, indicating that changing the acid type doesn't affect the optimal injection rate. However, the required breakthrough volume differed significantly across treatments (Gomaa and Nasr-El-Din, 2010).

3.3.3 Damköhler Number

The Damköhler number is the ratio of the overall rate of acid dissolution to the rate of acid convection (Elsayed et al., 2023). Fredd and Fogler (1999) first introduced the Damköhler number by conducting different theoretical and experimental investigations on a wide range of acid systems, and they observed that the optimum Damköhler number was 0.29. The optimum Damköhler number represents the optimum balance between reaction rate and transport rate at which a minimum number of pore volumes is required for channel breakthrough (Fredd and Fogler, 1999). In matrix acidizing, the Damköhler number is essential in determining the dissolution patterns of carbonate formation. Two cases of the Damköhler number formula exist based on the reaction rate. The first case is mass-transfer-limited, indicating that the movement of carbonic acid (H_2CO_3) from the solution to the calcite surface (where the solid and liquid meet) occurs more slowly than the reaction on the surface. The other case is reaction-rate-limited, indicating that the surface reaction rate (calcite dissolution) is the slowest step (Fredd and Fogler, 1998; Peng et al., 2015). The dissolution kinetics of calcite ($CaCO_3$) in carbonic acid (H_2CO_3) under varying conditions of temperature and pressure were investigated by using a rotating disc technique to study the effect of temperature and pressure on the reaction rate constant, where the carbonic acid

reacts with calcite and results in Ca^{+2} and HCO^{3-} as in the following formula (Peng et al., 2015):

$$CaCO_3 + H_2CO_3 \xrightarrow{K_r} Ca^{2+} + 2HCO_3^- \quad (8)$$

The following equation determines the Damkohler number (N_{Da}) for the reaction rate-limited case (Fredd and Fogler, 1999):

$$N_{Da(rxn)} = \frac{\pi \nu d L k_r}{q} \quad (9)$$

Where N_{Da} is the Damkohler number (dimensionless), k_r is the reaction rate constant (cm^2/s), ν is a variable that is influenced by the carbonate core (-), L is the wormhole length (cm), d is the wormhole diameter (cm), and q is the injection rate (cm^3/min).

The reaction-rate-limited case was used in this study because calcite dissolution by carbonic acid is controlled by surface reaction rather than mass transfer, given carbonic acid's weaker behavior compared to HCl.

In this study, The calculation of the Damkohler number is shown in Table 4, where the wormhole length and diameter can be obtained from the CT scan result for each injection rate, while the reaction rate constant can be obtained by using the chart developed by Peng et al., Figure 30, based on the temperature used in our experiment 333.15 K and 13.79 MPa, by crossing the inverse of temperature (1/T = 0.003 K) with the solve based on the pressure 13.8 MPa representing by shape triangle, we can get the ln Kr value from y-axis (Peng et al., 2015).

Table 4 The calculation of the Damkohler number

sample	Core length (mm)	L (cm)	Wormhole volume (mm^3)	d (cm)	q (cm^3/min)	q (cm^3/sec)	N_{Da}
IL1	64.68	3.234	495	0.312	5	0.0833	0.0031
IL2	63.36	3.168	209	0.205	2	0.0333	0.0050
IL3	65.95	3.2975	515	0.315	1	0.0166	0.0162
IL4	65.18	3.259	617	0.347	0.5	0.0083	0.0354

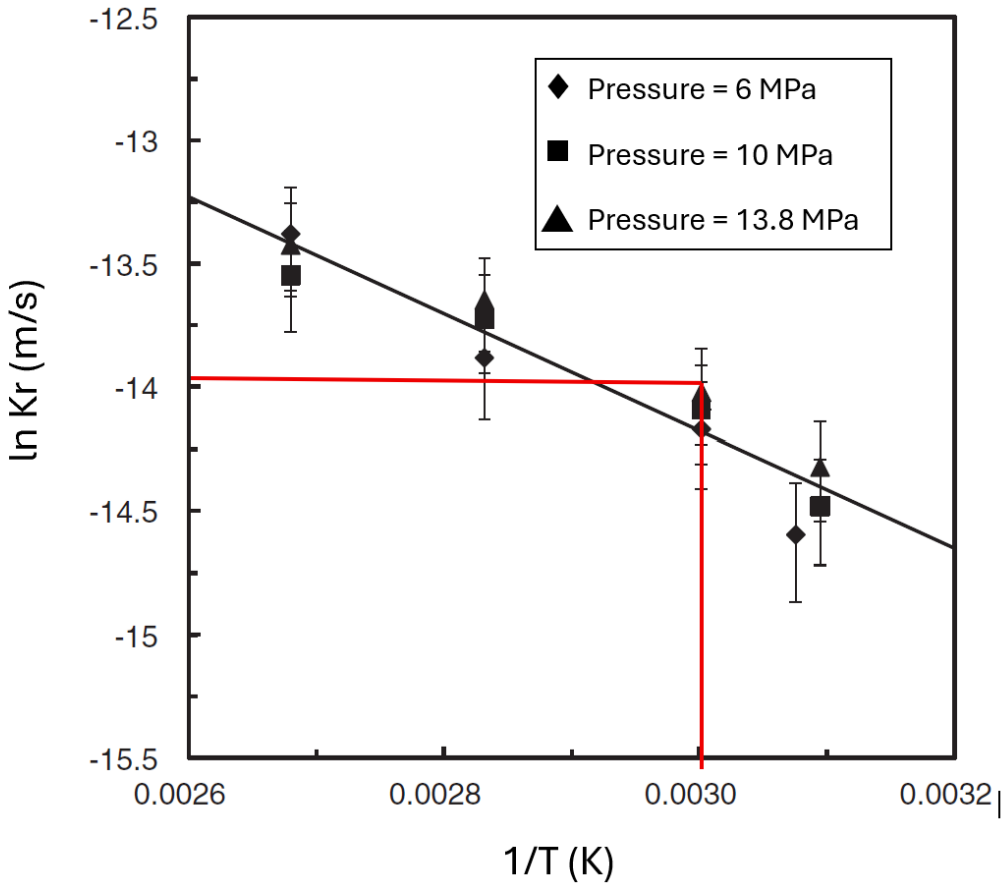

Figure 30 The impact of temperature on the reaction rate constant of calcite dissolution in carbonic acid (Peng et al., 2015)

Figure 31 displays a plot of the normalized number of pore volumes required to break through as a function of the inverse of the Damkohler number developed by Fredd and Fogler and the result obtained in this study. The observation that all points plotted from the experimental results are exclusively located on the right side of the optimum Damköhler number, rather than being distributed around it as expected, motivates further investigation into this phenomenon. Based on this study, the optimum Damköhler number for carbonic acid was 0.005. Fred and Fogler (1999), however, conducted their work using hydrochloric acid, formic acid, acetic acid, and other acids across a range of carbonate lithologies and didn't include carbonic acid in the analysis.

In contrast, this study focuses on carbonic acid, which is a significantly weaker acid. The slower dissolution kinetics and lower reactivity of carbonic acid shift the balance between reaction rate and transport rates, resulting in a much smaller optimum Damköhler number (0.005). This deviation from the value reported by Fred and Fogler can be attributed to the fundamentally weaker acid strength and slower reaction rate of carbonic acid with calcite.

Comparable findings have been reported in ongoing research at King Fahd University of Petroleum and Minerals, where experiments involving carbonic acid under different lithologies and salted carbonic acid yielded results consistent with those in this study. This

similarity in results suggests that the shift in optimum Damköhler number is a consistent behavior of carbonic acid rather than an experimental error.

Nevertheless, further investigation is required to strengthen these conclusions. Future work will aim to collect and consolidate all available experimental data on carbonic acid-based matrix acidizing, enabling the development of a generalized correlation of optimum Damköhler number for carbonic acid under a wide range of lithology and operational conditions.

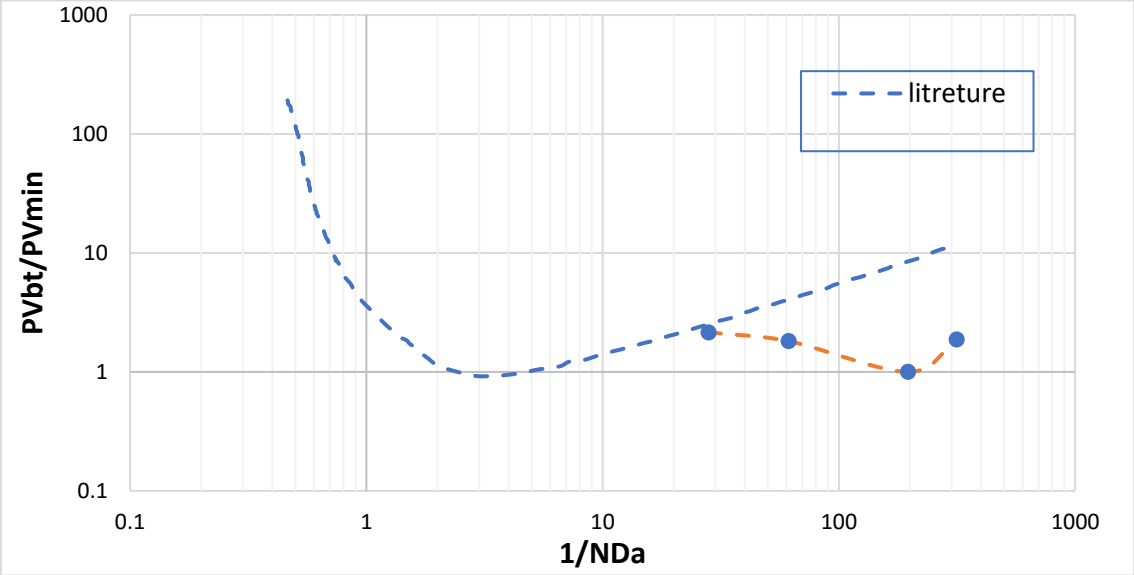

Figure 31 Plot the normalized number of pore volumes required to achieve a breakthrough against the reciprocal of the generalized Damkohler number of carbonic acid

3.3.4 Wormhole Morphology Analysis

A computerized tomography micro-CT scan was conducted to visualize the wormholes and estimate the volume created by acid injection after performing the single flooding experiments. The core samples were dried inside the oven at 100° C overnight. Figure 32 shows the samples' wormholes visualized using Pergeous software. Based on CT scan results, the wormhole radius (r_{wh}) can be calculated by using the following formula:

$$r_{wh} = \sqrt{\frac{V_{wh}}{3.14L}} \qquad (10)$$

V_{wh} is the wormhole volume estimated by CT scan (mm^3), L is the core length (mm)

At a low injection rate of 0.5 cm^3/min (Figure 32D), face dissolution did not occur due to carbonic acid's relatively slow reaction kinetics. However, this condition led to the formation of a branched wormhole, yielding the highest wormhole volume among the experiments. Increasing the injection rate slightly to 1 cm^3/min (Figure 32C) resulted in a notable acid loss on the wormhole's walls, leading to conical-shaped wormholes with multiple branches

within the core. A dominant, less branched wormhole was formed, requiring a minimal pore volume for breakthrough at an intermediate injection rate of 2 cm^3/min (Figure 32B). This type of wormhole, known as a dominant wormhole, exhibited the lowest wormhole volume. Further increasing the injection rate to 5 cm^3/min (Figure 32A) resulted in the acid penetrating tiny pores, increasing surface area contact, and higher acid consumption. This condition led to ramified wormholes characterized by branched flow channels. In all samples, the acid enters from a single dominant area rather than multiple areas, due to the natural heterogeneity of the core sample. Once the acid finds a slightly more permeable local zone at the inlet, the dissolution-enhanced local permeability and the wormhole continue to progress. These findings indicate that injection rate plays a crucial role in shaping the morphology and volume of wormholes formed during acid injection. Intermediate injection rates promote the formation of less branched, dominant wormholes, whereas higher and lower rates lead to more branched structures.

Inlet face after core flooding			
			
		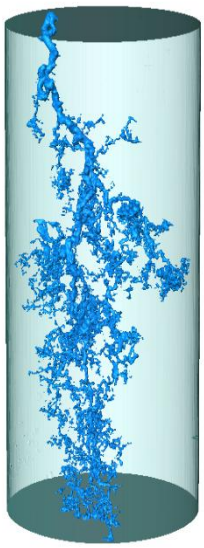	
IR= 5 cm^3/min Wormhole radius = 1.56 mm	IR= 2 cm^3/min Wormhole radius = 1.025 mm	IR= 1 cm^3/min Wormhole radius = 1.575 mm	IR= 0.5 cm^3/min Wormhole radius = 1.735 mm
(A)	(B)	(C)	(D)

Figure 32 Wormhole shapes of single core flooding experiments where (A) IL1, (B) IL2, (C) IL3, (D) IL4

3.3.5 Petrophysical properties

The interaction between carbonic acid and limestone altered the petrophysical characteristics, specifically porosity, while permeability became infinite after the wormhole was created. The following formula is used to calculate the change in porosity (Umer Shafiq et al., 2017):

$$\Delta\phi = \frac{\phi_2 - \phi_1}{\phi_1}.100\% \qquad (11)$$

Where ϕ_1 is the initial porosity, and ϕ_2 is the final porosity.

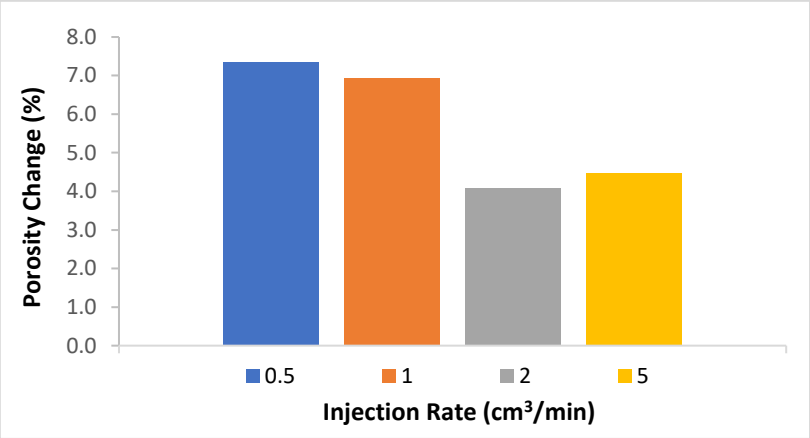

Figure 33 The effect of injection rate on porosity

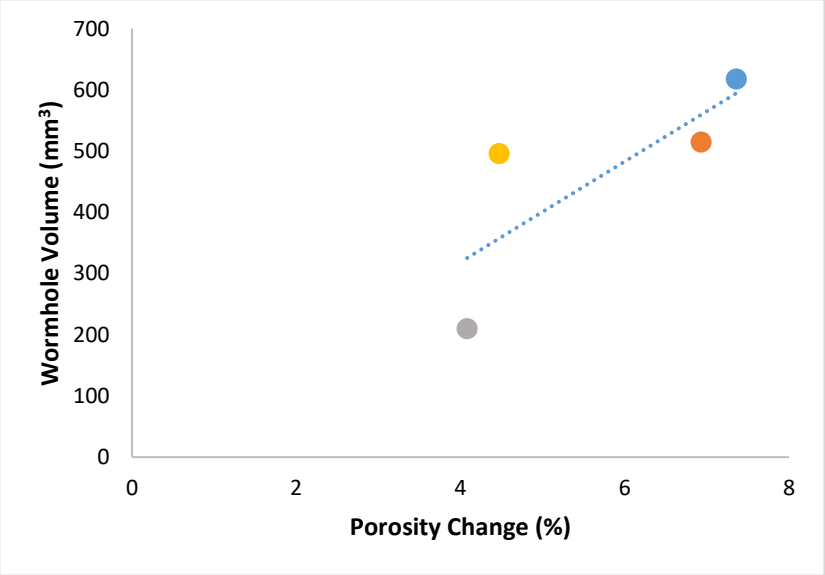

Figure 34 The porosity changes vs. wormhole volume

The results from the interaction between carbonic acid and calcite on petrophysical properties, particularly porosity and permeability, provide critical observations into the modification processes in geological formations. The porosity change is calculated using a formula highlighting the notable shifts observed in the samples. When examining the IL1,

IL2, IL3, and IL4 cores, there is a consistent increase in final porosity compared to initial porosity.

The porosity change observed at the optimal injection rate is the lowest among the analyzed cores (Figure 33 and Figure 34). This difference can be linked to the creation of a single, relatively straight, branchless wormhole. Contrary to the other cores, where the dissolution process may have resulted in complex and extensive networks of interconnected pores. Forming a single wormhole at the optimum injection rate limited the overall increase in porosity. This phenomenon indicates a localized dissolution effect, in which the acid primarily acts along a specific pathway, resulting in a moderate change in porosity. Although the porosity change is lower, the core's permeability after wormhole formation remains infinite, indicating a significant enhancement in fluid-flow pathways.

3.3.6 ICP analysis

Calcium is the major constituent of carbonate minerals such as calcite and dolomite, which comprise most carbonate reservoirs. Calcium-rich minerals dissolution during matrix acidizing significantly influences rock permeability and porosity, thereby impacting reservoir productivity. In this study, effluent samples were collected every 2 pore volumes in each experiment. The ICP test was then conducted to determine the calcium concentration. As shown in Figure 35, increasing the injection rate from 0.5 cm^3/min to 2 cm^3/min resulted in a significant increase in calcium concentration from 2770 ppm to 7070 ppm, whereas at the highest injection rate of 5 cm^3/min, the calcium concentration dropped significantly to 5146 ppm. The 2 cm^3/min injection rate yielded the greatest calcium concentration of 7070 ppm, indicating the most effective rate for promoting calcium dissolution in the specified experimental conditions. The ICP test results, plotted in Figure 35, agree with those presented in Figure 28, as the 2 cm^3/min experiment resulted in the fastest wormhole breakthrough.

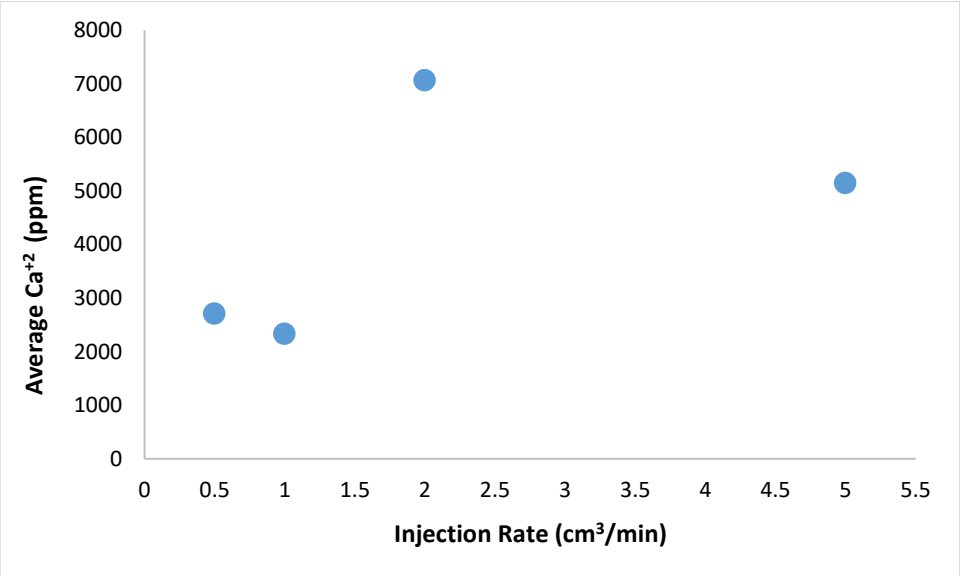

Figure 35 The average calcium concentration for each injection rate

3.3.7 Validation of Optimum Injection Rate

Validation experiments were performed with Indiana limestone cores, designated IL5 and IL6. Both cores were prepared as detailed in section 3.2 of the experimental methods; sample characteristics and preparation were thus identical, as shown in Table 5. The two experiments were conducted at the optimum injection rate of 1.7 cm³/min, where the differential pressure, pore volume to breakthrough (PVBT), and wormhole morphology were investigated (Figure 36 and Figure 37). The findings revealed PVBT values of 16 for IL5 and 20 for IL6, consistent with the anticipated values derived from prior experimental investigations. Post-experiment micro-CT scans revealed, in both cores, dominant, less branched wormhole structures similar to those observed in previous experiments (Figure 38 and Figure 39).

The experimental setup and available resources constrained the boundary conditions used in these experiments. Temperature and pressure defined the experimental conditions, with a system temperature of 60 °C and formation pressure of 2000 psi, porosity between 13-15% and permeability between 8-12 mD. While such laboratory limitations cannot fully replicate field-scale conditions, they provide a valuable investigation into the governing mechanisms under laboratory-scale conditions. To extend these findings to realistic reservoir conditions, numerical simulation is essential, enabling a wide range of temperatures and pressures, rock composition and mineralogy, and fault presence and orientation. The integrated approach bridges the gap between the laboratory and field scale, predicting a wide range of different scenarios under actual reservoir conditions.

The validation experiments using only two core samples were designed to confirm the repeatability of the previously determined optimum injection rate rather than to establish statistical generalization. The experiments used the optimum injection rate of 1.7 cm³/min under the same conditions in two experiments to verify that this rate consistently produces the desired dissolution behavior. The wormhole morphology observed in the two samples confirms that the optimal injection rate produces a single, dominant, non-branched wormhole structure. These results confirm that the selected injection rate is reliable under similar conditions and can be confidently used in further experiments and numerical simulations.

Table 5 Core Sample Characteristics for Validation Flooding Experiments

Core No.	D (cm)	L (cm)	Porosity (%)	Permeability (mD)
IL5	3.78	6.57	15.09	3.73
IL6	3.78	6.5	16.01	4

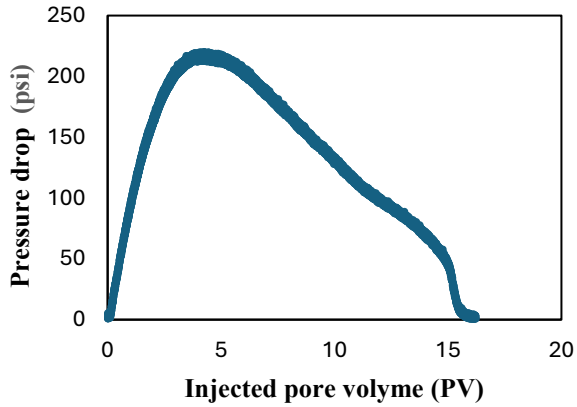

Figure 36 Pressure drop a cross IL5 sample with 1.7 (cm³/min) injection rate

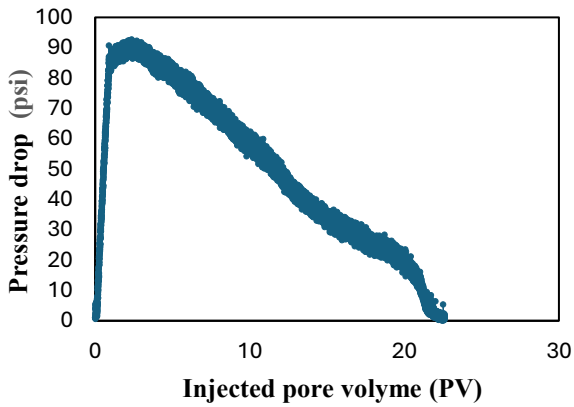

Figure 37 Pressure drop a cross IL6 sample with 1.7 (cm³/min) injection rate

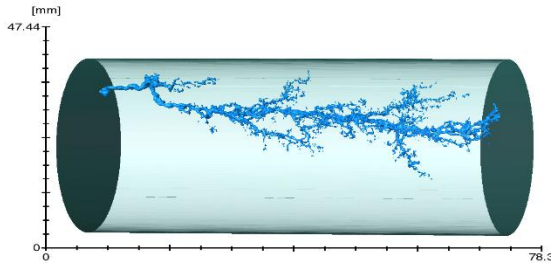

Figure 38 Wormholes generated during carbonic acid injection in the IL5 sample

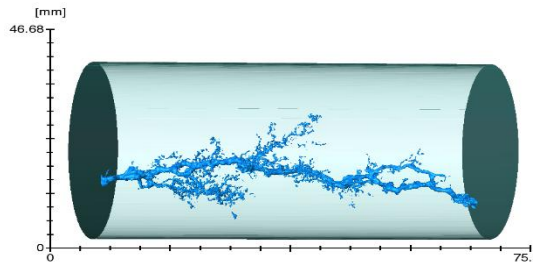

Figure 39 Wormholes generated during carbonic acid injection in IL6 sample

3.4 Conclusion

The comprehensive experimental study on carbonic acid injection into carbonate formations has yielded several significant findings that enhance our understanding of the process and its optimization. Below are the key findings derived from the results presented:

1. **Optimum Injection Rate:** Two models were presented to find the optimum injection rate; one based on the injection rate proposed by Wang. It's observed that the optimum injection rate is 2 cm^3/min, and the other is based on the interstitial velocity of acid proposed by Buijse and Glasbergen, which considers the relationship between PVBT and interstitial velocity (Vi), as expressed in Equations (3)-(8). By calculating parameters such as efficiency factor (Weff), B-factor (WB), and wormhole growth rate (Vwh), the model determines an optimum interstitial velocity of 1 cm/min, corresponding to an optimum injection rate of 1.7 cm^3/min. We can speculate that changes in the temperature and pressure might change the optimum injection rate and velocity. Wang's model determines the optimum injection rate based on the lowest PVBT obtained experimentally. However, because only a limited number of experiments can be conducted, the optimum obtained by Wang's method might not be the true optimum. Therefore, Buijse and Glasbergen's semiempirical model, which can be calibrated with a few experimental data, can be used to determine the true optimum PVBT.
2. **Wormhole Formation and Morphology:** The injection rate significantly impacts the morphology and volume of wormholes formed during acid injection. Intermediate rates (2 cm^3/min) tend to produce dominant, less branched wormholes, while higher and lower rates result in more branched structures. This insight is crucial for controlling the shape and size of wormholes for optimal reservoir performance.
3. **Damköhler Number Analysis:** The observation that all points are exclusively located on the right side of the optimum Damköhler number, rather than being distributed around it as expected, motivates further investigation into this phenomenon. Based on this study, the optimum Damköhler number for carbonic acid was 0.005. Fred and Fogler (1999) examined stronger acids, such as HCl, formic acid, and acetic acid, across various carbonate lithologies but did not include carbonic acid. In contrast, this study demonstrates that carbonic acid, being much weaker and slower reacting, produces a lower optimum Damköhler number (0.005). Similar results reported by ongoing work at King Fahd University confirm that this lower value is characteristic of carbonic acid across different lithologies. Nevertheless, further investigation is required to strengthen these conclusions. Future work will aim to collect and consolidate all available experimental data on

carbonic acid-based matrix acidizing, enabling the development of a generalized correlation of optimum Damköhler number for carbonic acid under a wide range of lithology and operational conditions.

4. **Petrophysical properties:** The reaction between carbonic acid and limestone significantly increased the final porosity while also causing the permeability to become infinite, indicating the presence of improved pathways for fluid flow. Optimal injection rates resulted in comparatively lower porosity changes, which can be attributed to the creation of a single, straight wormhole that facilitates liquid flow. This highlights the localized dissolution effects. However, the permeability continued to improve significantly, highlighting the efficacy of chemical dissolution in altering petrophysical properties.
5. **Calcium Dissolution:** The injection rate of the acid notably affects calcium dissolution. Increasing the rate from 0.5 cm^3/min to 2 cm^3/min resulted in a substantial rise in calcium concentration, peaking at 7070 ppm. However, further increasing the rate to 5 cm^3/min led to a decrease in concentration to 5146 ppm. This suggests that 2 cm^3/min is the most effective rate for promoting calcium dissolution. Optimizing injection rate is crucial for effective acid use.

In conclusion, the study determines the optimal injection rate for carbonic acid into carbonate formations. It also emphasizes the effects of this injection rate on wormhole formation, calcium dissolution, and petrophysical properties. Intermediate rates promote dominant wormholes, while higher and lower rates lead to more branched structures.

4 Acid Diversion Using a Dual-Core Flooding System

4.1 Introduction

This chapter introduced a novel approach to integrating carbonic acid with viscoelastic surfactant (VES) for acid diversion in a heterogeneous carbonate reservoir. This approach enhances acid distribution and provides significant environmental and operational benefits, including reduced hydrochloric acid consumption, minimized corrosion, and alignment with carbon capture and storage (CCS) initiatives. The rheological properties of the newly developed VES products FTS-20, S-2, and S-300 were measured, and the results revealed that FTS-20 exhibits shear-thinning behavior, making it a strong candidate for acid diversion. Indiana limestone core samples were flooded with different acid systems: hydrochloric acid alone, VES with hydrochloric acid, carbonic acid alone, and VES with carbonic acid to compare their performance and effectiveness comprehensively. Dual-core flooding experiments revealed that the VES carbonic acid system significantly improved acid distribution in heterogeneous formations, making it a viable alternative for carbonate rock matrix acidizing.

Viscoelastic surfactants have been extensively studied as diverting agents for HCl acid diversion due to their ability to enhance acid distribution in heterogeneous carbonate formations. However, the combination of VES with carbonic acid has not been investigated previously. To the best of our knowledge, this is the first time we have utilized the VES with carbonic acid as the primary stimulation solution in heterogeneous carbonate formation. VES with carbonic acid has several advantages. From an ecological perspective, this approach used CO2 as a reactant to minimize greenhouse gas emissions. Instead of releasing CO_2 as a result of conventional acidizing activity, as illustrated in equation 1 (Fredd and Fogler, 1998), this process consumes CO_2 during the acidizing, as shown in equation 2 (Almalichy et al., 2024; Peng et al., 2015). By doing so, it supports sustainable acidizing by minimizing HCl consumption. Furthermore, the viscosity of VES within the rock enhances acid distribution in heterogeneous formations. In addition, carbonic acid is less corrosive than HCl, reducing the damage to the wellbore and surface equipment.

$$2HCl^{+} + CaCO_3 \rightarrow Ca^{2+} + CO_2 + H_2O \quad (12)$$

$$H_2CO_3 + CaCO_3 \rightarrow Ca^{2+} + 2HCO_3^{-} \quad (13)$$

4.2 Material and Methods

4.2.1 Core sample

Core samples from Indiana limestone (outcrop formation), 2.5" in length and 1.5" in diameter, were used in this study. The initial porosity of the sample was measured using a helium porosimeter (AP-608), Table 6, ranging from 14% to 19%, and the permeability measured using a liquid permeameter LP-100A ranged from 4 mD to 33 mD. The samples were clustered based on their permeability, with high-permeability samples having about 6–7 times the values of low-permeability samples to achieve the acid diversion. XRD measurements indicate that the Indiana limestone is 100% calcite.

4.2.2 Fluids

DI water (DI) was used for saturation and for the pre- and post-flooding processes. The different acid systems used in the experiments are summarized in Table 6. In experiment 1, 15 wt% of hydrochloric acid was used, while 6 wt% of viscoelastic surfactant was mixed with the hydrochloric acid in experiment 2. 1 wt% corrosion inhibitor (CI) was included in the acid system used in experiments 1 and 2 to mitigate the corrosion caused by hydrochloric acid. The acid system used in experiment 3 was prepared by mixing 10 wt% $CaCl_2$ and 6wt% VES with DI water to produce a total liquid volume of 700 cm^3. The mixture was homogenized using an overhead stirrer, and then the solution was transferred to another accumulator containing CO_2. The resulting liquid-to-CO_2 ratio in the accumulator was 70:30 (v/v), corresponding to 70% DI water and 30% CO_2.

The 70:30 (v/v) liquid-to-CO2 ratio was selected based on Saudi Aramco's internal operational experience and experimental practices. According to this guidance, increasing the CO_2 fraction beyond 30% does not lead to complete dissolution of CO2 in the liquid phase, resulting in undissolved gas and making it difficult to maintain a stable carbonic acid system.

Table 6 Core sample and acid system details

Exp. No.	Core No.	Initial Porosity (%)	Final Porosity (%)	Permeability (mD)	Acid system
1	IL7	17.2	18.45	26	15 wt% HCl + 1 % corrosion inhibitor
	IL8	14	14.3	4	
2	IL9	19	20.6	25.3	15 wt% HCl + 10 wt% $CaCl_2$+ 6wt% VES+ 1 % corrosion inhibitor
	IL10	14.7	15.5	4	
3	IL11	17.3	17.7	25.5	(CO_2 +DI) Carbonic acid + 10 wt% $CaCl_2$+ 6 wt% VES
	IL12	14.8	15.1	4	

4.2.3 Experimental procedure

Figure 40 shows that the experimental procedure began by measuring the core samples' porosity using a helium porosimeter, followed by saturating the core samples with fresh water at 2,000 psi for 24 hours. The permeability of the core sample was then measured using a liquid permeameter, LP-100A. The experiment was followed by dual-core flooding, as detailed in the core flooding section, wherein the differential pressure (DP) and pore volume to breakthrough (PVBT) were recorded. After that, the core samples were dried in an oven at 100° C for 24 hours. Computerized Tomography (CT) scans were then used to visualize the samples containing wormholes.

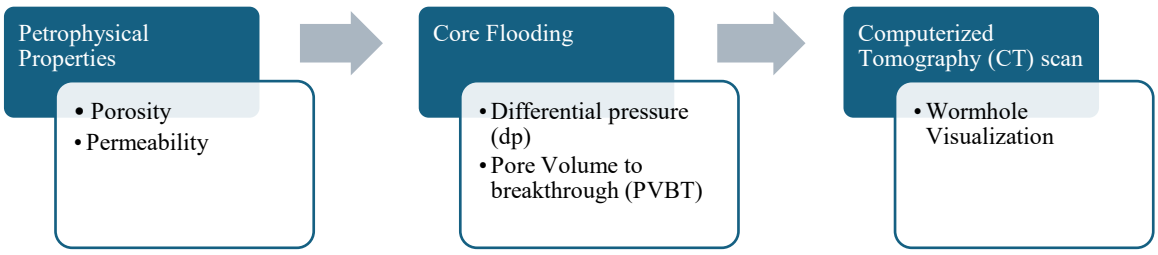

Figure 40 Experimental workflow of dual-core flooding experiments

4.2.4 Rheological measurements

The rheological measurements were performed using a Chandler HTTP 5550 Viscometer at a temperature of 60°C and 500 psi. The shear-thinning behavior of viscosity was monitored over time as the shear rate varied between 100 s^{-1} and 1000 s^{-1}. The aim was to evaluate the effect of varying $CaCl_2$ concentrations on micellar formation and the resulting viscosity. The solution was prepared by dissolving CaCl2 in DI water, adding 6 wt% of the newly developed VES, and mixing with an overhead stirrer. The preparation involved two concentrations of $CaCl_2$, starting with 20% for the initial tests conducted across all three surfactants (FTS-20, S-2, and S-300). Based on promising results observed with FTS-20 at this concentration, a second round of testing was performed using a 10% $CaCl_2$ solution, focusing exclusively on FTS-20.

4.2.5 Dual-core flooding

Figure 41 illustrates the schematic diagram of the flooding system used for Indiana limestone dual-core flooding experiments with different acid systems. The core holders and connecting lines are constructed from Hastelloy, a high-resistance material designed to withstand acidic conditions at elevated temperatures. The system features two high-pressure, high-temperature (HP/HT) core holders, also made of Hastelloy, which provide

excellent resistance to acid corrosion. Before each experiment, the low- and high-permeability core samples were loaded into the holders and subjected to a confining pressure of 3,500 psi. The core holder inlet is connected to two accumulators, one for DI water and the other for the acid system. At the same time, the outlet is linked to a production line. A CO_2 accumulator maintains a back pressure of 2,000 psi, and an isco pump injects the acid at 1 cm^3/min. A pressure transducer records the pressure difference between the inlet and outlet.

The core flooding experiments began by loading the core samples into the core holders and placing the holders in the core flooding system's oven, set to 60° C. A confining pressure of 3,500 psi and a back pressure of 2,000 psi were applied. Before each experiment, DI water was pumped as a pre-flush. Injections were conducted using an HP/HT Isco pump at 1 cm^3/min. The injection process was stopped once the breakthrough occurred in one or both core samples.

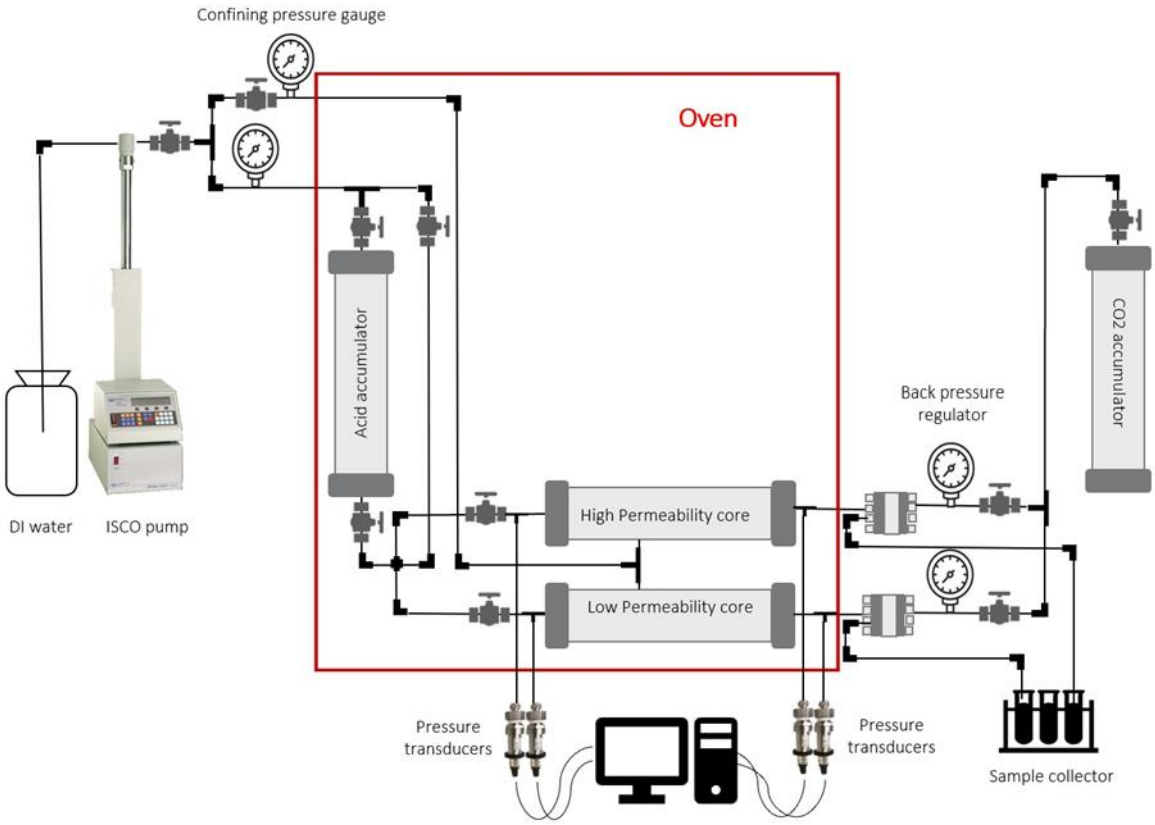

Figure 41 Dual-core flooding system

4.2.6 Computerized tomography (CT) scan

Computed tomography (CT) scan is a non-invasive technique that uses X-rays to create 2D cross-sectional images of rock samples, which can be reconstructed into 3D models using Pregeos software. The CT scan setup includes an X-ray source, a mechanical motion system, a data collection system, and an imaging process system (U. Alameedy et al., 2023;

Almalichy et al., 2024). In this study, CT scans were performed after core flooding to visualize the wormhole inside the core sample.

4.3 Results and discussions

4.3.1 Rheological results

Three newly developed viscoelastic surfactants (FTS-20, S-2, and S-300) were first tested with 20% CaCl2, and the results showed distinct behaviors influenced by their molecular structures and ionic interactions. Only FTS-20 achieved a 25 cp viscosity, while S-2 and S-300 showed no thickening at 1 cp, possibly due to an insufficient amphiphilic balance. A second-round test was conducted for FTS-20 using 10% CaCl2, and the result indicated a significant increase in viscosity to 150 cp, attributed to the optimal ionic condition, as shown in Figure 42.

4.3.1.1 Micelle Formation and Viscosity Response

In the case of FTS-20, huge differences in viscosities at both 20% and 10% $CaCl_2$ were present, especially at 100 s^{-1}, as shown in Figure 43 (100 s^{-1} is representative of the shear rate value experienced by the injected fluid near the formation) (Tie et al., 2019). At 20% $CaCl_2$, the micelles formed a low viscosity. However, viscosity was significantly increased at a 10% $CaCl_2$ concentration, indicating the formation of stronger rod-like or worm-like micelles (Figure 42). The FTS-20, when mixed with 10% CaCl2, can be more effective at blocking the high-permeability zones of a carbonate formation, making it a good candidate for acid diversion.

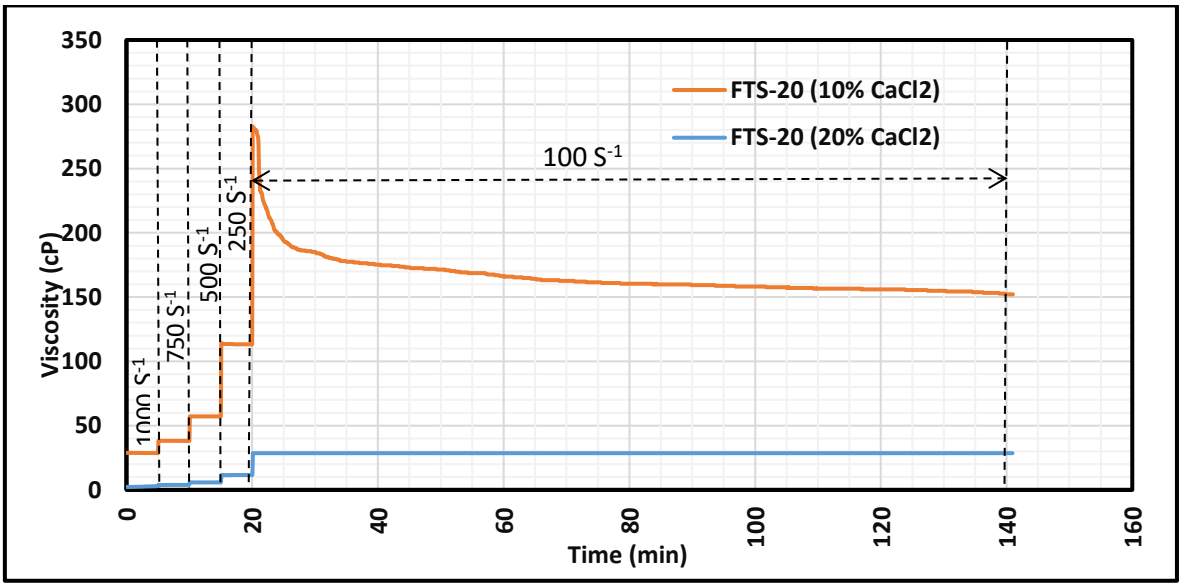

Figure 42 Viscosity as a function of time for FTS-20 at different $CaCl_2$ concentrations under a shear rate range of 1000 to 100 S^{-1} at 60° C

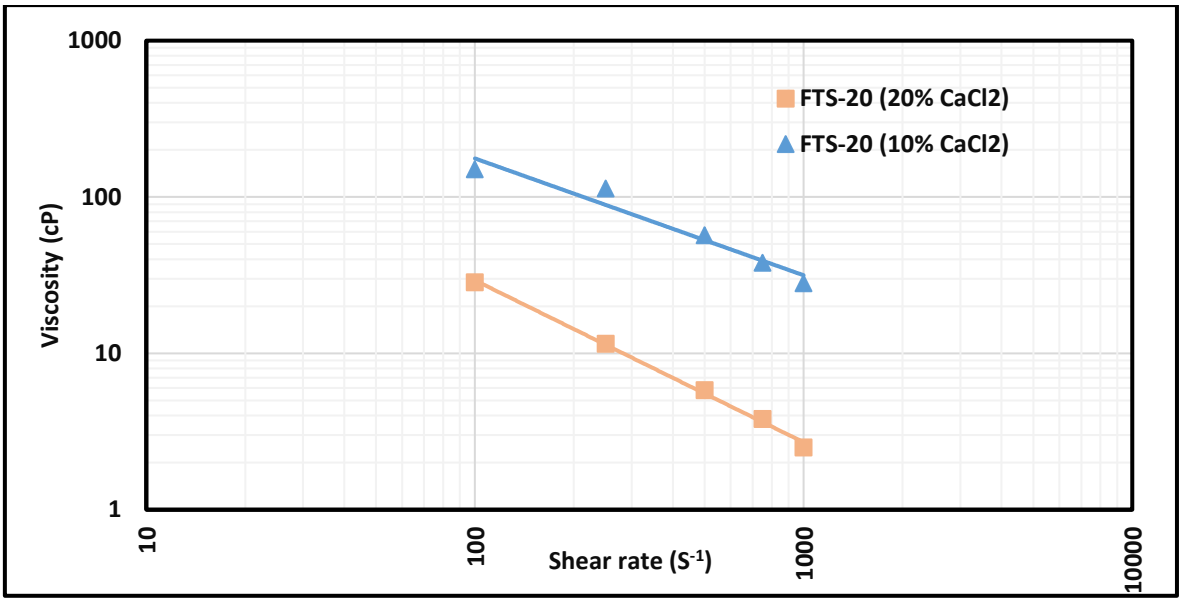

Figure 43 Viscosity as a function of shear rate for FTS-20 at different $CaCl_2$ concentrations at 60° C

4.3.1.2 Acid Diversion by Micellar Transition Effect

In acid diversion, spherical micelles should transition into rod-like micelles. While the acid reacts with the carbonate rock and releases Ca^{+2} ions, it increases the ionic strength and consequently forces the micelles in the VES solution to transform into rod-like or worm-like structures. These stretched micelles show higher viscosity and are crucial in blocking the high-permeability channels. FTS-20 forms these micellar structures under 10% and 20% $CaCl_2$ concentrations, indicating its ability to divert acid flow and allow the treatment to reach less permeable areas.

4.3.2 Dual Core flooding results

4.3.2.1 Neat Hydrochloric acid system

In the first experiment, the core characteristics and acid system are detailed in Table 6. The cores were pre-flushed with DI water for complete saturation. Acid injection started, and the breakthrough in the high-permeability core occurred 13 minutes after injecting 13 cm^3 of acid (58% of the total pore volume), as shown in Figure 44. In a low-permeability sample, the acid didn't penetrate. This is due to the high dissolution rate of hydrochloric acid when it reacts with calcite, resulting in a single dominant wormhole, as shown in Figure 45. However, in heterogeneous formations, this is a significant drawback, as in our case, the low-permeability core sample was subject to surface dissolution, and the acid did not penetrate it because it preferred to flow through the high-permeability path, leaving the low-permeability core untreated.

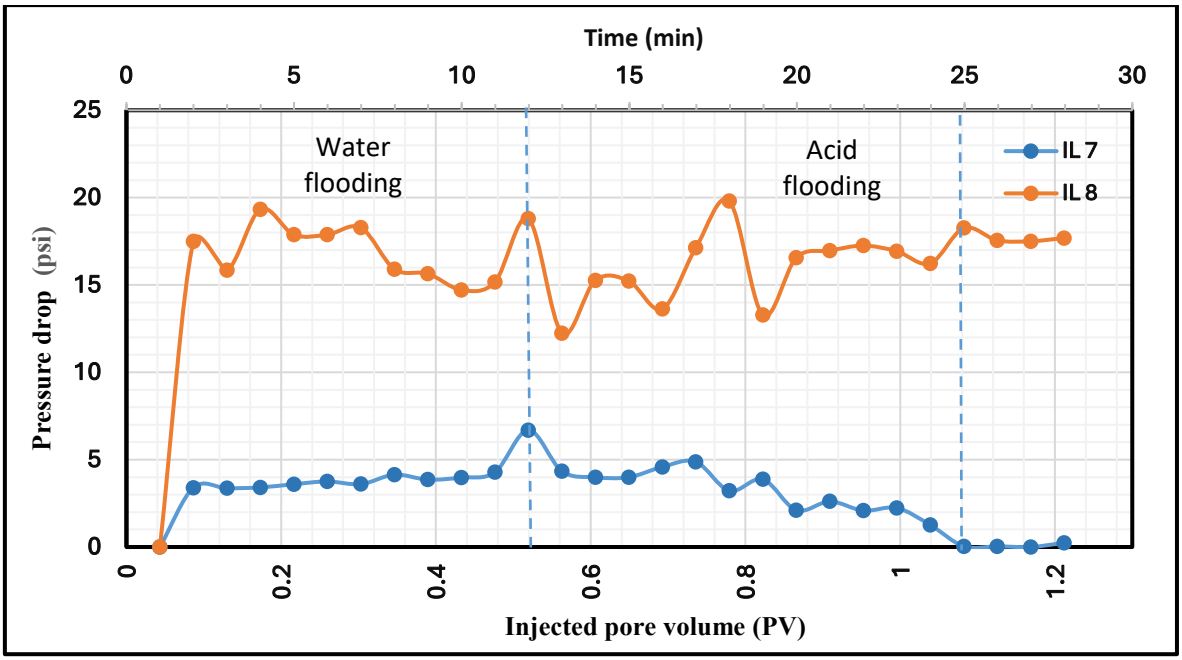

Figure 44 Pressure drop of IL7 (high permeability) and IL8 (low permeability) samples during neat acid injection.

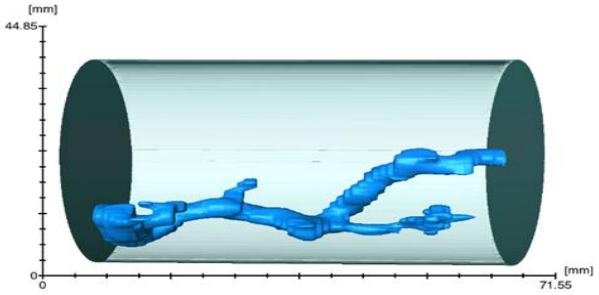

Figure 45 Wormholes generated during neat HCl acid injection in the IL7 sample

4.3.2.2 Hydrochloric acid mixed with VES

In the second experiment, the acid system and core sample details are outlined in Table 6. As per the experimental method, DI water was initially injected to saturate the cores. The 15 wt% HCl mixed with 6 wt% VES injection began afterward, and the breakthrough in the high permeability core was observed after 32 minutes of the acid injection, corresponding to 1.6 PV of acid, as shown in Figure 46. Meanwhile, the low-permeability core reached breakthrough at 36 minutes into the acid injection, as shown in Figure 46. Despite the permeability contrast between cores, their breakthrough times were remarkably close. Compared with the case of HCl alone in experiment No. 1, the extended breakthrough time is due to the VES, which reduces HCl's high reactivity. This performance showed the effectiveness of the newly developed VES FTS-20, making it an excellent choice for acidizing highly heterogeneous formations. The CT scan results in Figure 47 and Figure 48 revealed the wormholes generated in low- and high-permeability cores. Notably, the

wormholes were single and similar in width, regardless of the permeability contrast between the cores.

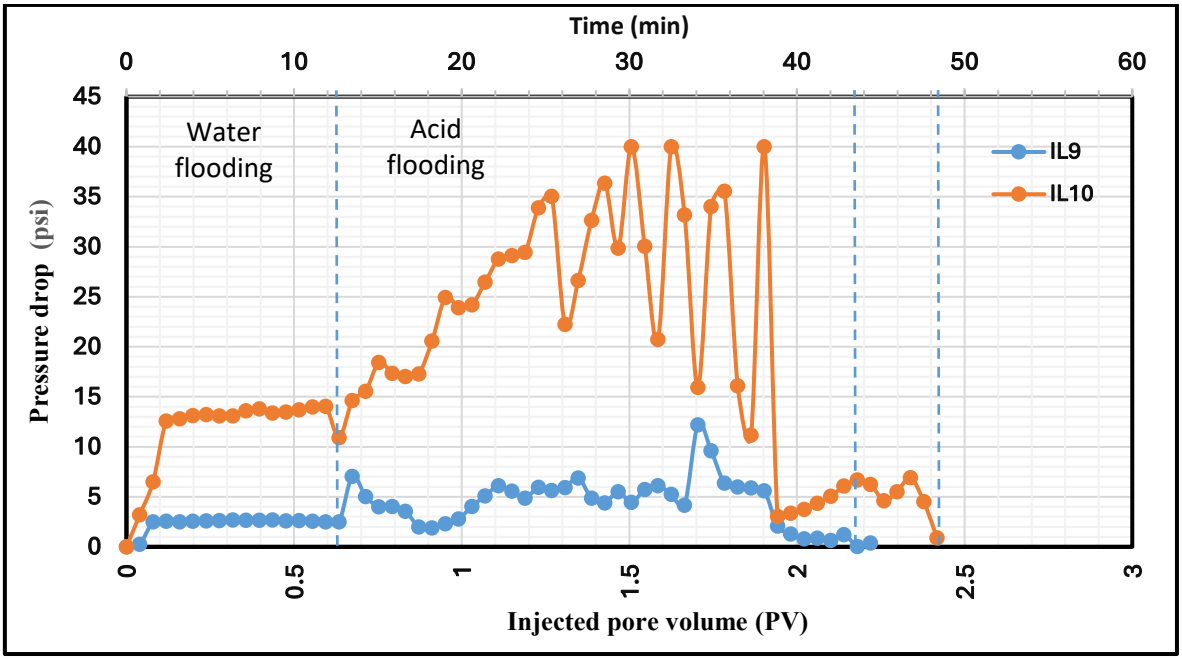

Figure 46 Pressure drop of IL9 (high permeability) and IL10 (low permeability) samples during VES acid system injection

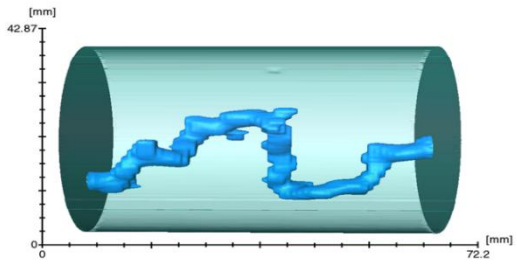

Figure 47 Wormholes generated during VES acid system injection in IL9 sample

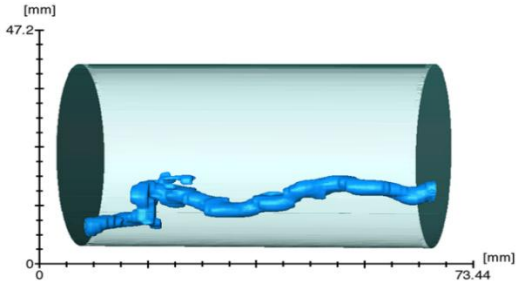

Figure 48 Wormholes generated during VES acid system injection in IL10 sample

4.3.2.3 VES carbonic acid system

In the third experiment, the acid system described in Table 6 includes carbonic acid mixed with 6 wt% VES and 10 wt% $CaCl_2$. Initially, DI water was injected as a part of the pre-flush process. The carbonic acid mixed with 6 wt% VES injection led to a breakthrough in both high- and low-permeability cores at around 150 minutes, after injecting 7 PV of acid. Notably, the pressure curve behavior was identical, as shown in Figure 49. However, the shapes of the wormholes formed in the two samples differed. Two wormholes were created in the high-permeability core: one extending through the entire sample and another partially

formed, as shown in Figure 50 and Figure 51. This confirms that diversion occurred within the same sample and between the high- and low-permeability samples.

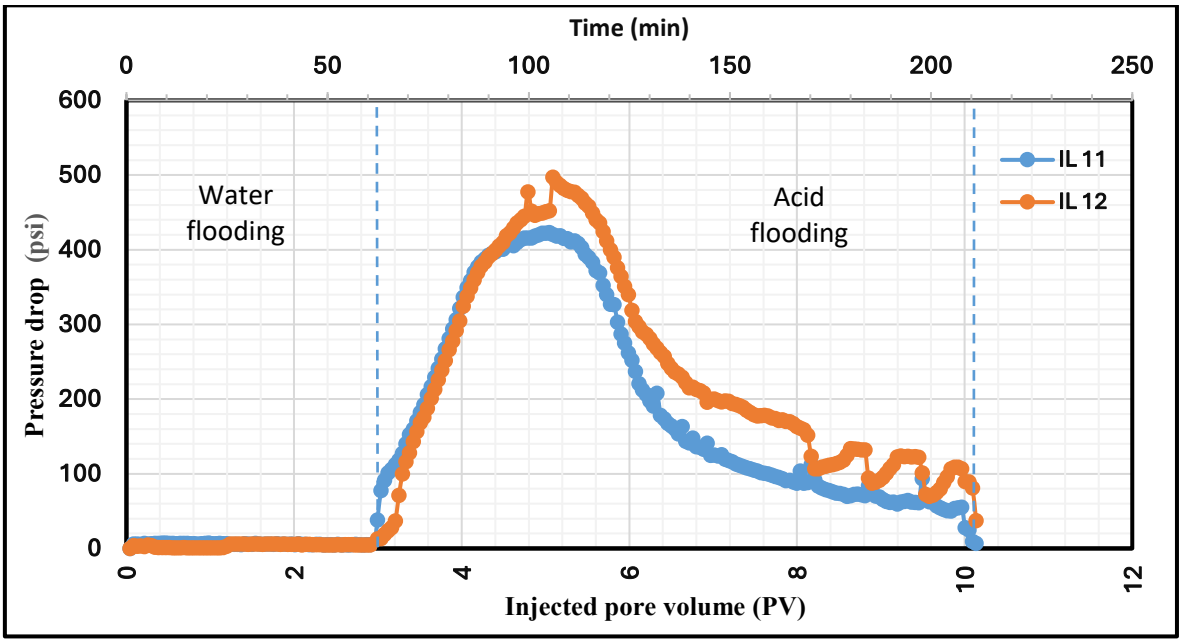

Figure 49 Pressure drop of IL11 (high permeability) and IL12 (low permeability) samples during VES carbonic acid system injection

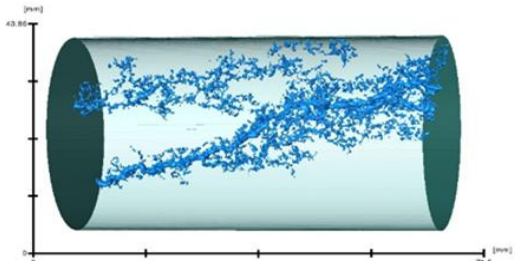

Figure 50 Wormholes generated during VES carbonic acid system injection in IL11 sample

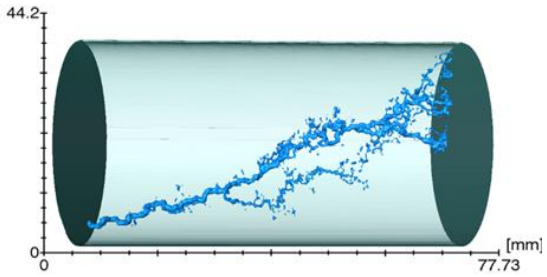

Figure 51 Wormholes generated during VES acid system injection in IL12 sample

The experiments showed that the volume required to achieve a breakthrough with carbonic acid was approximately 7 pore volumes (PV). In contrast, only about 1.7 PV was needed with a hydrochloric acid VES system. This is expected because hydrochloric acid, a strong acid, is highly reactive compared to carbonic acid, which is very weak (Hydrochloric acid has a pH of approximately 1 to 2 at 1M concentration, while carbonic acid has a pH of around 4.2 to 4.7 under natural equilibrium conditions in water). In previous studies addressing carbonate matrix acidizing, a large volume of injected acid is often considered a disadvantage due to economic and operational concerns. However, in the case of carbonic acid, the requirement for a larger volume is seen as an advantage because it aligns

with the intent to inject as much CO_2 as possible into the subsurface. This supports carbon capture and storage (CCS) initiatives to reduce greenhouse gas emissions.

4.4 Conclusions

This study introduced a novel integration of carbonic acid and viscoelastic surfactant (VES) for acid diversion in a heterogeneous carbonate reservoir. This study evaluated four acid systems to compare their performance and effectiveness comprehensively. The findings reveal the following conclusion:

- A rheological test of newly developed viscoelastic surfactants (FTS-20, S-2, and S-300) showed that FTS-20 at 10 wt% of CaCl2 exhibited exceptional performance, behaving like a shear-thinning fluid, making it a perfect choice for acid diversion.
- VES carbonic acid significantly improved acid distribution in heterogeneous formations; however, it required a longer time to achieve results than the VES-hydrochloric acid system.
- Using carbonic acid is environmentally beneficial because it reduces hydrochloric acid consumption, minimizing associated issues such as pipe and surface equipment corrosion, and supporting carbon capture and storage (CCS) by injecting CO2 into subsurface formations.

5 Acid Diversion Using a Novel Single-Core Design

5.1 Introduction

Using an acid to stimulate a heterogeneous carbonate reservoir during matrix acidizing may result in over-treating the high-permeability zones, leaving the low-permeability zones untreated. This is particularly exacerbated in long, horizontal sections, necessitating the use of acid diverters to distribute acid throughout the formation evenly. In previous studies, conventional core flooding systems used single inlet and outlet lines or, at best, two outlet lines for dual-core flooding. This study proposes a new method for simulating matrix acidizing in horizontal wells by introducing five injection points and two production outlets. The injection points are perpendicular to the core samples to simulate multiple perforations in a horizontal well, while the outlet lines are parallel to each other. Four experiments were conducted in this study using Indiana limestone cores that were 1.5 inches in diameter. For the first three tests, the core length was 12 inches, and the cores' average permeability was 16 mD. Two 6 inches long cores with different average permeabilities (10 and 50 mD) were employed for the fourth one. Hydrochloric acid was used in the first experiment, while hydrochloric acid with viscoelastic surfactant (VES) was used in subsequent experiments. To the best of our knowledge, this is the first study to introduce a multi-point injection system with enhanced coverage and distribution, resulting in a more precise representation of acidizing a horizontal well.

5.2 Experimental Setup and Materials

5.2.1 Samples

Indiana limestone core samples were utilized in this study. After obtaining the core samples from the source, they were cleaned, dried, and cut to the desired lengths of 6 and 12 inches. The porosity of the samples was measured as shown in Table 7. The mineralogy of the samples was determined by XRD, which showed that all samples were 100% calcite.

5.2.2 Chemicals

DI water is used for saturation and pre- and post-flooding. The acid systems used in the experiments are summarized in Table 7. The acid system used in experiments 2, 3, and 4 was prepared by adding 10 wt% calcium chloride ($CaCl_2$) to a solution containing 15 wt% hydrochloric acid (HCl) and 1 wt% corrosion inhibitor (CI), and mixing with a corrosion-

resistant overhead stirrer made of titanium. Then, 6 wt% of viscoelastic surfactant (VES) was added gradually to the solution. The acid system used in the first experiment consisted of only 15 wt% HCl mixed with 1 wt% CI. To investigate the flow behavior of the viscoelastic surfactant, the viscosity was measured across a range of shear rates, from 100 to 1000 sec^{-1}. The results show a non-linear relationship between shear rate and viscosity. As the shear rate increased, the viscosity of the viscoelastic surfactant decreased, with values of 153 mPa·s at 100 sec^{-1}, 113 mPa·s at 250 sec^{-1}, and continuing to decline to 28 mPa·s at 1000 sec^{-1}.

5.2.3 Experimental design

A systematic approach was undertaken across 4 experiments to understand wormhole propagation in porous media. In the first experiment, neat hydrochloric acid (HCl) was injected to establish a baseline for diversion behavior. Breakthrough refers to the point at which the injected acid penetrates the outer surface of the sample and forms a continuous flow path (wormhole) between the injection point and one of the outlets. Subsequently, viscoelastic surfactants (VES) were introduced alongside HCl in the second experiment, with injection stopped after the breakthrough to analyze the immediate impact on wormhole formation. The third experiment extended this inquiry by continuing the injection after the breakthrough to evaluate the continuous influence on wormhole propagation. Finally, a heterogeneous sample with varying permeability was introduced to simulate heterogeneous conditions. By systematically varying parameters and conditions across these experiments, a comprehensive understanding of wormhole propagation mechanisms and the influence of different factors on diversion behavior was gained, offering valuable insights for enhanced acid diversion strategies.

Table 7 Specifications of Single Long Core Experiments

Exp. No.	Core No.	Core dimensions	Inj. rate (cm^3/min)	Acid system	Permeability (mD)	Porosity (%)
1	IL1	1.5 in × 12 in	1	15 wt% HCl + 1% CI	16	15.77
2	IL2	1.5 in × 12 in	1	15 wt% HCl+6 wt% VES+10% $CaCl_2$+ 1% CI	16	16.02
3	IL3	1.5 in × 12 in	1	15 wt% HCl +6 wt% VES+10% $CaCl_2$+ 1% CI	16	16.61
4	IL4	1.5 in × 6 in	1	15 wt% HCl +6 wt% VES+10% $CaCl_2$+ 1% CI	10	16.47
	IL5	1.5 in × 6 in	1		50	19.06

5.2.4 Core Flooding Setup

Figure 52 shows the schematic drawings of the flooding system used for acidizing experiments. The experiments were conducted at 60 °C, 3500 psi confining, and 2000 psi back pressure. In this context, back pressure refers to the pressure used to simulate the formation pressure in an oil well. The novated flooding system can handle cores up to 12 inches in length and 1.5 inches in diameter. The core flooding system operates under demanding conditions of 10,000 psi and 150 °C, necessitating materials such as Hastelloy for the core holder and lines to withstand high-temperature, acidic conditions. The HP/HT Coreholder is made from Hastelloy. As shown in Figure 53, the core holder consists of five injection points connected to accumulators that hold DI water and the acid system solution. At the same time, the two outlets are linked to the production line of effluent sample collection. A CO_2 accumulator applies 2000 psi back pressure. The 100 DX ISCO pump delivers the acid solution at a specified contact flow rate. Pressure transducers measure the pressure differential between the inlet and outlet, while a fraction collector collects effluent samples. These components comprise a robust system for conducting experiments under simulated reservoir conditions.

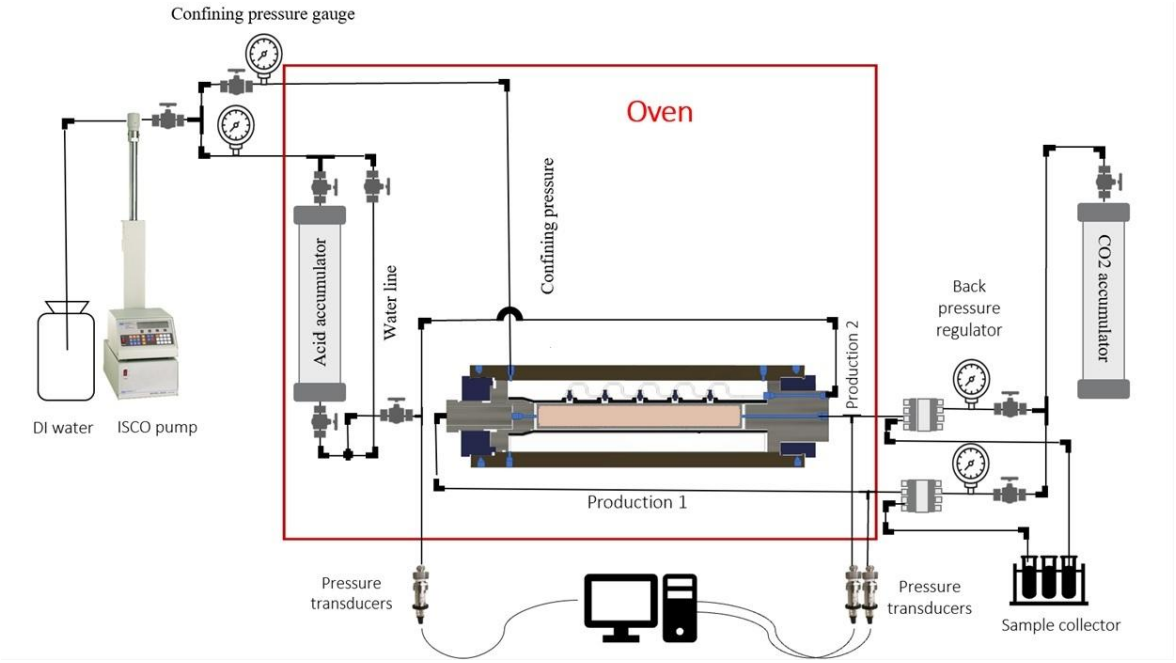

Figure 52 Schematic drawings of the laboratory flooding system

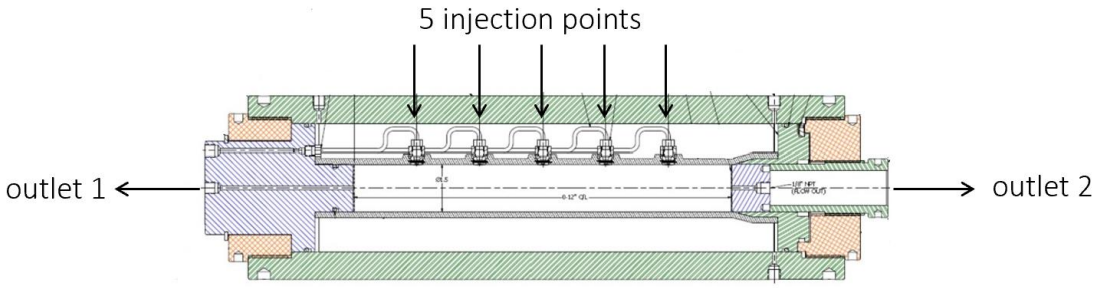

Figure 53 Illustration of injection points and production points

5.2.5 Experimental Procedure

The experimental procedure commenced with measuring sample porosity using a helium porosimeter (AP-608) in accordance with API RP 40. Subsequently, the samples underwent meticulous preparation, including vacuuming for 3 hours and saturation with DI water for 24 hours, in accordance with API RP 40 guidelines for proper core handling and fluid saturation. The samples were carefully loaded into a core holder and placed inside the oven. An oven was heated to 60 °C, with a 3-hour wait to ensure uniform temperature throughout the flooding system. Once equilibrium was reached, the inlet and outlet pressures were recorded, indicating the commencement of core flooding with DI water before acid injection. Upon completion of the acid injection, the system underwent a post-flush with DI water. Subsequently, the samples were offloaded and transferred to a drying oven set at 100 °C for 24 hours, in accordance with the API RP 40 recommendations for post-experiment sample drying. Finally, computerized tomography was used to visualize the generated wormholes, following the guidelines in ASTM E1441-11, thereby providing crucial insights into the effectiveness of the experimental procedure.

5.3 Results

5.3.1 Core flooding results

5.3.1.1 Neat acid system

An Indiana limestone core with a diameter of 1.5 in and a length of 12 in, with a permeability of around 16 mD, was used in this experiment. The acid system used in this experiment, as shown in Table 7, consists of 15 wt% HCl mixed with 1% CI. As mentioned in the experimental procedure, the experiment began with DI water injection as a pre-flush to saturate the sample fully. Injection of the acid system began, and 9 minutes later, a breakthrough occurred at outlet 2, followed by one at outlet 1 15 minutes later. According to the plan, the acid injection continued for 25 minutes after the breakthrough at both outlet

points to monitor wormhole propagation. The DI water flushing of the system followed this process. Figure 54 illustrates the relationship between the pressure drop and the number of pore volumes injected. The breakthrough occurred at outlet 2 after a total of 0.19 PV of acid had been injected. At outlet point 1, a total of 0.27 PV was used before the breakthrough occurred.

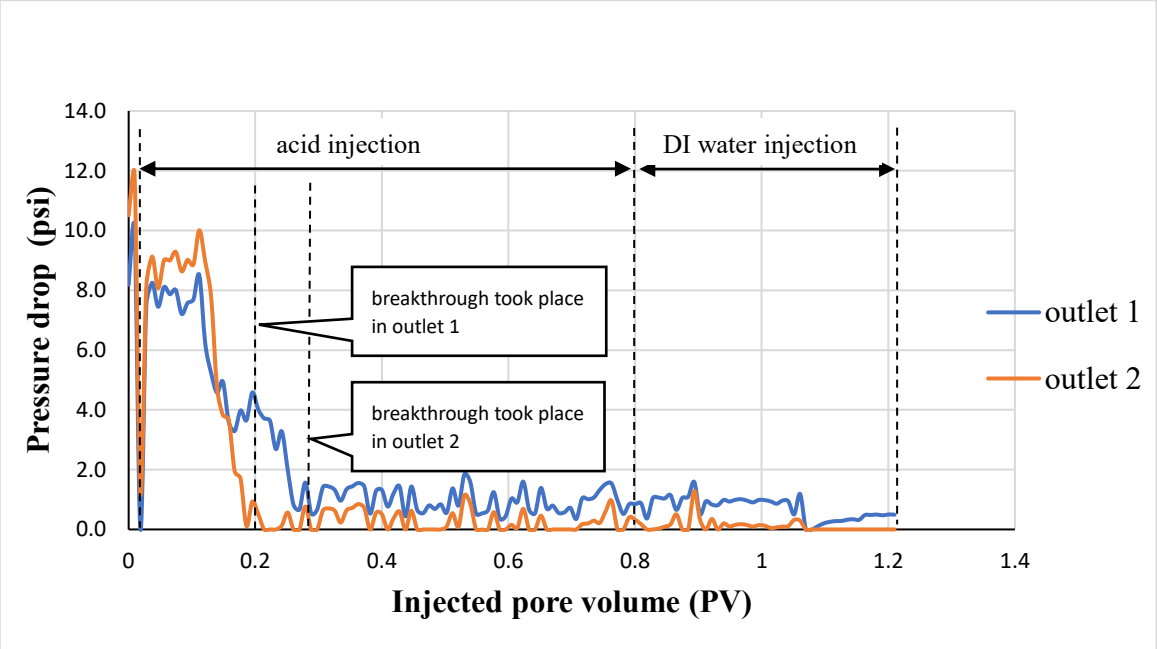

Figure 54 Pressure drop of a cross IL1 sample during 15wt% HCl acid injection

5.3.1.2 VES acid system (injection stops after breakthrough)

An Indiana limestone core with a diameter of 1.5 in and a length of 12 in, with a permeability of around 16 mD, was used in this experiment. The acid system of this experiment, as shown in Table 7, consists of 15 wt% HCl, 10 wt% $CaCl_2$, and 6 wt% of VES mixed with 1 wt% CI. As mentioned in the experimental procedure, the experiment began with DI water injection as a pre-flush to saturate the sample fully. Then, after injecting the acid system, a breakthrough occurred in outlet 2 after 5 minutes, and 23 minutes after the experiment started, a breakthrough occurred in outlet 1. According to the plan, acid injection was stopped after a breakthrough occurred in outlet 1. The system was then flushed with DI water.

As shown in Figure 55, the breakthrough occurred on the high-permeability side (outlet 2), with a lower pressure difference than in the other part. After that, the flow stopped at outlet 2 due to increased spent acid viscosity, leading to a temporary blockage, and the acid diverted to the lower-permeability side (outlet 1).

Figure 55 shows the pressure drop as a function of the number of pore volumes injected. The breakthrough occurred in outlet point 2 after pumping 1.6 pore volumes (PV) of the acid. While at outlet point 1, 2 PVs were consumed before the breakthrough occurred.

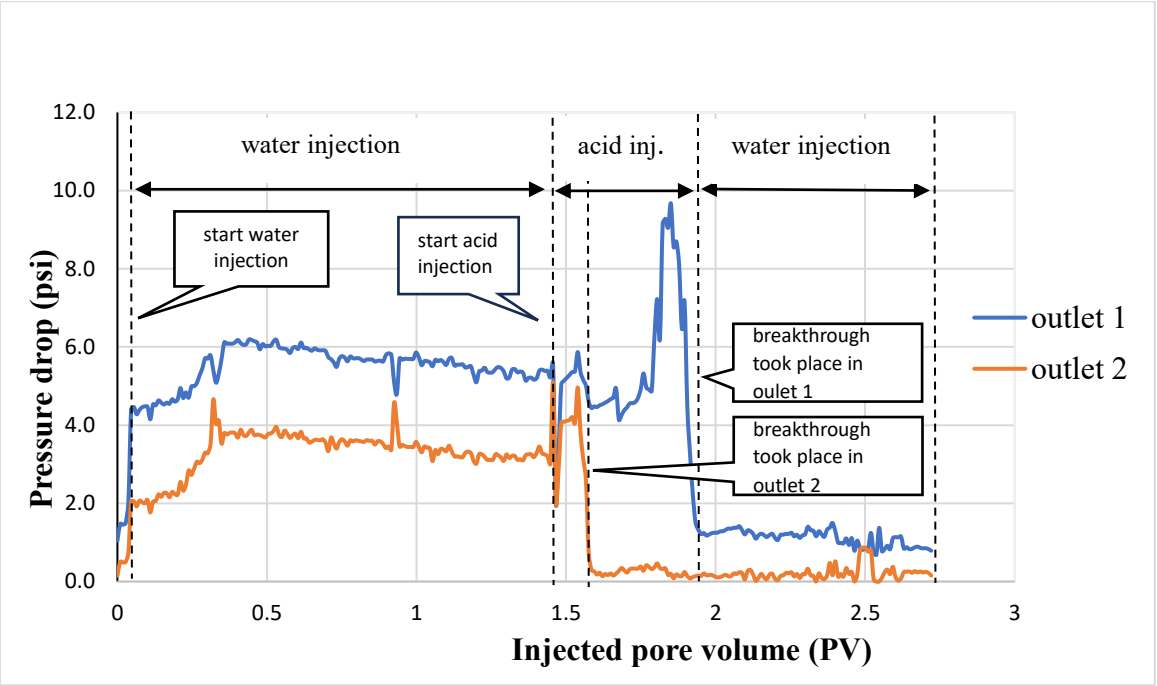

Figure 55 Pressure drop of a cross IL2 sample during the 15 wt% HCl acid injection mixed with 6 wt% VES

5.3.1.3 VES acid system (injection continues after breakthrough)

An Indiana limestone core, 1.5 in diameter and 12 in length, with a permeability of approximately 16 mD, was used in this experiment. The acid system used in this experiment, as shown in Table 7, consists of 15 wt% HCl mixed with 10 wt% $CaCl_2$, 6 vol% VES, and 1% CI. As mentioned in the experimental procedure, the experiment began with DI water injection as a pre-flush to saturate the sample fully. Then, after injecting the acid system, a breakthrough occurred in outlet 2 after 10 minutes, and 115 minutes after the acid injection started, a breakthrough occurred in outlet 1. According to the plan, the acid injection continued even after a breakthrough occurred at both outlet points in this experiment. Finally, the system was flushed with DI water.

As shown in Figure 56, the breakthrough occurred on the high-permeability side (outlet 2), with a lower pressure difference than in the other part. After that, the flow stopped at outlet 2 due to increased spent acid viscosity, leading to a temporary blockage, and the acid diverted to the lower-permeability side (outlet 1).

Figure 56 shows the pressure drop as a function of the number of pore volumes injected. The breakthrough occurred in outlet point 2 after pumping 0.22 PV of the acid. At outlet point 1, a total of 2.4 PV was consumed before the breakthrough happened. After the breakthrough at both outlet points, the flow alternated between the first and second outlet points due to increased viscosity, resulting in temporary blockages and changes in direction.

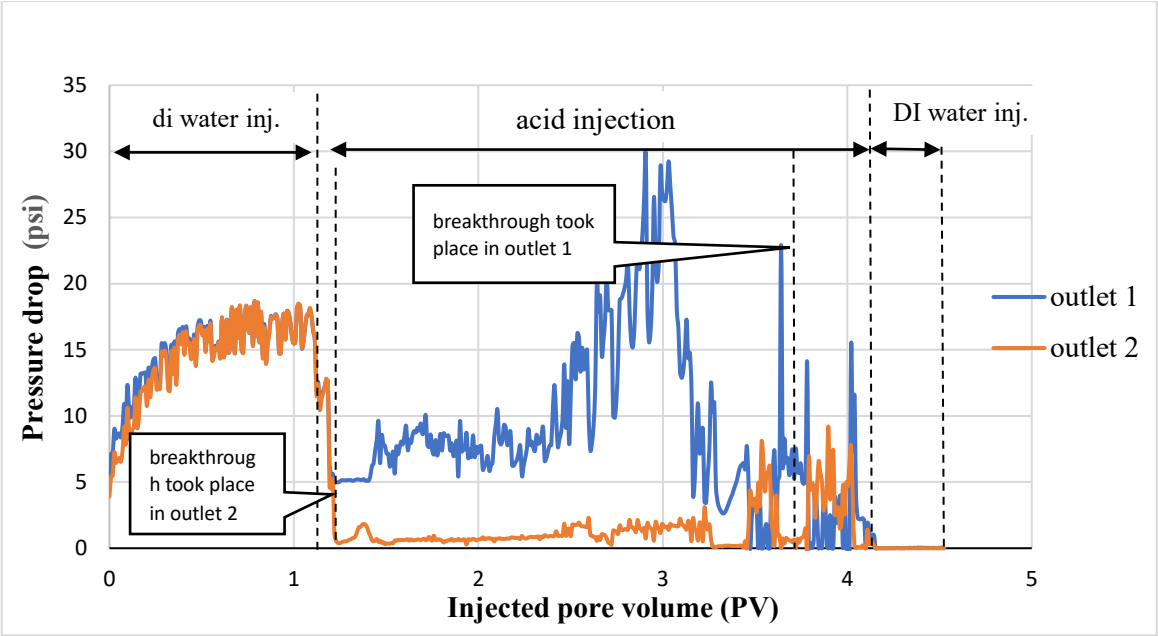

Figure 56 Pressure drop of a cross IL3 sample during the 15 wt% HCl acid injection mixed with 6 wt% VES

5.3.1.4 VES acid system (heterogeneous permeability)

In this experiment, two Indiana limestone samples were used simultaneously. The samples had a diameter of 1.5 in and a length of 6 in. The cores had different permeabilities: the tight one had a permeability (low K) of 10 mD, while the high-permeability (high K) zone had a permeability of 50 mD. The acid system used in this experiment, as shown in Table 7, consists of 15 wt% HCl mixed with 10 wt% $CaCl_2$, 6 wt% VES, and 1 wt% CI. As mentioned in the experimental procedure, the experiment began with DI water injection as a pre-flush to saturate the sample fully. Then, after injecting the acid system, the breakthrough occurred in the high-permeability core (outlet 2) after 26 minutes, and 31 minutes after the acid injection began (a 5 min gap), the breakthrough occurred in the low-permeability core (outlet 1). The acid injection continued after a breakthrough occurred at both outlet points in this experiment. Finally, the system was flushed with DI water.

As shown in Figure 57, the flow from the high-permeability core stopped after the breakthrough occurred in both core samples. The flow continued from the low-permeability core; the wormhole widened without diversion to the other side for 60 minutes; later, the flow alternated between outlet points 1 and 2.

Figure 57 shows the pressure drop as a function of the number of pore volumes injected. The breakthrough occurred in outlet point 2 after pumping 0.5 PV of the acid. At outlet point 1, 0.77 PVs were consumed before breakthrough. After the breakthrough in both outlet points, the flow alternated between the first and second outlet points due to increased viscosity. This is caused by a temporary flow blockage, leading the flow to switch direction.

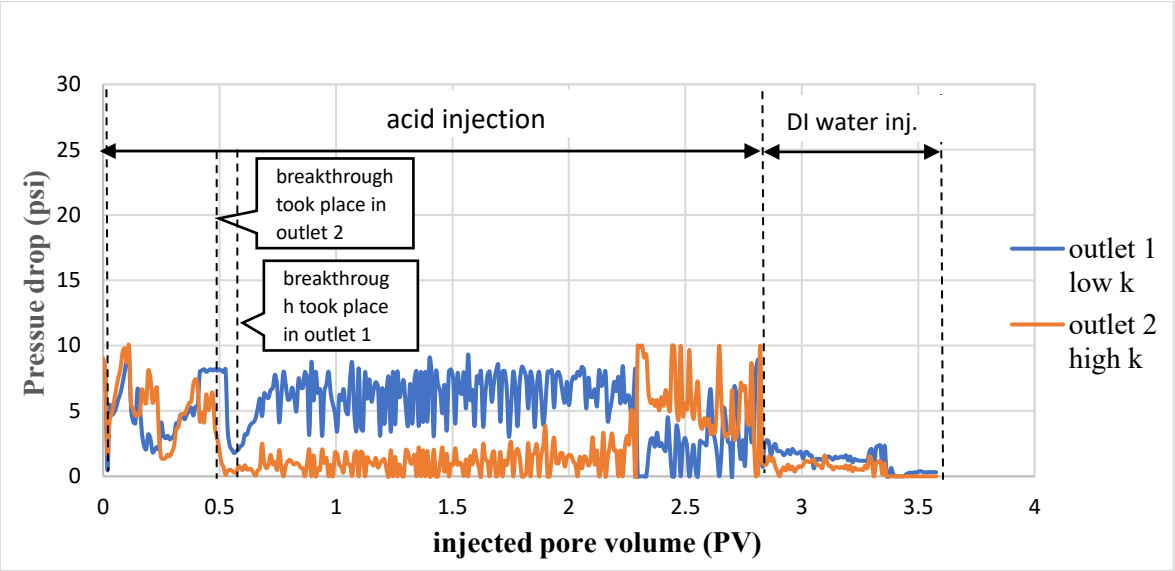

Figure 57 Pressure drop of a cross IL4 and IL5 sample during the 15 wt% HCl acid injection mixed with 6 wt% VES

5.3.2 Computerized tomography (CT) scan results

After the core flooding experiments, a computerized tomography (CT) scan was used to visualize the wormholes created and estimate their volume. Table 8 summarizes the parameters of the wormholes generated in the experiments shown here; CT scan results determine the values.

Table 8 Main parameters of generated wormholes according to CT scan results

Sample No	Wormhole volume fraction	Sample length (mm)	BV (mm^3)	Wormhole volume (mm^3)	Wormhole diameter (mm)
IL1	0.018	305.21	340.70	6.27	0.078
IL2	0.030	305.30	340.80	10.38	0.100
IL3	0.034	305.24	340.73	11.65	0.106
IL4	0.025	152.21	179.97	4.63	0.095
IL5	0.024	152.38	174.64	4.19	0.091

In the first experiment, hydrochloric acid was used, and wormholes were generated on both sides, with a short time gap between the first and second breakthroughs. As shown in Figure 58, there was no diversion in the wormhole, even with continued acid injection after the breakthrough.

Figure 59 shows the CT scan result of Experiment 2. In that case, the wormhole formed on the high-permeability side and was then diverted to the lower-permeability side. The wormhole did not divert to the opposite side because acid injection stopped after the breakthrough occurred on both sides.

In the third experiment, hydrochloric acid with viscoelastic surfactant was used; the wormhole was first generated on the high-permeability side from the closest spot to the edge, and then the acid was diverted to the other side, as shown in Figure 60. As indicated in Table 8, the wormhole volumes generated in Experiments 2 and 3 are close to each other, 11.6 and 10.3, respectively. However, the wormhole length was greater in experiment 3 due to the effect of acid diversion, which produced a longer wormhole with lower acid volume consumption.

In Experiment 4, hydrochloric acid with a viscoelastic surfactant was used; the wormhole was first created on the high-permeability side (point 2), and the flow slowed after breakthrough at outlet 2. The flow increased at outlet 1, and after 4 minutes, a breakthrough occurred at point 1. As shown in Figure 61, the wormhole generated in the low-permeability core was wider and showed no diversion in the opposite direction; in contrast, the wormhole generated in the high-permeability core was thinner and branched in both directions from the initiation point.

IL1 (12 in)	Volume fraction =0.018

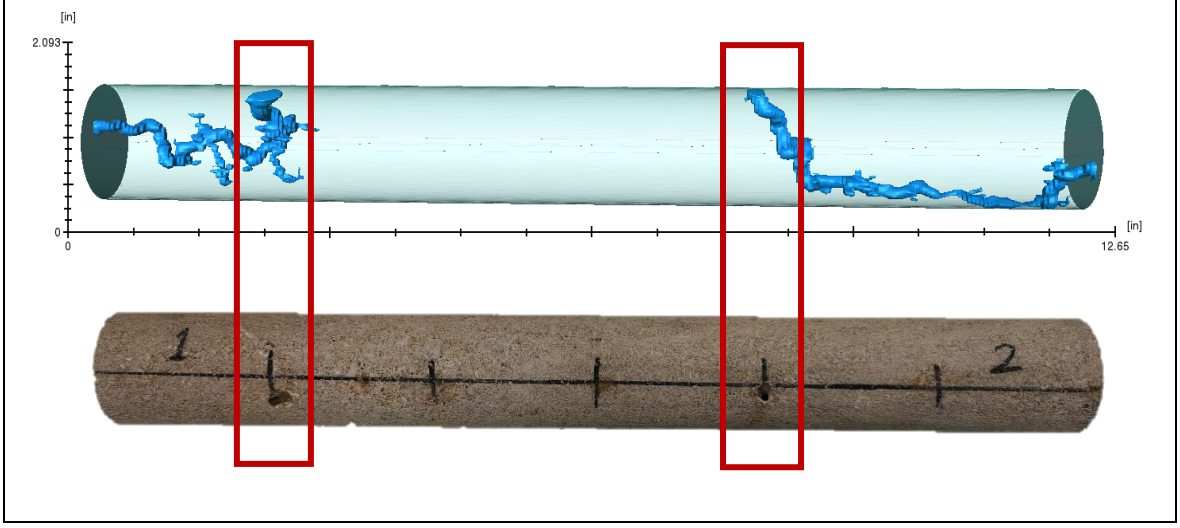

Figure 58 Wormholes generated during Experiment 1

IL2 (12 in)	Volume fraction = 0.030

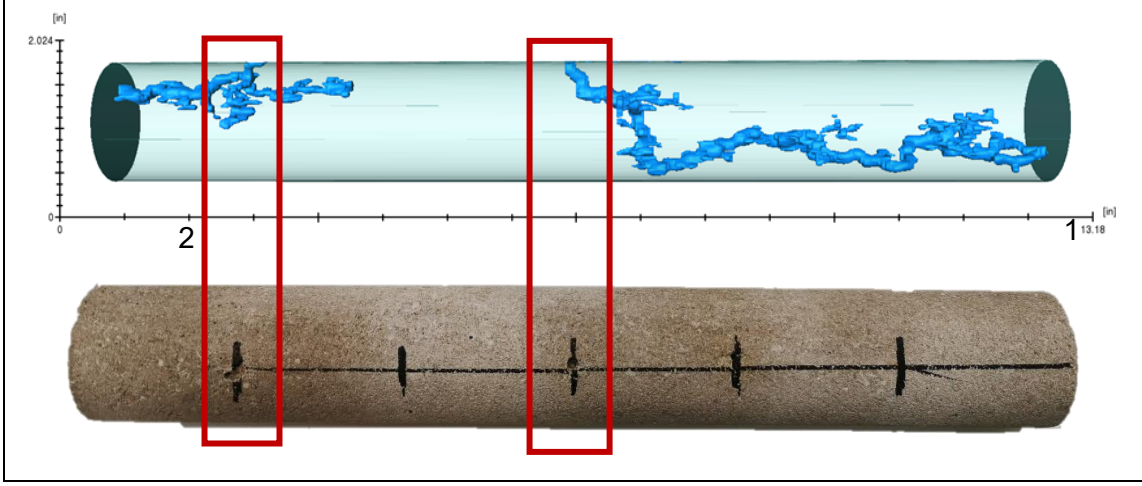

Figure 59 Wormholes generated during Experiment 2

IL3 (12 in)	Volume fraction = 0.034

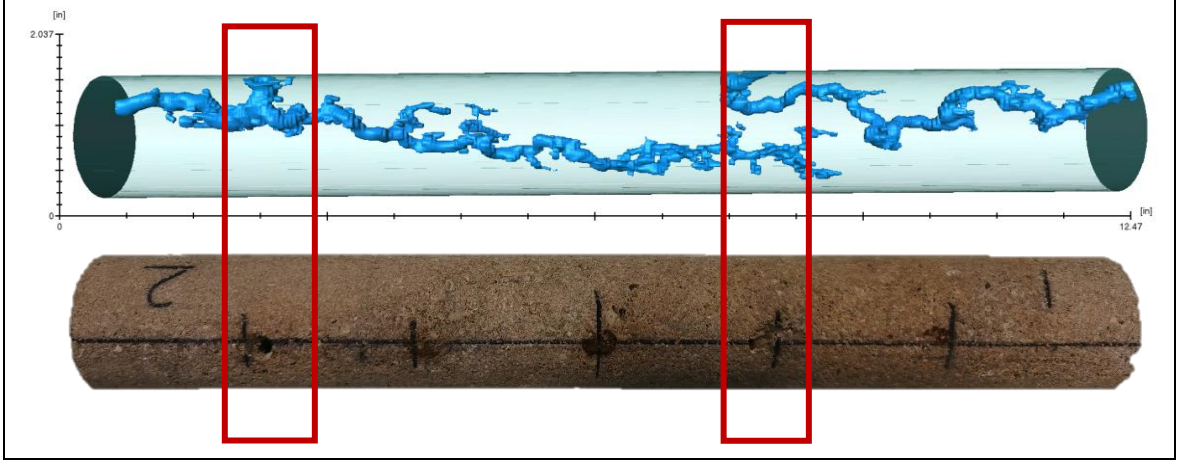

Figure 60 Wormholes generated during Experiment 3

IL4 (6 in) high permeability	IL5 (6 in) low permeability
Volume fraction = 0.024	Volume fraction = 0.025

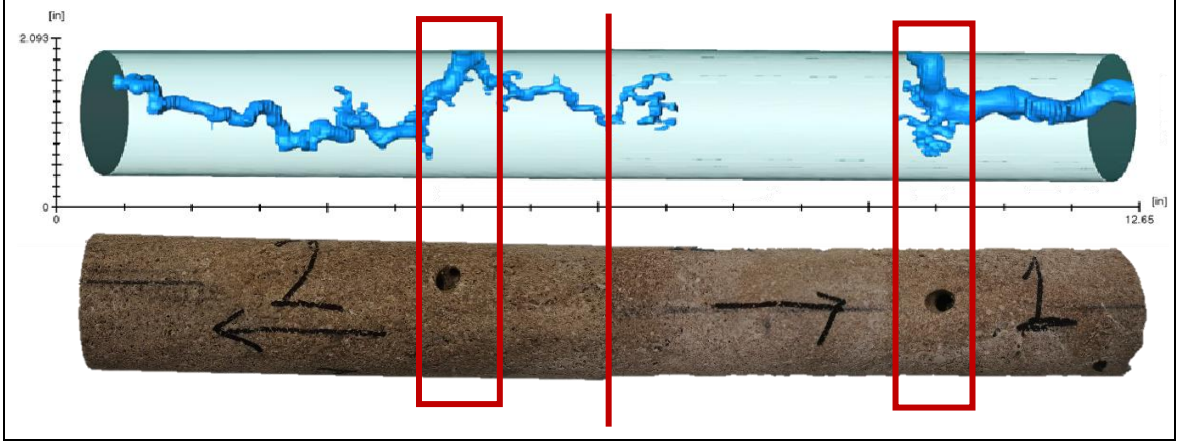

Figure 61 Wormholes generated during Experiment 4

5.4 Discussion:

The introduction of the novel multi-point injection system offers a significant advantage in evaluating the diversion efficiency of certain chemicals during matrix acidizing in horizontal wells. This innovative design aims to more accurately replicate the perforation distribution in horizontal wells, thereby improving acid distribution and diversion efficiency by incorporating five injection points and two outlet lines. This allows researchers to systematically assess the performance of chemical diverters, such as the viscoelastic surfactants (VES) utilized in our study, in directing acid flow across heterogeneous carbonate formations.

The flooding outcomes from the four experiments using the novel multi-point injection technique yield significant insights into acid distribution and diversion performance during matrix acidizing in horizontal wells. Experiment 1 (IL1), which used only hydrochloric acid (HCl), showed limited diversion, resulting in wormholes on both sides of the sample, highlighting the need for improved acid placement strategies. Experiments 2 (IL2) and 3 (IL3), which used HCl with viscoelastic surfactants (VES), showed more successful diversion than the first experiment, as evidenced by higher wormhole volumes and longer wormhole lengths. Experiment IL4 demonstrated the potential for improved diversion in heterogeneous reservoir conditions using two samples with different permeabilities.

I conducted rheological tests on the fluid at 60 °C and measured its viscosity at various shear rates after acid treatment. The results showed shear-thinning behavior, where viscosity decreased as the shear rate increased. The reason for fluid diversion is the higher viscosity of the viscoelastic surfactant (VES) compared to that of hydrochloric acid. To support this, our rheological tests confirmed that the VES produced a significant increase in viscosity, reaching 153 cP, validating the enhanced flow resistance and effective diversion it caused.

The computed tomography (CT) scan results demonstrate the new multi-point injection technique's efficacy in evaluating the diversion efficiency of specific chemicals during matrix acidizing in horizontal wells. The wormhole volumes of Samples IL2 and IL3 are much higher, suggesting improved diversion efficiency, particularly when using chemical diverters such as viscoelastic surfactants (VES). The results emphasize the importance of using modern CT scans to precisely assess acid-diversion schemes, thereby enabling improved reservoir stimulation and optimal hydrocarbon extraction.

Investigations of this novel approach provide insights into acid-diversion behavior and wormhole-propagation mechanisms. The study highlights the influence of chemical diversion on acid placement and distribution by systematically evaluating the efficiency of different acid systems, such as hydrochloric acid (HCl) alone and HCl mixed with VES. The

experiments demonstrate that introducing VES results in longer, more evenly distributed wormholes, indicating improved diversion efficiency compared to conventional methods.

5.5 Conclusions and recommendations

This study used a new flooding system to understand better acidizing in horizontal wells and to identify how acid behaves and diverts in heterogeneous carbonate formations, using viscoelastic surfactant (VES) as a diverting solution. Computerized tomography (CT) scans were also used to visualize the wormholes generated inside the rock samples. The findings and conclusions that resulted from this research can be briefly described as follows:

- Wormhole locations initiated in each experiment differed from one another due to the heterogeneity of formation.
- In each experiment, wormholes occurred far apart. This suggests that the generated wormholes are competing with one another.
- In all experiments, only two wormholes were formed among the five injection points, indicating that not all perforations in the horizontal wells can receive acid.
- Continued injection after the breakthrough, as in Experiment 3, led to a longer wormhole than in Experiment 2, where injection was stopped after the breakthrough.
- In both Experiment 1 (HCl only) and Experiment 3 (HCl+VES), injection continued after breakthrough, but the wormhole generated in Experiment 3 was longer than that in Experiment 1.
- When using only HCl, continuing the injection after the breakthrough leads to a wider wormhole, whereas using HCl with VES produces a longer wormhole with less acid consumption.

6 Conclusion

6.1 Key Findings:

Optimized injection rate: the optimum injection rate for carbonic acid was identified at 2 cm^3/min using the Wang model and at 1.7 cm^3/min using Buijse and Glasbergen's semiempirical model.

Wormhole Morphology: The injection rate of carbonic acid significantly affects the wormhole structure. The intermediate injection rate generates dominant, single, and less branching wormholes.

Petrophysical Alterations: Carbonic acid effectively increased the porosity and permeability of the core sample. The optimum injection rate results in less porosity change but infinite permeability.

Dual-core system advantages: VES carbonic acid significantly improved acid distribution in heterogeneous formations; however, it required a longer time to achieve results than the VES-hydrochloric acid system.

Environmental benefits: Using carbonic acid is environmentally beneficial because it reduces hydrochloric acid consumption, minimizing associated issues such as pipe and surface equipment corrosion, and supporting carbon capture and storage (CCS) by injecting CO2 into subsurface formations.

6.2 Implications for Industry

Carbonic Acid as Green Alternative: These findings establish the efficacy of carbonic acid as a green alternative to HCl in acidizing carbonate formations and provide a solution to both environmental concerns and corrosion-related problems.

Acid diversion system: The combination of the VES-carbonic acid system improves acid distribution, especially in heterogeneous reservoirs.

Economic and Operational Advantages: Reduced consumption of conventional acid and enhanced diversion efficiency may result in lower operational costs and improved safety during well stimulation.

Novel Design: the novel core holder with 5 injection points helps understand acid diversion in a horizontal well and opens the window to identify the best chemical for optimal acid diversion.

6.3 Limitations

Core Sample Constraints: This study was conducted on Indiana limestone. The experiments were performed at 60 °C and under a backpressure of 2000 psi, which was

applied to represent the reservoir pressure. Therefore, the findings are directly valid within this temperature and pressure range; however, they may not apply to all carbonate formations with different mineralogical characteristics.

Scale Limitations: Laboratory-scale experiments cannot perfectly replicate field-scale conditions of pressure, temperature, and heterogeneity.

VES Stability Challenges: While further validation of VES carbonic acid systems is needed under extremely high-temperature/high-pressure conditions. Our experiments confirm the system's stability and diversion efficiency at 60 °C and 2000 psi, which are representative of moderate carbonate reservoir conditions.

6.4 Future Research Directions

Field-Scale Validation: Upgrade laboratory-scale findings to field scale using STIM Pro software.

Comparative Studies: A comparison of the performance of carbonic acid with other acid systems, such as organic or foamed acids, in different types of carbonate formations.

Dynamic Reservoir Modeling: Incorporating specific reservoir considerations into models to predict acid behavior and optimize injection protocols in various field conditions.

7 New scientific achievements

1- Introduction of carbonic acid as a matrix acidizing fluid for carbonate formation

This study experimentally introduced carbonic acid (H_2CO_3), prepared from a mixture of 30% CO_2 and 70% DI water, as an eco-friendly and less corrosive alternative to traditional acid for matrix acidizing in carbonate formation. Unlike previous studies that used salted water for carbonic acid preparation, this work used DI water to better control fluid composition and reaction behavior.

2- Identification of the optimum injection rate for carbonic acid in carbonate limestone.

The study determined the optimum injection rate of carbonic acid during matrix acidizing in carbonate formations. The study investigates different injection rates and their impact on wormhole formation, dissolution rate, and changes in petrophysical properties. Two models were used to determine the optimum injection rate: the Wang model and the Bujis & Glasbergen semi-empirical model approach, yielding results of 2 and 1.7 cm^3/min, respectively.

3- Identification of a new optimum Damköhler number for carbonic acid

While the standard literature Damkohler number introduced by Fredd and Fogler is 0.29, this study showed that the optimum Damkohler number is lower, around 0.005, proving the weak nature of carbonic acid.

4- Development and validation of a novel single-core holder design with five injection points.

A novel core flooding system was developed featuring five injection spots positioned perpendicular to the core samples, simulating perforations in a horizontal well. The new setup provides a more realistic evaluation of wormhole propagation and acid diversion efficiency in heterogeneous carbonate rocks. The research highlights how different acid systems influence the development and propagation of wormholes within the rock.

5- The first experimental study of acid diversion used carbonic acid with VES in a dual-core flooding system.

For the first time, this study introduced the combination of carbonic acid with viscoelastic surfactant for acid diversion in heterogeneous carbonate formation. Diversion efficiency was evaluated using a dual-core flooding system. The experiments confirmed the performance of the VES carbonic acid system and its effectiveness in acid distribution and in redirecting acid flow from high- to low-permeability zones.

8 List of Publications and Presentations

8.1 Publications by the Candidate

1. Abdulameer Almalichy, Usama Alameedy, and Zoltan Turzo, CARBONATE ROCK MATRIX ACIDIZING: A REVIEW OF ACID SYSTEMS AND REACTION MECHANISMS, XXV Spring Wind Conference, 26/05/2022.
2. Abdulameer Almalichy, Zoltan Turzo, Murtada Aljawad, Ahmed Alyasri, A Novel Approach to Assess Acid Diversion Efficiency in Horizontal Wells – Scientific report - 2025 https://doi.org/10.1038/s41598-024-84671-y
3. Abdulameer Almalichy, Murtada Aljawad, Ahmed Alyasri, A novel core flooding system for simulating acid diversion in horizontal wells – Patent submission- USPTO- application No.18/946,725
4. Abdulameer Almalichy, Zoltan Turzo, Murtada Aljawad, Ahmed Alyasri, A Study of The Optimum Injection Rate of Carbonic Acid During Matrix Acidizing of Carbonate Reservoirs: Implications For Reducing CO2 Emissions- Heliyon- 2024- https://doi.org/10.1016/j.heliyon.2024.e39955
5. Abdulameer Almalichy, Zoltan Turzo, The Impact of Carbonic Acid on Porosity and Pore Structure During Matrix Acidizing of Carbonate Reservoirs: Implications for Reducing CO2 Emissions, Civil and Environmental Engineering Reports, 2025 DOI: https://doi.org/10.59440/ceer/200053

8.2 Conference Presentations

1. Carbonate Rock Matrix Acidizing: A Review Of Acid Systems And Reaction Mechanisms, Spring Wind Conference 2022, University of Pécs, 07/05/2022
2. Matrix Acidizing in a tight oil reservoir, Forum of Doctoral Students conference, University of Miskolc, 17/11/2022
3. Assessing Petrophysical Changes During Carbonic Acid Matrix Acidizing- Multiscience - XXXVII. Microcad International Multidisciplinary Scientific Conference- University of Miskolc- 30-31 May 2024
4. The Impact of Carbonic Acid On Porosity During Matrix Acidizing Of Carbonate Reservoirs: Implications For Reducing CO2 Emissions- XXIV Conference of Ph.D. Students and Young Scientists- Wroclaw, Poland on October 23-25, 2024

9 References

Abdollahi, R., Esfandyari, H., Nadri Pari, M., Davarpanah, A., 2021. Conventional diverting techniques and novel fibr-assisted self-diverting system in carbonate reservoir acidizing with successful case studies. Petroleum Research 6, 247–256. https://doi.org/10.1016/j.ptlrs.2021.01.003

Akrad, O., Miskimins, J., 2023. The Use of Biodegradable Particulate Diverting Agents in Hydraulic Fracturing and Refracturing: An Experimental Study. Presented at the International Petroleum Technology Conference, OnePetro. https://doi.org/10.2523/IPTC-23059-MS

Al Ayesh, A.H., Salazar, R.., Farajzadeh, R.., Vincent-Bonnieu, S.., Rossen, W.R., 2017. Foam Diversion in Heterogeneous Reservoirs: Effect of Permeability and Injection Method. SPE Journal 22, 1402–1415. https://doi.org/10.2118/179650-PA

Alameedy, U., Al-Haleem, A., Al-Saedi, A., Kadhim, H., Khan, D., 2023. An experimental study of the effects of matrix acidising on the petrophysical characteristics of carbonate formation. Materials Today: Proceedings. https://doi.org/10.1016/j.matpr.2023.04.128

Alameedy, Usama, Fatah, A., Abbas, A.K., Al-Yaseri, A., 2023. Matrix acidizing in carbonate rocks and the impact on geomechanical properties: A review. Fuel 349, 128586. https://doi.org/10.1016/j.fuel.2023.128586

Al-Douri, A.F., Sayed, M.A., Nasr-El-Din, H.A., Aften, C., 2013. A New Organic Acid To Stimulate Deep Wells in Carbonate Reservoirs. Presented at the SPE International Symposium on Oilfield Chemistry, OnePetro. https://doi.org/10.2118/164110-MS

Alghamdi, A., 2011. Experimental and Theoretical Study of Surfactant-Based Acid Diverting Materials.

Al-Ghamdi, A.H... H., Mahmoud, M.A... A., Wang, G.., Hill, A.D.. D., Nasr-El-Din, H.A.. A., 2014. Acid Diversion by Use of Viscoelastic Surfactants: The Effects of Flow Rate and Initial Permeability Contrast. SPE Journal 19, 1203–1216. https://doi.org/10.2118/142564-PA

Al-Hulail, I., Eoff, L., Anazi, M., 2019. Assessment of Biodegradable Diverter for Acid Fracturing of Highly Fractured Formations. Presented at the Abu Dhabi International Petroleum Exhibition & Conference, OnePetro. https://doi.org/10.2118/197687-MS

Aljawad, M.S., Aboluhom, H., Schwalbert, M.P., Al-Mubarak, A., Alafnan, S., Mahmoud, M., 2021. Temperature impact on linear and radial wormhole propagation in limestone, dolomite, and mixed mineralogy. Journal of Natural Gas Science and Engineering 93, 104031. https://doi.org/10.1016/j.jngse.2021.104031

Almalichy, A., Aljawad, M.S., Turzo, Z., Al-Yaseri, A., 2025. A novel approach to assess acid diversion efficiency in horizontal wells. Sci Rep 15, 1080. https://doi.org/10.1038/s41598-024-84671-y

Almalichy, A., Aljawad, M.S., Turzo, Z., Al-Yaseri, A., 2024. A study of the optimum injection rate of carbonic acid during matrix acidizing of carbonate reservoirs: Implications for reducing CO2 emissions. Heliyon 10, e39955. https://doi.org/10.1016/j.heliyon.2024.e39955

Almalichy, A., Turzó, Z., Alameedy, U., 2022. Carbonate Rock Matrix Acidizing: A Review of Acid Systems and Reaction Mechanisms.

Al-Mutawa, M., Al-Anzi, E., Ravula, C., Al Jalahmah, F., Jemmali, M., Samuel, E., Samuel, M., 2003. Field Cases of a Zero Damaging Stimulation and Diversion Fluid from the Carbonate Formations in North Kuwait. Presented at the International Symposium on Oilfield Chemistry, OnePetro. https://doi.org/10.2118/80225-MS

AlOtaibi, F., Dahlan, M., Khaldi, M., AlGhamdi, A., Al-Hulail, I., 2020. Evaluation of Inorganic-Crosslinked-Based Gelled Acid System for High-Temperature Applications. Presented at the SPE International Conference and Exhibition on Formation Damage Control, OnePetro. https://doi.org/10.2118/199258-MS

Al-Othman, M., A-Matrouk, Y., Ahmed, Z., Ashkanani, M., Buhamad, A., Al-Dousari, M., Ahmed, A.-S., Fidan, E., Mahmoud, W., Liu, H., Salem, A., Nikolaev, M., 2017. New Approach to Chemical Diversion Using Biodegradable Particulates and Fibers in Matrix Acidizing: Kuwait Case Studies. Presented at the Abu Dhabi International Petroleum Exhibition & Conference, OnePetro. https://doi.org/10.2118/188834-MS

Al-Sadat, W., Nasser, M.S., Chang, F., Nasr-El-Din, H.A., Hussein, I.A., 2014. Laboratory evaluation of the effects of additives and pH on the thermorheological behavior of a viscoelastic zwitterionic surfactant used in acid stimulation. Journal of Petroleum Science and Engineering 122, 458–467. https://doi.org/10.1016/j.petrol.2014.08.006

Al-Shargabi, M., Davoodi, S., Wood, D.A., Ali, M., Rukavishnikov, V.S., Minaev, K.M., 2023. A critical review of self-diverting acid treatments applied to carbonate oil and gas reservoirs. Petroleum Science 20, 922–950. https://doi.org/10.1016/j.petsci.2022.10.005

Al-Yaseri, A., Al-Mukainah, H., Yekeen, N., Al-Qasim, A.S., 2023. Experimental investigation of hydrogen-carbonate reactions via computerized tomography: Implications for underground hydrogen storage. International Journal of Hydrogen Energy 48, 3583–3592. https://doi.org/10.1016/j.ijhydene.2022.10.148

Ba Alawi, M., Hassan, A., Aljawad, M.S., Kamal, M.S., Mahmoud, M., Al-Nakhli, A., 2020. A Novel Approach to Improve Acid Diversion in Carbonate Rocks Using Thermochemical Fluids: Experimental and Numerical Study. Molecules 25, 2976. https://doi.org/10.3390/molecules25132976

Bale, G.E., 1984. Matrix Acidizing in Saudi Arabia Using Buoyant Ball Sealers. Journal of Petroleum Technology 36, 1748–1752. https://doi.org/10.2118/11500-PA

Bashir, A., Ali, M., Patil, S., Aljawad, M.S., Mahmoud, M., Al-Shehri, D., Hoteit, H., Kamal, M.S., 2024. Comprehensive review of CO2 geological storage: Exploring principles, mechanisms, and prospects. Earth-Science Reviews 249, 104672. https://doi.org/10.1016/j.earscirev.2023.104672

Bazin, B., 2001. From Matrix Acidizing to Acid Fracturing: A Laboratory Evaluation of Acid/Rock Interactions. SPE Production & Facilities 16, 22–29. https://doi.org/10.2118/66566-PA

Bazin, B., Roque, C., Bouteca, M., 1995. A Laboratory Evaluation of Acid Propagation in Relation to Acid Fracturing: Results and Interpretation. Presented at the SPE European Formation Damage Conference, OnePetro. https://doi.org/10.2118/30085-MS

Bernadiner, M.G., Thompson, K.E., Fogler, H.S., 1992. Effect of Foams Used During Carbonate Acidizing. SPE Production Engineering 7, 350–356. https://doi.org/10.2118/21035-PA

Buijse, M., Glasbergen, G., 2005. A Semiempirical Model To Calculate Wormhole Growth in Carbonate Acidizing. Presented at the SPE Annual Technical Conference and Exhibition, OnePetro. https://doi.org/10.2118/96892-MS

Buijse, M.A., 2000. Understanding Wormholing Mechanisms Can Improve Acid Treatments in Carbonate Formations. SPE Production & Facilities 15, 168–175. https://doi.org/10.2118/65068-PA

Buijse, M.A., 1997. Mechanisms of Wormholing in Carbonate Acidizing. Presented at the International Symposium on Oilfield Chemistry, OnePetro. https://doi.org/10.2118/37283-MS

Caldeira, K., Wickett, M.E., 2003. Anthropogenic carbon and ocean pH. Nature 425, 365–365. https://doi.org/10.1038/425365a

Cao, C., Zhou, F., Cheng, L., Liu, S., Lu, W., Wang, Q., 2021. A comprehensive method for acid diversion performance evaluation in strongly heterogeneous carbonate reservoirs stimulation using CT. Journal of Petroleum Science and Engineering 203, 108614. https://doi.org/10.1016/j.petrol.2021.108614

Chacon, O.G., Pournik, M., 2022. Matrix Acidizing in Carbonate Formations. Processes 10, 174. https://doi.org/10.3390/pr10010174

Chang, F., Qu, Q., Frenier, W., 2001. A Novel Self-Diverting-Acid Developed for Matrix Stimulation of Carbonate Reservoirs. Presented at the SPE International Symposium on Oilfield Chemistry, OnePetro. https://doi.org/10.2118/65033-MS

Chang, F.F., Nasr-El-Din, H.A., Lindvig, T., Qiu, X.W., 2008. Matrix Acidizing of Carbonate Reservoirs Using Organic Acids and Mixture of HCl and Organic Acids. Presented at the SPE Annual Technical Conference and Exhibition, OnePetro. https://doi.org/10.2118/116601-MS

Chang, F.F., Qiu, X., Nasr-El-Din, H.A., 2007. Chemical Diversion Techniques Used for Carbonate Matrix Acidizing: An Overview and Case Histories. Presented at the International Symposium on Oilfield Chemistry, OnePetro. https://doi.org/10.2118/106444-MS

Chen, X., Lu, Y., 2023. A perspective review on degradable polylactic acid diverters for well stimulations. Fuel 348, 128557. https://doi.org/10.1016/j.fuel.2023.128557

Coulter, G.R., Jennings, A.R., Jr., 1999. A Contemporary Approach to Matrix Acidizing. SPE Production & Facilities 14, 150–158. https://doi.org/10.2118/56279-PA

Daccord, G., Touboul, E., Lenormand, R., 1989. Carbonate Acidizing: Toward a Quantitative Model of the Wormholing Phenomenon. SPE Production Engineering 4, 63–68. https://doi.org/10.2118/16887-PA

Domelen, V., S, M., 2017. A Practical Guide to Modern Diversion Technology. Presented at the SPE Oklahoma City Oil and Gas Symposium, OnePetro. https://doi.org/10.2118/185120-MS

Dong, K., 2018. A new wormhole propagation model at optimal conditions for carbonate acidizing. Journal of Petroleum Science and Engineering 171, 1309–1317. https://doi.org/10.1016/j.petrol.2018.08.055

Dong, K., Zhu, D., Hill, A.D., 2016. Theoretical and Experimental Study on Optimal Injection Rates in Carbonate Acidizing. SPE Journal 22, 892–901. https://doi.org/10.2118/178961-PA

Elsayed, M., BinGhanim, A., Aljawad, M.S., El-Husseiny, A., Al-Abdrabalnabi, R., Mahmoud, M., 2023. Quantifying acid diversion efficiency through NMR tortuosity measurements. J Petrol Explor Prod Technol 13, 917–927. https://doi.org/10.1007/s13202-022-01587-x

Evgenievich Folomeev, A., Azatovich Taipov, I., Rustemovich Khatmullin, A., Khanifovich Mukhametov, F., Alexandrovich Vakhrushev, S., Kanafeevich Mingalishev, F., Filusovich Abrarov, V., Viktorovich Akimkin, A., 2021. Gelled Acid vs. Self-Diverting Systems for Carbonate Matrix Stimulation: an Experimental and Field Study. Presented at the SPE Russian Petroleum Technology Conference, OnePetro. https://doi.org/10.2118/206647-MS

Fatah, W.A., Nasr-El-Din, H.A., Moawad, T., Elgibaly, A., 2008. Effects of Crosslinker Type and Additives on the Performance of In-Situ Gelled Acids. Presented at the SPE International Symposium and Exhibition on Formation Damage Control, OnePetro. https://doi.org/10.2118/112448-MS

Fredd, C.N., Fogler, H.S., 1999. Optimum Conditions for Wormhole Formation in Carbonate Porous Media: Influence of Transport and Reaction. SPE Journal 4, 196–205. https://doi.org/10.2118/56995-PA

Fredd, C.N., Fogler, H.S., 1998. Influence of transport and reaction on wormhole formation in porous media. AIChE Journal 44, 1933–1949. https://doi.org/10.1002/aic.690440902

Frenier, W.W., Wilson, D., Crump, D., Jones, L., 2000. Use of Highly Acid-Soluble Chelating Agents in Well Stimulation Services. Presented at the SPE Annual Technical Conference and Exhibition, OnePetro. https://doi.org/10.2118/63242-MS

Furui, K.., Burton, R.C.. C., Burkhead, D.W.. W., Abdelmalek, N.A.. A., Hill, A.D.. D., Zhu, D.., Nozaki, M.., 2011. A Comprehensive Model of High-Rate Matrix-Acid Stimulation for Long Horizontal Wells in Carbonate Reservoirs: Part I—Scaling Up Core-Level Acid Wormholing to Field Treatments. SPE Journal 17, 271–279. https://doi.org/10.2118/134265-PA

Garrouch, A.A., Jennings, A.R., 2017. A contemporary approach to carbonate matrix acidizing. Journal of Petroleum Science and Engineering 158, 129–143. https://doi.org/10.1016/j.petrol.2017.08.045

Ghommem, M., Zhao, W., Dyer, S., Qiu, X., Brady, D., 2015. Carbonate acidizing: Modeling, analysis, and characterization of wormhole formation and propagation. Journal of Petroleum Science and Engineering 131, 18–33. https://doi.org/10.1016/j.petrol.2015.04.021

Glasbergen, G., Kalia, N., Talbot, M., 2009. The Optimum Injection Rate for Wormhole Propagation: Myth or Reality? Presented at the 8th European Formation Damage Conference, OnePetro. https://doi.org/10.2118/121464-MS

Gomaa, A.M., Mahmoud, M.A., Nasr-El-Din, H.A., 2010. A Study of Diversion Using Polymer-Based In-Situ Gelled Acids Systems. Presented at the Trinidad and Tobago Energy Resources Conference, OnePetro. https://doi.org/10.2118/132535-MS

Gomaa, A.M., Nasr-El-Din, H.A., 2010. New Insights into Wormhole Propagation in Carbonate Rocks Using Regular, Gelled and In-situ Gelled Acids. Presented at the SPE Production and Operations Conference and Exhibition, OnePetro. https://doi.org/10.2118/133303-MS

Gomaa, A.M.M., Mahmoud, M.A.. A., Nasr-El-Din, H.A.. A., 2011. Laboratory Study of Diversion Using Polymer-Based In-Situ-Gelled Acids. SPE Production & Operations 26, 278–290. https://doi.org/10.2118/132535-PA

Gonzalez, D., Ulloa, J., Safari, R., Al-Rawi, A., Babey, A., 2017. State of the Art Biodegradable Diversion Technology Applied on Tight Carbonates Reservoir Leads to Maximized Production. Presented at the Abu Dhabi International Petroleum Exhibition & Conference, OnePetro. https://doi.org/10.2118/188632-MS

Huang, J., Safari, R., Fragachan, F.E., 2018. Applications of Self-Degradable Particulate Diverters in Wellbore Stimulations: Hydraulic Fracturing and Matrix Acidizing Case Studies. Presented at the SPE International Hydraulic Fracturing Technology Conference and Exhibition, OnePetro. https://doi.org/10.2118/191408-18IHFT-MS

Huang, Tianping, Hill, A.D., Schechter, R.S., 2000. Reaction Rate and Fluid Loss: The Keys to Wormhole Initiation and Propagation in Carbonate Acidizing. SPE Journal 5, 287–292. https://doi.org/10.2118/65400-PA

Huang, T., Ostensen, L., Hill, A.D., 2000. Carbonate Matrix Acidizing with Acetic Acid. Presented at the SPE International Symposium on Formation Damage Control, OnePetro. https://doi.org/10.2118/58715-MS

Jafarpour, H., Moghadasi, J., Petrakov, D.G., Khormali, A., 2018. Investigating the Necessity of Developing the Self-diverting Emulsified Acid (SDEA) System for Stimulation of a Middle-Eastern Carbonate Reservoir. Presented at the Saint Petersburg 2018, European Association of Geoscientists & Engineers, pp. 1–5. https://doi.org/10.3997/2214-4609.201800302

Jain, R., McCool, C.S., Green, D.W., Willhite, G.P., Michnick, M.J., 2005. Reaction Kinetics of the Uptake of Chromium(III) Acetate by Polyacrylamide. SPE Journal 10, 247–255. https://doi.org/10.2118/89399-PA

Kalfayan, L.J., Martin, A.N., 2009. The Art and Practice of Acid Placement and Diversion: History, Present State and Future. Presented at the SPE Annual Technical Conference and Exhibition, OnePetro. https://doi.org/10.2118/124141-MS

Khan, A., Raza, M., 2015. Coiled Tubing Acidizing: An Innovative Well Intervention for Production Optimization. International Journal of Engineering Research and Technology 2278-0181 Volume 4, 497–500.

Letichevskiy, A., Nikitin, A., Parfenov, A., Makarenko, V., Lavrov, I., Rukan, G., Ovsyannikov, D., Nuriakhmetov, R., Gromovenko, A., 2017. Foam Acid Treatment - The Key to Stimulation of Carbonate Reservoirs in Depleted Oil Fields of the Samara Region. Presented at the SPE Russian Petroleum Technology Conference, OnePetro. https://doi.org/10.2118/187844-MS

Li, S., Li, Z., Lin, R., 2008. Mathematical models for foam-diverted acidizing and their applications. Pet. Sci. 5, 145–152. https://doi.org/10.1007/s12182-008-0022-4

Li, Y., Deng, Q., Zhao, J., Liao, Y., Jiang, Y., 2018. Simulation and analysis of matrix stimulation by diverting acid system considering temperature field. Journal of Petroleum Science and Engineering 170, 932–944. https://doi.org/10.1016/j.petrol.2018.06.050

Liu, M., Zhang, S., Mou, J., Zhou, F., Shi, Y., 2013. Diverting mechanism of viscoelastic surfactant-based self-diverting acid and its simulation. Journal of Petroleum Science and Engineering 105, 91–99. https://doi.org/10.1016/j.petrol.2013.03.001

Liu, N., Liu, M., 2016. Simulation and analysis of wormhole propagation by VES acid in carbonate acidizing. Journal of Petroleum Science and Engineering 138, 57–65. https://doi.org/10.1016/j.petrol.2015.12.011

Liu, P., Xue, H., Zhao, L.Q., Fu, Y., Luo, Z., Qu, Z., 2015. Analysis and simulation of rheological behavior and diverting mechanism of In Situ Self-Diverting acid. Journal of Petroleum Science and Engineering 132, 39–52. https://doi.org/10.1016/j.petrol.2015.04.042

Lungwitz, B., Fredd, C., Brady, M., Miller, M., Ali, S., Hughes, K., 2007. Diversion and Cleanup Studies of Viscoelastic Surfactant-Based Self-Diverting Acid. SPE Production & Operations 22, 121–127. https://doi.org/10.2118/86504-PA

Lynn, J.D., Nasr-El-Din, H.A., 2001. A core based comparison of the reaction characteristics of emulsified and in-situ gelled acids in low permeability, high temperature, gas bearing carbonates. Presented at the SPE International Symposium on Oilfield Chemistry, OnePetro. https://doi.org/10.2118/65386-MS

Ma, L., Fauchille, A.-L., Ansari, H., Chandler, M., Ashby, P., Taylor, K., Pini, R., Lee, P.D., 2021. Linking multi-scale 3D microstructure to potential enhanced natural gas recovery and subsurface CO2 storage for Bowland shale, UK. Energy Environ. Sci. 14, 4481–4498. https://doi.org/10.1039/D0EE03651J

Moffitt, P.D., Moradi-Araghi, A., Ahmed, I., Janway, V.R., Young, G.R., 1996. Development and Field Testing of a New Low Toxicity Polymer Crosslinking System. Presented at the Permian Basin Oil and Gas Recovery Conference, OnePetro. https://doi.org/10.2118/35173-MS

Mohammed, A., Velledits, F., 2024a. Microfacies impacts on reservoir heterogeneity of early Cretaceous Yamama carbonate reservoir in South Iraq. Sci Rep 14, 24184. https://doi.org/10.1038/s41598-024-74640-w

Mohammed, A., Velledits, F., 2024b. Microfacies impacts on reservoir heterogeneity of early Cretaceous Yamama carbonate reservoir in South Iraq. Sci Rep 14, 24184. https://doi.org/10.1038/s41598-024-74640-w

Mou, J., Liu, M., Zheng, K., Zhang, S., 2015. Diversion Conditions for Viscoelastic-Surfactant-Based Self-Diversion Acid in Carbonate Acidizing. SPE Production & Operations 30, 121–129. https://doi.org/10.2118/173898-PA

Nasr-El-Din, H.A., Al-Ghamdi, A.H., Al-Qahtani, A.A., Samuel, M.M., 2008. Impact of Acid Additives on the Rheological Properties of a Viscoelastic Surfactant and Their Influence on Field Application. SPE Journal 13, 35–47. https://doi.org/10.2118/89418-PA

Nasr-El-Din, H.A., Samuel, M., 2007. Lessons Learned From Using Viscoelastic Surfactants in Well Stimulation. SPE Production & Operations 22, 112–120. https://doi.org/10.2118/90383-PA

Ortega, A., 2015. Acidizing High-Temperature Carbonate Formations Using Methanesulfonic Acid (Thesis).

Panga, M.K.R., Ziauddin, M., Gandikota, R., Balakotaiah, V., 2004. A New Model for Predicting Wormhole Structure and Formation in Acid Stimulation of Carbonates. Presented at the SPE International Symposium and Exhibition on Formation Damage Control, OnePetro. https://doi.org/10.2118/86517-MS

Peiwu, L., Al-Mefleh, K., van Dijk, K., Ajayi, A., Fidan, E., Al-Salali, Y., Naqi, Y., Alaabdin, Z., 2023. A Novel Hybrid Acid Stimulation/Fracturing Technique Developed for North Kuwait Jurassic Gas, Utilizing Particulate Diverters for Wellbore Diversion.

Presented at the SPE International Hydraulic Fracturing Technology Conference and Exhibition, OnePetro. https://doi.org/10.2118/215664-MS

Peng, C., Crawshaw, J.P., Maitland, G.C., Trusler, J.P.M., 2015. Kinetics of calcite dissolution in CO2-saturated water at temperatures between (323 and 373) K and pressures up to 13.8 MPa. Chemical Geology 403, 74–85. https://doi.org/10.1016/j.chemgeo.2015.03.012

Punnapala, S., Rahman, M.A., Misra, S., 2014. Challenge of Acidizing Horizontal Wells in Tight Carbonate Reservoirs - Weak Acid and Non-acid Alternates. Presented at the Abu Dhabi International Petroleum Exhibition and Conference, OnePetro. https://doi.org/10.2118/171766-MS

Ratnakar, R.R., Kalia, N., Balakotaiah, V., 2012. Carbonate Matrix Acidizing with Gelled Acids: An Experiment-Based Modeling Study. Presented at the SPE International Production and Operations Conference & Exhibition, OnePetro. https://doi.org/10.2118/154936-MS

Reddy, B.R., Cortez, J., 2013. Activator Development for Controlling Degradation Rates of Polymeric Degradable Diverting Agents. Presented at the SPE International Symposium on Oilfield Chemistry, OnePetro. https://doi.org/10.2118/164117-MS

Rodrigues, M.A.F., Arruda, G.M., da Silva, D.C., da Costa, F.M.F., de Brito, M.F.P., Antonino, A.C.D., Wanderley Neto, A. de O., 2021. Application of nonionic surfactant nonylphenol to control acid stimulation in carbonate matrix. Journal of Petroleum Science and Engineering 203, 108654. https://doi.org/10.1016/j.petrol.2021.108654

Safari, R., Shahri, M.P., Smith, C., Fragachan, F., 2017. Analysis and Design Method for Particulate Diversion in Carbonate Acidizing. Presented at the SPE Eastern Regional Meeting, OnePetro. https://doi.org/10.2118/187525-MS

Shafiq, M.U., Ben Mahmud, H.K., Arif, M., 2018. Mineralogy and pore topology analysis during matrix acidizing of tight sandstone and dolomite formations using chelating agents. Journal of Petroleum Science and Engineering 167, 869–876. https://doi.org/10.1016/j.petrol.2018.02.057

Shah, M., Agarwal, J.R., Patel, D., Chauhan, J., Kaneria, D., Shah, S.N., 2020. An assessment of chemical particulate technology as diverters for refracturing treatment. Journal of Natural Gas Science and Engineering 84, 103640. https://doi.org/10.1016/j.jngse.2020.103640

Shahri, M.P., Huang, J., Smith, C.S., Fragachán, F.E., 2017. An Engineered Approach to Design Biodegradables Solid Particulate Diverters: Jamming and Plugging. Presented at the SPE Annual Technical Conference and Exhibition, OnePetro. https://doi.org/10.2118/187433-MS

Shank, R.A., McCartney, T.R., 2013. Synergistic and Divergent Effects of Surfactants on the Kinetics of Acid Dissolution of Calcium Carbonate Scale. Presented at the CORROSION 2013, OnePetro.

Talbot, M.S., Gdanski, R.D., 2008. Beyond the Damkohler Number: A New Interpretation of Carbonate Wormholing. Presented at the Europec/EAGE Conference and Exhibition, OnePetro. https://doi.org/10.2118/113042-MS

Taylor, D., Kumar, P.S., Fu, D., Jemmali, M., Helou, H., Chang, F., Davies, S., Al-Mutawa, M., 2003. Viscoelastic Surfactant Based Self-Diverting Acid for Enhanced Stimulation in Carbonate Reservoirs. Presented at the SPE European Formation Damage Conference, OnePetro. https://doi.org/10.2118/82263-MS

Taylor, K.C., Nasr-El-Din, H.A., 2003. Laboratory Evaluation of In-Situ Gelled Acids for Carbonate Reservoirs. SPE Journal 8, 426–434. https://doi.org/10.2118/87331-PA

Taylor, K.C., Nasr-El-Din, H.A., 2002. Coreflood Evaluation of In-Situ Gelled Acids. Presented at the International Symposium and Exhibition on Formation Damage Control, OnePetro. https://doi.org/10.2118/73707-MS

Thomas, A., Ramkumar, A., Shanmugam, A., 2022. CO2 acidification and its differential responses on aquatic biota – a review. Environmental Advances 8, 100219. https://doi.org/10.1016/j.envadv.2022.100219

Thomas, R.L., Saxon, A., Milne, A.W., 1998. The Use of Coiled Tubing During Matrix Acidizing of Carbonate Reservoirs Completed in Horizontal, Deviated, and Vertical Wells. SPE Production & Facilities 13, 147–162. https://doi.org/10.2118/50964-PA

Tie, L., Yu, M., Li, X., Liu, W., Zhang, B., Chang, Z., Zheng, Y., 2019. Research on polymer solution rheology in polymer flooding for Qikou reservoirs in a Bohai Bay oilfield. J Petrol Explor Prod Technol 9, 703–715. https://doi.org/10.1007/s13202-018-0515-7

Umer Shafiq, M., Khaled Ben Mahmud, H., Rezaee, R., Testamanti, N., 2017. Investigation of Changing Pore Topology and Porosity During Matrix Acidizing using Different Chelating Agents. IOP Conf. Ser.: Mater. Sci. Eng. 217, 012023. https://doi.org/10.1088/1757-899X/217/1/012023

Wang, Y., Hill, A.D., Schechter, R.S., 1993. The Optimum Injection Rate for Matrix Acidizing of Carbonate Formations. Presented at the SPE Annual Technical Conference and Exhibition, OnePetro. https://doi.org/10.2118/26578-MS

Yan, Y., Xi, Q., Una, C., He, B., Wu, C., Dou, L., 2019a. A novel acidizing technology in carbonate reservoir: In-Situ formation of CO2 foamed acid and its self-diversion. Colloids and Surfaces A: Physicochemical and Engineering Aspects 580, 123787. https://doi.org/10.1016/j.colsurfa.2019.123787

Yan, Y., Xi, Q., Una, C., He, B., Wu, C., Dou, L., 2019b. A novel acidizing technology in carbonate reservoir: *In-Situ* formation of CO2 foamed acid and its self-diversion. Colloids and Surfaces A: Physicochemical and Engineering Aspects 580, 123787. https://doi.org/10.1016/j.colsurfa.2019.123787

Yousufi, M.M., Mohyaldinn Elhaj, M.E., Dzulkarnain, I.B., 2024. A Review on Use of Emulsified Acids for Matrix Acidizing in Carbonate Reservoirs. ACS Omega 9, 11027–11049. https://doi.org/10.1021/acsomega.3c07132

Zakaria, A.S., Nasr-El-Din, H.A., 2016a. A Novel Polymer-Assisted Emulsified-Acid System Improves the Efficiency of Carbonate Matrix Acidizing. SPE Journal 21, 1061–1074. https://doi.org/10.2118/173711-PA

Zakaria, A.S., Nasr-El-Din, H.A., 2016b. A Novel Polymer-Assisted Emulsified-Acid System Improves the Efficiency of Carbonate Matrix Acidizing. SPE Journal 21, 1061–1074. https://doi.org/10.2118/173711-PA

Zakaria, A.S., Nasr-El-Din, H.A., 2015. Application of Novel Polymer Assisted Emulsified Acid System Improves the Efficiency of Carbonate Acidizing. Presented at the SPE International Symposium on Oilfield Chemistry, OnePetro. https://doi.org/10.2118/173711-MS

Zerhboub, M., Ben-Naceur, K., Touboul, E., Thomas, R., 1994. Matrix Acidizing: A Novel Approach to Foam Diversion. SPE Production & Facilities 9, 121–126. https://doi.org/10.2118/22854-PA

Zhang, L., He, J., Wang, H., Li, Z., Zhou, F., Mou, J., 2021. Experimental investigation on wormhole propagation during foamed-VES acidizing. Journal of Petroleum Science and Engineering 198, 108139. https://doi.org/10.1016/j.petrol.2020.108139

Zhang, L., Zhou, F., Zhang, S., Wang, Jie, Wang, Jin, Pournik, M., 2019. Fracture Conductivity Analysis on the Degradable Particle Diverter Combined with Engineered Proppant. Presented at the 53rd U.S. Rock Mechanics/Geomechanics Symposium, OnePetro.

Zheng, N., Zhu, J., Yang, Z., Li, X., Chen, H., Su, H., Qiao, L., 2024. Molecular dynamics simulation and key performance study of VES self-diverting acid system for deep carbonate reservoirs. Journal of Molecular Liquids 401, 124645. https://doi.org/10.1016/j.molliq.2024.124645

Zhu, D., Wang, Y., Cui, M., Zhou, F., Zhang, Y., Liang, C., Zou, H., Yao, F., 2022. Effects of spent viscoelastic-surfactant acid flow on wormholes propagation and diverting performance in heterogeneous carbonate reservoir. Energy Reports 8, 8321–8332. https://doi.org/10.1016/j.egyr.2022.06.056

Ziauddin, M., Bize, E., 2007. The Effect of Pore-Scale Heterogeneities on Carbonate Stimulation Treatments. Presented at the SPE Middle East Oil and Gas Show and Conference, OnePetro. https://doi.org/10.2118/104627-MS